
Increased sedimentation and habitat change following dynamic dune restoration, Mason Bay, New Zealand

Ella Buckley

A thesis submitted in partial fulfilment of the degree of

Master of Science

At the University of Otago, Dunedin, New Zealand

August 2015

Abstract

Since 2002 *Ammophila arenaria* has been progressively eradicated from the transgressive dune system at Mason Bay, Stewart Island, New Zealand in a bid to restore dune dynamics. Little is known, however, about the impact of restored dune dynamics on downwind landforms and associated plant communities. With the aim of predicting the response of the Mason Bay stonefield to dynamic restoration, this study examines the patterns of sand transport and accumulation downwind of the dynamic restoration project and considers the implications for plant communities and key species. The Mason Bay stonefield is a deflation surface which is recognised as nationally threatened as it is inhabited by at-risk native plants and is an important habitat for the endangered Dotterel (*Caradrius o. obscurus*). Sand accumulation in the stonefield may cause a shift from a deflation surface to other dune forms, including nabkha, given the presence of indigenous sand-colonising species.

The methodology of this study reflected the spatial and temporal scales at which *A. arenaria* invasion and dynamic restoration could impact the stonefield. First the historic development of the Mason Bay landforms was described in relation to *A. arenaria* invasion and its subsequent removal using a series of historic photographs. Since *A. arenaria* invasion in 1958, the area of the stonefield has significantly increased by 39% and moved inland. Since *A. arenaria* removal in 2002, the stonefield has increased in area by 7%. This was attributed to the remnant *A. arenaria* rhizome and dead plant material creating a lag in geomorphic response to revegetation.

The current sand accumulation in the stonefield was examined over a nine month period, using a series of erosion pins within a 200m x 50m plot in the stonefield. Digital elevation models were derived from regular total station surveys to determine whether sand-drift was accumulating around low *Ficinia spiralis* nabkha. During the nine month survey period the surface of the study area accreted on average only 3.22mm. Accretion and erosion was not strongly correlated with vegetation cover. The dimensions of the surveyed nabkha did not change significantly during this period. The lack of sand deposition downwind of eroding dunes is attributed to the topography and exposure of the bed.

The importance of the event-scale sedimentation patterns was investigated by measuring the wind speed, direction and sand transport, to determine whether such events deposit or erode

sand in the study area. The wind speed and direction measured during two discrete wind events showed that there is no decline in wind speed across the study area, creating little potential for aeolian deposition in the stonefield.

Lastly, the impact of the observed sand burial on the sand binding and non-sand binding stonefield plant communities was assessed. This investigation suggested that at risk non-sand binding plant communities might have a degree of tolerance to sand burial. Increased sand deposition, however, may favor the sand binding plant species and exclude the native non-sand binders like *Raoulia hookeri* var. *hookeri*.

The geography of the stonefield has shown to be remarkably dynamic and the ability of plant species to keep pace is evidence of their ability to colonise. Since 2011, approximately five years after *A. arenaria* spray efforts began the depositional lobes have started to elongate into the stonefield. This suggests that the remnant *A. arenaria* rhizome is breaking down and sand inputs in the stonefield may be increasing. Sand deposition around *F. spiralis* plants in the stonefield and the elongation of the depositional lobes may reduce the stonefield area and break up the continuous stonefield feature. To date, the stonefield has been a continuous feature which has most likely aided in the stonefield species' ability to keep pace with the evolution of the stonefield. However, it is unknown whether the colonisation abilities of these species will be able to adapt to the fragmentation of the stonefield habitat by sand burial from recent destabilisation.

Acknowledgements

Thanks must go to everyone who has been involved and contributed to this research:

Doctor Mike Hilton, Doctor Teresa Konlechner and Doctor Janice Lord; for the invaluable experience and knowledge that you have each brought to this research. I would like to also thank you all for your patience and support over the course of my research.

To the many field assistants, this study would not have been possible without all of your endless hours of erosion pin measuring and surveying. The enthusiasm and great personalities you each brought to Mason Bay will be something I will always treasure from my research experience.

The technical staff of the Geography Department, especially Nigel McDonald; thank you for assisting with the array of technical equipment used in this research.

Department of Conservation for providing the opportunity to carry out this research in Mason Bay, a truly unique location, for which your tireless efforts in the removal of *Ammophila arenaria* continues to amaze me.

To my friends in the Geography Department, you have accepted me into your family and the support and advice you have all provided has been greatly appreciated. Our lunch time conversations will be sorely missed.

To my family, friends and Hamish for your endless love and support. A special thanks to those of you who helped with proof reading.

Lastly a huge thanks to Mum and Dad (Diane and Bob), for your endless support from afar. Your passion for the coast has been a true inspiration for this research.

Table of contents

Abstract.....	i
Acknowledgements	iii
Table of contents	iv
List of Tables.....	vii
List of Figures.....	viii
Chapter 1: Introduction	1
1.1 Overview	1
1.2 Dynamic restoration, Mason Bay, Stewart Island	5
1.3 Research Objectives.....	10
1.4 Thesis structure.....	12
Chapter 2: Evolution of the Mason Bay stonefield in conjunction with the invasion and recent removal of <i>Ammophila arenaria</i>.....	14
2.1 Introduction	14
2.2 Method.....	16
2.2.1 Aerial photography	16
2.2.2 Mapping the current stonefield.....	17
2.2.3 Limitations of aerial photography	18
2.2.4 Analysis of stonefield land form changes	18
2.3 Results	19
2.3.1 Stonefield evolution before <i>A. arenaria</i> control (between 1958 and 2000).....	19
2.3.2 <i>A. arenaria</i> eradication programme (between 2002 and 2015).....	25
2.3.3 Relationship between the stonefield and foredune growth.....	26
2.4 Discussion.....	27

Chapter 3: Short-term sedimentation patterns within the stonefield.....	29
3.1 Introduction	29
3.2 Method.....	31
3.2.1 Stonefield area survey	32
3.2.2 <i>Ficinia spiralis</i> nabkha development	33
3.2.3 Soil profiles	35
3.2.4 Data Analysis.....	36
3.3 Results	37
3.3.1 Sedimentation patterns recorded by the erosion pins	37
3.3.2 Patterns in <i>F. spiralis</i> nabkha size and development	40
3.3.3 Spatial distribution of recent burial patterns.....	42
3.3.4 Wind regime during the study period	45
3.4 Discussion.....	46
Chapter 4: Event-scale stonefield sedimentation.....	48
4.1 Introduction	48
4.2 Method.....	51
4.2.1 Study site	51
4.2.2 Wind analysis	52
4.2.3 Sediment budget analysis	53
4.2.4 Analysis	55
4.3 Results	58
4.3.1 Spatial wind analysis	58
4.3.2 Stonefield digital terrain model	62
4.3.3 Mason Bay sand drift potential.....	64
4.4 Discussion.....	65
Chapter 5: The impact of sedimentation on the native dune species <i>Raoulia hookeri</i> var. <i>hookeri</i> and <i>Ficinia spiralis</i>.....	67
5.1 Introduction	67

5.2 Method.....	70
5.2.1 Relationship between <i>F. spiralis</i> and <i>R. hookeri</i> var. <i>hookeri</i> surface area and sedimentation patterns	70
5.2.2 <i>Raoulia hookeri</i> burial experiment.	70
5.2.3 Analysis	72
5.3 Results	74
5.3.1 Stonefield plant communities	74
5.3.2 <i>R. hooker</i> var. <i>hookeri</i> and <i>F. spiralis</i> surface area patterns	75
5.3.3 <i>R. hookeri</i> burial experiment	76
5.4 Discussion.....	79
Chapter 6: Conclusion.....	83
6.1 Introduction	83
6.2 The historic development of the Mason Bay stonefield and deflation surfaces	84
6.3 Is sand liberated from recent and ongoing destabilisation accumulating in the stonefield?	85
6.4 Are the observed sedimentation patterns adversely affecting the native plant communities in the stonefield?.....	87
6.4 Concluding remarks.....	89
6.5 Future Research	90
References.....	92
Appendix I.....	103
Appendix II	107

List of Tables

Chapter 1

Table 1.1: Summary of dynamic restoration programmes around the world using destabilisation and their restoration goals. In alphabetical order of countries.....4

Chapter 2

Table 2.1: Aerial photographs and satellite images were sourced from New Zealand Aerial Mapping (NZAM), private collections (PC) and Google Earth (GE).....16

Chapter 4

Table 4.1: Fryberger's (1979) classification of wind energy environments using total drift potential (DP) and directional variability (RDP/DP) ratio. Adapted by Bullard (1997) to m/s.....57

Chapter 5

Table 5.1: The six *R. hookeri* burial treatments. Three direct burial and three incremental burial depths. There were three replicates for each burial treatment.72

Table 5.2 Species found in the stonefield, and the percentage of quadrats in which they were found.....74

Table 5.3 Linear regression analysis between the burial treatments and the number of weeks after burial.....77

List of Figures

Chapter 1

Figure 1.1: Mason Bay transgressive dune system on the west coast of Stewart Island, New Zealand. The associated landforms; foredune, deflation surface, parabolic dune (comprised of the trailing arms and depositional lobe), stonefield, wetland and sand sheet.....8

Figure 1.2: Oblique image of the Mason Bay stonefield facing East (landwards) into the study area, taken in June 2014. Note the stony lag deposit, *R. hookeri* var. *hookeri* cushion plants and the *F. spiralis* nabkha.....9

Figure 1.3: Temporal and spatial scales of investigations used in this study.....11

Chapter 2

Figure 2.1: Mason Bay central transgressive dune system. The rectangle is the area analysed for each aerial photograph (area = 675612m^2 , width = 514m, length = 1313 m). The horizontal lines outline the six transects used to measure the movement of stonefield. They are running in the direction of parabolic central axis. The dashed lines represent the outline of the 2015 stonefield.....17

Figure 2.2: Landforms within the Mason Bay central transgressive dune system. a) 2013 satellite image of the central dunes. b) Outline of the landforms in 2013. The long walled parabolic dunes encompass the trailing arms and the depositional lobes.....18

Figure 2.3: Aerial photographs of a section of the Mason Bay dune system, from 1958 to 2013, with an interpretation of the extent of deflation surface (red). In the 1958 image the dashed lines indicate the smaller of the stonefield outlines. In the 2013 image the dashed line is the outline of the 2015 stonefield (surveyed by GPS). The aerial images outlined in black are after the removal *A. arenaria* commenced in 2002. The blue dashed line in the 2011 image outlines the western margin of the spray efforts. The black arrow in the 2011 image indicates where the depositional lobe has extended into the stonefield.....20

Figure 2.4: Outline of the key landforms through the two key stages of the stonefield's evolution. The invasion of *A. arenaria* into the Mason Bay transgressive dune system took place prior to 1958. 2000 saw the maximum level of *A. arenaria* invasion, just prior to start of the eradication programme in 2002. 2013 is the current stonefield, the dashed line indicates the western extent of the eradication programme.....21

Figure 2.5: Mason Bay transgressive dune system in 1929. This photo is looking southwest towards the Earnest Islands. A stonefield is discernable in the center of the image. Source: Stewart Island Museum.....	22
Figure 2.6: Spatial and temporal changes in the morphology of the Mason Bay central stonefield derived from the aerial photographic analysis and GPS data.....	23
Figure 2.7: Oblique images of the parabolic depositional lobes extending into the stonefield. a) Parabolic depositional lobe in 1998, white arrow indicated <i>A. arenaria</i> colonisation (source Mike Hilton). b) <i>F. spiralis</i> has since colonised the leeward side of the depositional lobes, which has slowed but not prevented this erosion parabolic, white arrow indicates <i>F. spiralis</i> colonisation.....	24
Figure 2.8: Plot of the stonefield area (m ²) each year between 1958 and 2013. The solid line is the regression of the stonefield areas prior to <i>A. arenaria</i> removal between 1958 – 2000 (p.value = 0.028, r ² = 0.81, df =2). The dashed line is the regression of the stonefield areas post <i>A. arenaria</i> removal 2002 – 2013 (p.value = 0.131, r ² = 0.92, df =1).....	24
Figure 2.9: Oblique images looking landwards through the stonefield. a) Stonefield in 1998, white arrow indicates <i>A. arenaria</i> nabkha. b) Stonefield in 2015, white arrow indicated <i>F. spiralis</i> nabkha.....	25
Figure 2.10: Linear regression analysis between the stonefield area and the area of the foredune. The solid line is the regression of the stonefield areas and the foredune areas prior to <i>A. arenaria</i> removal between 1978-2000 (r ² = 0.95, df = 2). The dashed line is the regression of the stonefield areas and the foredune areas after <i>A. arenaria</i> removal between 2002-2013 (r ² = 0.24, df = 1).	26

Chapter 3

Figure 3.1: The formation of nabkha around isolated sand binding species such as <i>Ficinia spiralis</i> . a) Arrows show the air flow around vegetation. Sand deposition occurs along the centerline where the opposing vortices meet. b) The depositional form of nabkha in relation to the prevailing wind. Adapted from Hesp, 1981 and Lang <i>et al.</i> , 2013.....	30
Figure 3.2: Ground survey in Mason Bay central stonefield. a) Ground survey in the Mason Bay Central stonefield. b) Area of survey 200m x 50m running (west to east), divided into 100 quadrants of 10m ² . c) Location of five 1m ² quadrats within each 10m ² quadrant. The size of the quadrats has been exaggerated to make them visible in this diagram.....	33

Figure 3.3: a) <i>Ficinia spiralis</i> nabkha. Note the distinct tail in the lee of the <i>F. spiralis</i> . b) Location of the 18 surveyed <i>F. spiralis</i> nabkha within the study site (black rectangle). The prevailing westerly winds blow right to left in the top image and left to right in the lower images.....	34
Figure 3.4: Stratigraphic layers of a soil pit dug downwind of a depositional lobe of a parabolic dune. The distinct roots and darker appearance identify the organic layer. The width of the sand layer above the organic layer was recorded and compared spatially between the soil profiles.....	35
Figure 3.5: The average accretion and erosion (mm) for each 10m ² quadrant (average of the five 1m ² quadrats). The negative values represent sand erosion and the positive values represent accretion. The solid black line is the regression line and the dashed line represents 0. a) Average between June 2014 and February 2015 (df = 97). b) Average between January 2015 and February 2015 (p.value = 0.01, r ² = 0.056, df = 67).....	38
Figure 3.6: Net volume of the <i>F. spiralis</i> nabkha versus distance from the foredune, (r ² of 0.692). The net volume is relative to the total station (located on the North West post of the study site), hence the negative volumes which indicate that the nabkha were at a lower elevation than the total station.....	39
Figure 3.7: Net volume of the <i>F. spiralis</i> nabkha versus distance from the parabolic depositional lobe, (r ² of 0.692, df = 17, SE<0.00).....	40
Figure 3.8: a) <i>F. spiralis</i> nabkha net volume change (m ³) between August 2014 and February 2015. The dashed line equals 0. (r ² = 0.294, df=17, SE<0.00). b) <i>F. spiralis</i> nabkha maximum height change (mm) between August 2014 and February 2015. The dashed line equals 0. (r ² = 0.434, df = 17, SE<0.00).....	41
Figure 3.9 Soil profiles measured in August 2014 in the Mason Bay stonefield study site. The grey tone is the depth of burial (mm) with the dune surface at 0mm. The soil profiles correspond to the pits (black dots) located on the right hand side of each set of profiles.....	43
Figure 3.10: Soil profiles measured in August 2014 in the Mason Bay stonefield study site. The grey tone is the depth of burial (mm) with the dune surface at 0mm. The soil profiles numbers correspond with the number and location of each soil pit (black dot).....	44
Figure 3.11: Wind roses for the South West Cape Weather station, Stewart Island. a) Wind regime during the study period (May 2014 – April 2015). b) Wind regime during the period 1991 – 2012.....	45

Chapter 4

Figure 4.1: June 2011 till March 2014 wind record from the Mason Bay foredune anemometer (green dot in Figure 4.2).....50

Figure 4.2: The anemometer layout in the stonefield study site. At the seaward (black dot) and landward (red dot) margin four anemometers were erected on a vertical mast. The red rectangle is the reoriented sediment budget plot and the black rectangle is the original study area.....52

Figure 4.3: a) Fixed sand traps (without sand bags). b) Wind anemometer mast. c) Swing traps with bags.....53

Figure 4.4: The anemometer and sand trap layout. a) Layout of fixed and swing sand traps, and anemometer mast. The layout is repeated at the landward and seaward edge of the study site, facing west. b) The configuration of fixed traps at 40 and 20cm from the ground. c) Configuration of swing traps at 46, 26, 16, 6cm from the ground. d) Configuration of the anemometers on the mast 20, 40, 80, 160cm.....54

Figure 4.5: The two profiles to be extracted from the digital terrain model (DTM). The first is through the center of the study site (black dashed line through the black rectangle), the second is between the anemometer masts (red line through the red rectangle).....56

Figure 4.6: Summary vector diagram of the average wind direction for the August (blue arrows N=12) and March (black arrows, N=5) study periods at each of the four anemometer locations.....59

Figure 4.7: Comparisons of wind direction (a) and wind speed (b) between the landward and seaward stonefield, regional (Vaisala) and foredune anemometers. Each represents a three to five minute section of the wind record when either the regional or foredune anemometers were at a constant direction (17, three to five minute sections were analysed). The wind events were recorded in August 2014 (N=12) and March 2015 (N=5).....60

Figure 4.8: Regression analysis of wind direction ($^{\circ}$) at the landward and seaward margins of the study area for 17 trials ($r^2 = 0.969$, $df=15$).....61

Figure 4.9: Regression analysis of wind speed (m/s) at the landward and seaward margins of the study area for 17 trials ($r^2 = 0.941$, $df=15$).....61

Figure 4.10: Digital terrain model of the study areas in the stonefield. The dashed rectangle is the outline of the main study site. The solid rectangle is the outline of the sediment budget plot. The white dots are the locations of the landward and seaward anemometer masts. The coordinate system is in meters.....62

Figure 4.11: Cross section through the short term sedimentation study area heading eastwards. The intersecting lines indicate the start and finish of the study area.....63

Figure 4.12: Cross section through the sediment budget plot heading landwards. The intersecting lines outline the start and finish of the sediment budget site.....63

Figure 4.13: Sand drift rose calculated via the Fryberger model (Eq. (1)), with wind values from the Mason Bay foredune anemometer between 2011 and 2014. The rose represents the Drift Potential (DP) for 16 equal compass directions. The bold line indicates the Resultant Drift Direction (RDD) and the Resultant Drift Potential (RDP). The aerial photograph is from 2013 Google Earth image. The black rectangle represents the study area and the red rectangle represents the outline area in which the sediment budget analysis was carried out.....64

Chapter 5

Figure 5.1: Changes in temperature, moisture, bulk density, organic matter (OM) and other environmental factors at different burial depths (adapted from Maun, 1998 and Maun, 2009).....68

Figure 5.2: a) *R. hookeri* species from Moa nurseries (Dunedin). b) *R. hookeri* var. *hookeri* found in the Mason Bay stonefield. c) *R. hookeri* var. *hookeri* plant in the Mason Bay stonefield.....73

Figure 5.3: Standardised major axis regression between the log transformed average sedimentation over nine months (mm) and average *R. hookeri* var. *hookeri* surface area per 10m² (cm²) ($r^2 = 0.01$, $df = 67$).....75

Figure 5.4: Standardised major axis regression between the log transformed average sedimentation over nine months (mm) and average *F. spiralis* surface area per 10m² (cm²) ($r^2 = 0.001$, $df = 39$, $p\text{-value} < 0.05$).....76

Figure 5.5: Burial trial after two weeks of incremental burial, at a depth of 1.25mm per week.....77

Figure 5.6: Average number of stems visible at the end of each week after burial. Direct burial is represented by a diamond, and the incremental burial is represented by a square. a) 20 mm, b) 10mm, c) 5mm. N=3 plants per burial treatment.78

Figure 5.7: Vertical growth of individual plants in treatments three months after the start of burial treatments. The dashed lines indicate treatment burial depth, therefore growth above this line is growth above the sand surface. X indicates plants that died. The control had no sand applied, but was exposed to the same climatic conditions. N=3 plants per burial treatment. There was no statistical difference between the treatments.....79

Chapter 6

Figure 6.1: Oblique views of the parabolic depositional lobes extending into the stonefield. a) parabolic depositional lobe in 1998, white arrow indicated *A. arenaria* colonisation (source Mike Hilton). b) *F. spiralis* has since colonised the leeward side of the depositional lobes, which has slowed but not prevented this erosion parabolic, white arrow indicates *F. spiralis* colonisation.....87

Figure 6.2: Oblique images looking landwards through the stonefield. A) Image A shows the coarse texture of the central stonefield in 1998. B) The same location in 2015. Notice the similar surface texture approximately five years after the initial destabilisation efforts bega.....88

Chapter 1

Introduction

1.1 Overview

Coastal dunes lie at the interface between the marine and terrestrial environment, providing key habitats for a unique array of flora and fauna (Hesp, 2013). Transgressive dunes are actively migrating sand deposits situated over vegetated to semi-vegetated terrain (Hesp and Thom, 1990). The term encompasses a range of landforms, including blowouts, parabolic dunes, transgressive dune fields and deflation surfaces. They generally develop through reworking of pre-existing dune deposits, such as foredunes or parabolic dunes and are characterised by mobile substrate and frequent disturbance regimes of burial and erosion (Hesp and Thom, 1990). The cycles of erosion and stabilisation generated by the geomorphic processes in transgressive dunes provide environmental conditions and gradients required by a suite of different ecological communities (Grootjans *et al.*, 2013; Martinez *et al.*, 2013; Rhind *et al.*, 2013; Nordstrom *et al.*, 2000). The ecological communities that persist within these dynamic environments are unique in that they have adapted to adverse conditions like sand burial, erosion, salt and high solar radiation (Maun, 2009).

Historically management of transgressive dunes has been concerned with erosion control (Klijn, 1990; Van der Meulen *et al.*, 1989). Dune systems were stabilised, usually through the deliberate planting of dune vegetation to halt the natural geomorphic processes of aeolian sand transport and dune migration. The introduction of sand dune stabilising plants, commonly *Ammophila arenaria*, have suppressed aeolian processes, leading to a loss in landform complexity and dynamics (Arens *et al.*, 2013a; Hilton, 2006; Hilton *et al.*, 2005; Wiedemann and Pickart, 1996).

Over the last three decades awareness of the importance of dune mobility for coastal biodiversity has grown (Walker *et al.*, 2013; Hilton *et al.*, 2005; Wiedemann and Pickart, 1996; Van der Meulen *et al.*, 1989), and consequently, dune management today is largely concerned with restoring aeolian dynamics in order to restore populations of specific species or habitats (Arens *et al.*, 2013b). The dynamics of aeolian processes create the erosional and dispositional disturbances required to maintain an array of coastal dune habitats (Konlechner *et al.*, 2014; Walker *et al.*, 2013). The reduction in landform complexity following dune stabilisation has often lead to the following ecological impacts: loss of pioneer species, decreased species richness and decreased species diversity (Konlechner *et al.*, 2014; Arens *et al.*, 2013b; Walker *et al.*, 2013). Specifically *A. arenaria* stabilised dunes have caused the decline in early successional species (Arens *et al.*, 2013b; Maun, 2009; Wiedemann and Pickart, 1996), and a corresponding loss of ecosystem function and resilience (Nordstrom, 2008; Grootjans *et al.*, 2002).

The management of transgressive dunes to restore aeolian dynamics is termed ‘dynamic restoration’ (Nordstrom, 2008, Arens and Geelen, 2006). Dynamic restoration aims to re-establish the natural geomorphic processes, with the goal of restoring the landform complexity and therein protecting the diversity of coastal dune ecosystems (Table 1.1) (Hesp and Hilton, 2013; Martinez *et al.*, 2013; Walker *et al.*, 2013). Key geomorphic processes are the aeolian dynamics and dune mobility, often restored through the deliberate removal of vegetation by either manual or chemical means at a range of scales, i.e., from a few square meters to hectares (Konlechner *et al.*, 2014; Arens *et al.*, 2013b). Vegetation removal exposes the dune forms to aeolian erosion and subsequent deposition allowing the dune system to equilibrate to a hopefully more natural state. If dynamic restoration is successful, the reinstated aeolian dynamics will contribute to protecting or recreating landscape complexity, thus potentially supporting the range of successional communities naturally occurring in a coastal dune system. Once a range of successional communities have re-established native biodiversity is likely to be greater, facilitating a recovery of coastal dune ecosystem functionality (Provoost *et al.*, 2011).

There has been little consideration of the possible adverse effects of short term dune system responses following dynamic restoration. Hesp and Hilton (2013) indicated that release of foredunes from unnatural stabilisation might adversely affect downwind ecosystems. It has been predicted that after the remobilisation of dune forms there will be increased sand

deposition downwind (Arens *et al.*, 2013a; Eamer *et al.*, 2013). Ecosystems that are at risk of being adversely affected in the short term are pre-existing native habitats such as deflation surface communities and wetlands (Hesp and Hilton, 2013; Grootjans *et al.*, 2002). These are often fragmented or uncommon habitats of threatened species. A sudden substantial increase in sand deposition may lead to the short term or permanent loss of these habitats and consequently the biodiversity of the transgressive dune system. Sand mobility represents a major environmental constraint during early succession. The colonisation and succession in dunes systems is limited by the seed dispersal and colonisation abilities of plant species (Lichter, 2000). Dynamic restoration projects expect that over time, processes of plant dispersal and colonisation will result in an increasingly ‘natural’ distribution of plant species (Provoost *et al.*, 2011).

Dynamic restoration projects provide essential research opportunities into understanding the morphological and vegetative responses of coastal transgressive dunes after destabilisation (Arens *et al.*, 2013b; Walker *et al.*, 2103). Recent studies, such as Eamer *et al.*, (2013), have focused on foredune growth and decay and local downwind sand drift. Few have considered the effect of an increased sand budget on the habitats downwind of the foredune environment (Hesp and Hilton, 2013). This project considers the effect of a dynamic dune restoration at Mason Bay, Southern New Zealand on the downwind plant communities. In doing so, this may provide valuable information to local authorities regarding the costs and benefits of dynamic dune restoration as a result of invasive species removal, particularly with regard to its effectiveness as a tool for preserving and restoring coastal transgressive dune systems.

Table 1.1: Summary of dynamic restoration programmes around the world using destabilisation and their restoration goals. In alphabetical order of countries

Author	Country	Cause of stabilisation	Restoration goals	Restoration methods
Sturgess and Atkinson., 1993	Britain	Pine plantation	Restoring dune mobility and increasing biodiversity	<ul style="list-style-type: none"> • Mechanical removal of vegetation and topsoil • Disturbance of dunes on the windward side of stabilised areas to mobilise sand and seeds.
Bar, 2013	Israel	Natural (low wind velocity) Little traditional human interference	Restoring dune mobility and increasing biodiversity	<ul style="list-style-type: none"> • Beach nourishment • Mechanical shrub and topsoil removal • Deep ploughing
Arens <i>et al.</i> , 2013a	Netherlands	Erosion control	Restoring dune mobility and increasing biodiversity	<ul style="list-style-type: none"> • Mechanical vegetation and topsoil removal
Konlechner <i>et al.</i> , 2014	New Zealand	Plant invasion	Restoring dune mobility and increasing biodiversity	<ul style="list-style-type: none"> • Removal of invasive species (herbicides) • Planting natives
Pickart, 2013	USA, California	Plant invasion	Restoring biotic and abiotic processes	<ul style="list-style-type: none"> • Removal of invasive species (manual digging and pulling) • Planting natives
Rhind <i>et al.</i> , 2013	Wales	Loss of herbivores	Restoring dune mobility and increasing biodiversity	<ul style="list-style-type: none"> • Grazing • Mechanical removal of vegetation and top soil

1.2 Dynamic restoration, Mason Bay, Stewart Island

Mason Bay is situated on the west coast of Stewart Island, New Zealand (46°55'S, 167°47'E) (Figure 1. 1). The high sediment availability and prevailing strong onshore winds in Mason Bay has created a large transgressive dune system (Hilton *et al.*, 2005). The bay runs for approximately 13 km alongshore and the dune system extends 3.5 km inland, with little human interference or modification when compared to dune systems on mainland New Zealand. The transgressive dune system is one of the most physically diverse and ecologically important dune systems left in New Zealand (Johnson, 1992).

The transgressive dunes at Mason Bay have stabilised since 1958 (Hilton *et al.*, 2005), due to the deliberate introduction and subsequent invasion of the non-native dune-binder, *A. arenaria*. *A. arenaria* was first planted at the southern end of the dunes near Kilbride Homestead in the early 1930s, and later at the Island Hill Homestead in the 1960s, to prevent sand encroachment on agricultural land (Hilton *et al.*, 2005). Since the initial planting and the establishment of marine-dispersed rhizome, *A. arenaria* has colonised the foredune environment and close to 60% of the hinterland between Martins Creek and Duck Creek (Figure 1.1).

Prior to *A. arenaria* colonisation the Mason Bay foredune comprised of isolated high shadow dunes formed around the native sand binding sedge *Ficinia spiralis* (Hart *et al.*, 2012). The irregularity of the foredune allowed for the formation of blowouts through the foredune and a sediment exchange into the backdune environment. The rapid *A. arenaria* colonisation between 1958 and 1978, however, saw the merging of *A. arenaria* shadow dunes as the vegetation cover increased (Hilton *et al.*, 2005). This displaced native species such as *Ficinia spiralis* and *Euphorbia glauca* from the foredune (Hilton *et al.*, 2005; Cockayne, 1909a). Between 1978 and 2001 the foredune prograded seaward and accreted, forming a large, stable, densely vegetated, continuous alongshore foredune (Hart *et al.*, 2012). The growth of the continuous foredune has meant that sand transport through the parabolic dunes was inhibited, causing the present parabolic dunes to migrate landwards creating long walls and a large deflation surface (Hart *et al.*, 2012; Hilton *et al.*, 2005). *A. arenaria* invasion resulted in the loss of dune dynamics essential to maintaining the integrity and resilience of the transgressive dune ecosystem.

Today the transgressive dune system is comprised of primary and secondary dune forms, which combined run three km's inland (Figure 1.1). The foredune is 8-15m high, 100-150m wide and

continuous alongshore. A series of long walled U shaped parabolic dunes lie to the east, and behind them is a broad gently sloping deflation zone known as the 'stonefield' (Hilton *et al.*, 2005). These various landforms support an array of plant species: the native sand binders *F. spiralis* and *Poa billardiarei* but also non-sand binding plant such as *Coprosma acerosa* and the native cushion plant *Raoulia hookeri* var. *hookeri* in the deflation zones (Hilton *et al.*, 2005; Cockayne, 1909a).

The Department of Conservation (DOC) started a dynamic restoration effort at Mason Bay in 2002, which aims to restore and safeguard the geomorphic processes of aeolian sand transport and dune mobility that underpin the natural character of the pre-*A. arenaria* system at Mason Bay through the eradication of *A. arenaria* (Hilton and Konlechner, 2010). *A. arenaria* is removed by applying a grass-specific herbicide via knapsacks, argo and helicopter. Between 2002 and 2005 the goals of the initial restoration effort were largely focused on removing small isolated patches of *A. arenaria* scattered throughout the central dune system. Eradication efforts post 2005 were concerned with destabilisation of landforms. Initial efforts were concentrated on the parabolic dunes and, since 2010, the foredune (Hilton, M., pers. Comm. 2014; Hilton and Konlechner, 2010).

The rhizome of the parabolic dunes and foredune is persistent and its breakdown has been a slow process (Hilton and Konlechner, 2010). It is, therefore, timely to consider the impact of sand drift in the deflation environments, because sand is yet to significantly start moving. Hesp and Hilton (2013) predicted that once *A. arenaria* and its rhizome has been removed sand will eventually move into hinterland environments. Of future interest to coastal managers is the effect the foredune and parabolic breakdown will have on the entire dune system. This research will examine the response of hinterland habitats to increased sand released by *A. arenaria* removal in a bid to restore the dynamic potential of the Mason Bay transgressive dune system.

In the Mason Bay transgressive dune system there is a large deflation area called the 'stonefield' which is characterised by a distinct stony lag deposit between the parabolic dunes and the sand sheet (Figure 1. 1 and Figure 1.2). Deflation zones are a common habitat in the lee of *A. arenaria* stabilised dune forms, created as a result of sand starvation (Wiedemann and Pickart, 1996). Deflation surfaces such as dune slacks, ponds, sabkhas (evaporate interdunes) and stonefield, harbor a unique assemblage of flora and fauna (Wiedemann and Pickart, 2004; Carter *et al.*, 1990). These deflation communities play an integral role in the conservation or

restoration of dune ecosystem biodiversity. The stonefield will be used as a case study, as it provides a unique research opportunity into the effects of destabilisation on downwind habitats, as the parabolic dunes have started to erode after *A. arenaria* removal efforts began in 2006. Increased sand accumulation in deflation communities like the stonefield, will have profound physical and ecological changes such as landform changes towards a dune field and shifts in plant species dominance. These changes can be monitored effectively through plant community changes and sand accumulation (Levin, 2006).

The stonefield habitat has been recognised as nationally threatened, as it is home to an array of ‘at-risk’ native plants and an important breeding and foraging site for the endangered New Zealand Dotterel (*Charadrius o. obscurus*) and Banded Dotterel (*Charadrius b. bicinctus*) (Holdaway *et al.*, 2012; Hilton *et al.*, 2005). Key species present in the stonefield habitat include: *Raoulia hookeri* var. *hookeri*, *Gentianella saxosa*, *Coprosma acerosa* (at risk/declining), *Colobanthus muelleri*, *Luzula celata* (at risk/declining), *Pimelea lyallii* (at risk) and the sand binding sedge *F. spiralis* (at risk/ declining) (Hilton *et al.*, 2005). These stonefield plant communities persist in a transient habitat where their final density depends on the stability of the adjacent dunes (Garcia-Mora *et al.*, 1999).

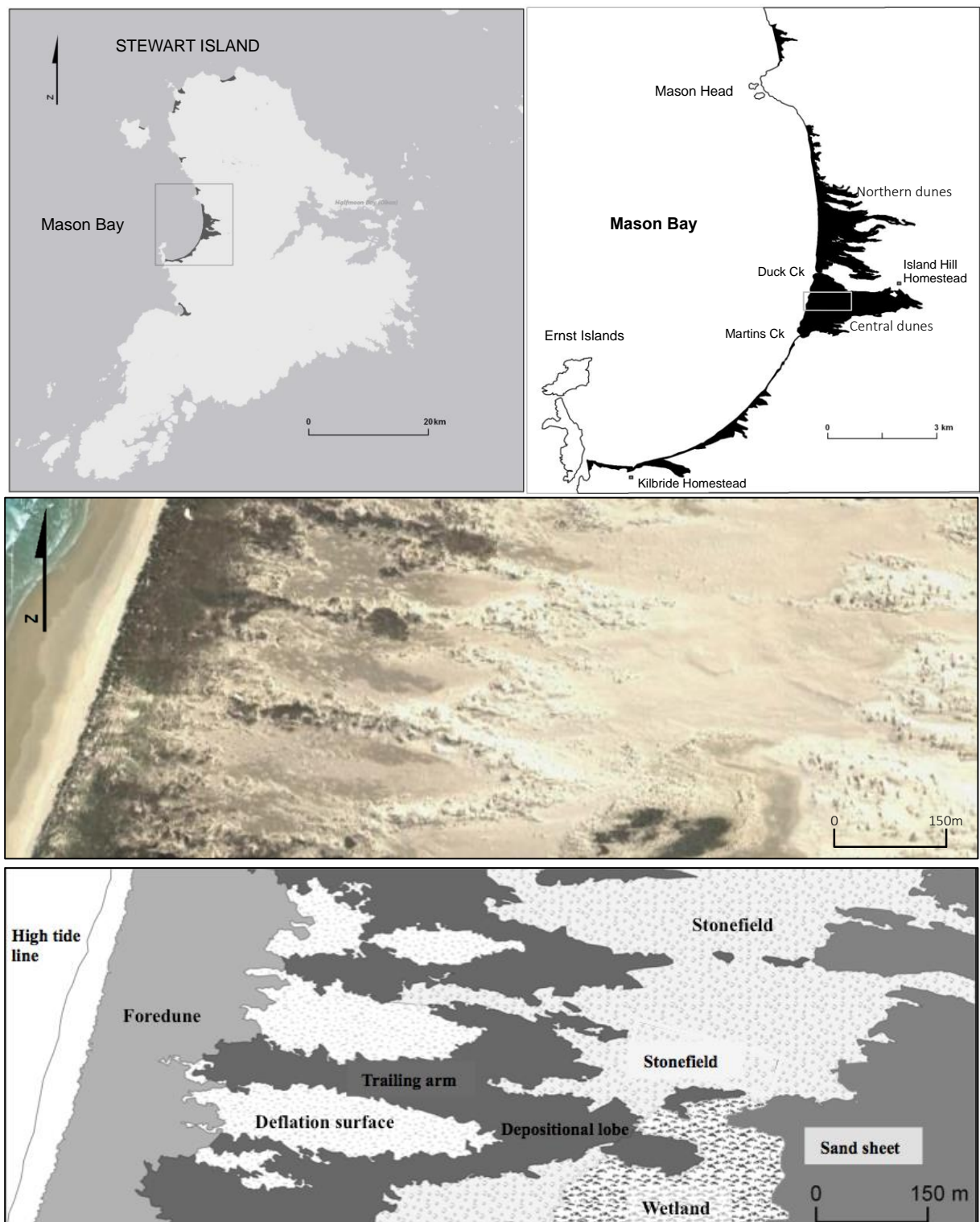


Figure 1.1: Mason Bay transgressive dune system on the west coast of Stewart Island, New Zealand. The associated landforms; foredune, deflation surface, parabolic dune (comprised of the trailing arms and depositional lobe), stonefield, wetland and sand sheet.

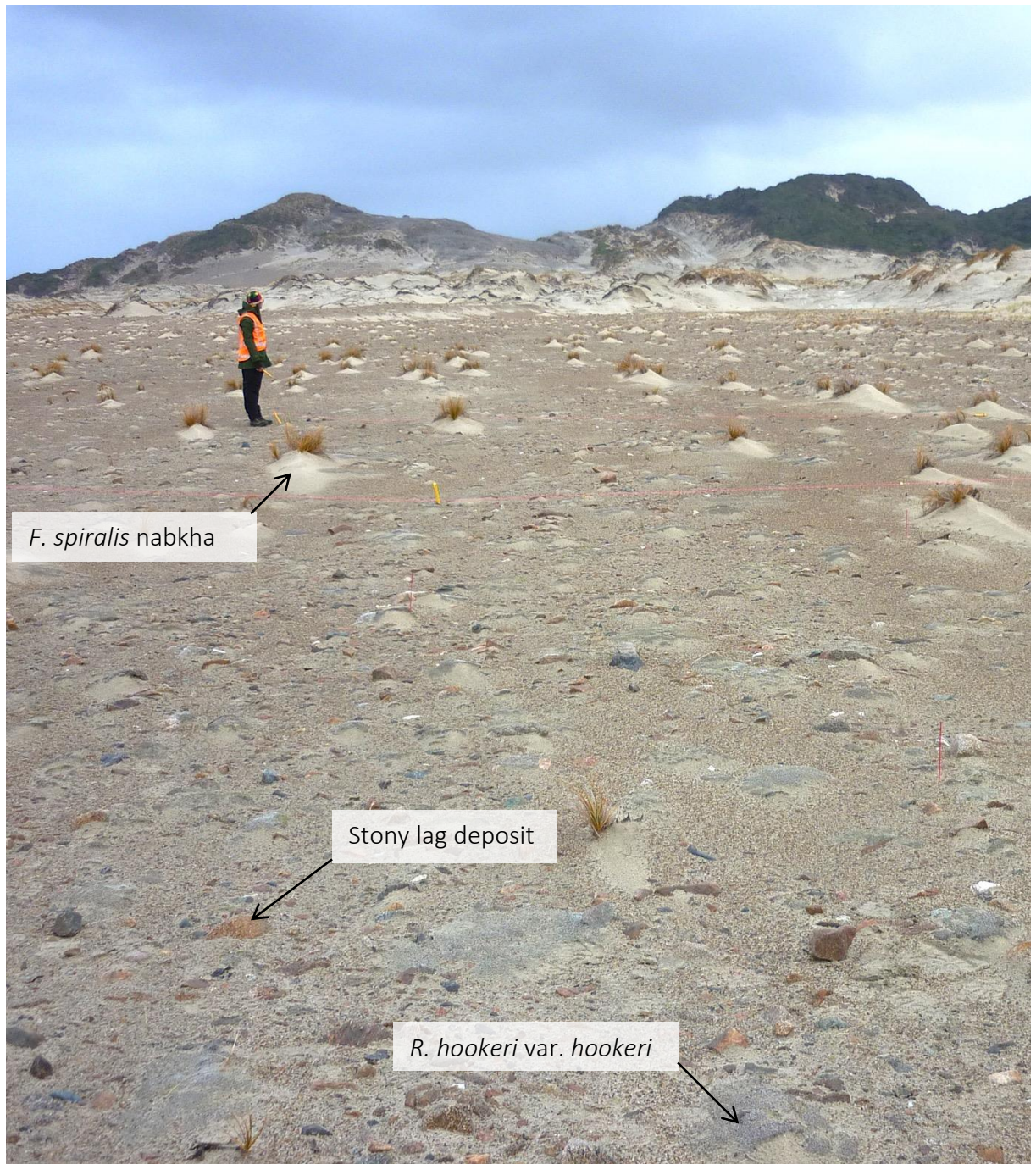


Figure 1.2: Oblique image of the Mason Bay stonefield facing East (landwards) into the study area, taken in June 2014. Note the stony lag deposit, *R. hookeri* var. *hookeri* cushion plants and the *F. spiralis nabkha*.

1.3 Research Objectives

The impact of dynamic dune restoration on downwind habitats needs to be addressed. Mason Bay, Stewart Island, provides a unique opportunity to address this knowledge gap and resides in a well understood and relatively simple dune system that has had little or no human development (Hart *et al.*, 2012; Hilton and Konlechner, 2010). *A. arenaria* invasion at Mason Bay has been well documented by aerial photographs from 1958, (i.e. prior to invasion) to present day, allowing for an in depth study on the development of the stonefield over various temporal and spatial scales (Figure 1.3).

This project aims to predict the response of the dynamic restoration project on the Mason Bay stonefield. Specifically it aims to:

- 1. Describe the historic development of the Mason Bay stonefield and deflation surfaces in relation to *Ammophila arenaria* invasion.**

Previous studies have recorded landform changes in the foredune and parabolic environments associated with *A. arenaria* invasion. Transgressive dune systems are highly connected, therefore, it is reasonable to hypothesise that landform changes upwind of the stonefield may have impacted on the stonefield. The historic development of the Mason Bay dune system may demonstrate the geomorphic coupling between the foredune and hinterland, and increase our understanding of the dynamic nature of the landscape. It may also provide a frame of reference for assessing modern patterns and processes and their implications for the stonefield habitat (over the period of years to decades, Figure 1.3).

- 2. Assess whether sand liberated from recent and ongoing destabilisation is accumulating in the stonefield.**

It is also reasonable to hypothesise that the destabilised parabolic dune forms will cause increased deposition of sand in the stonefield. To establish the validity of this prediction, the sedimentation patterns and processes need to be identified within the stonefield (over the period of hours to months, Figure 1.3). These investigations will identify whether sand accumulation is a future threat to stonefield communities, if so, at what rate and where is this process occurring?

3. To assess the impact of observed sedimentation patterns on native plant communities in the stonefield.

How will changes in patterns of sedimentation affect the native stonefield communities? The biodiversity of the stonefield plant communities are integral to the ecological functioning of the Mason Bay dune system. In order to assess the response of the stonefield communities, their current distribution needs to be identified. The species at risk of increased sand deposition also need to be identified. This will provide an understanding into the future of the stonefield's ecological values.

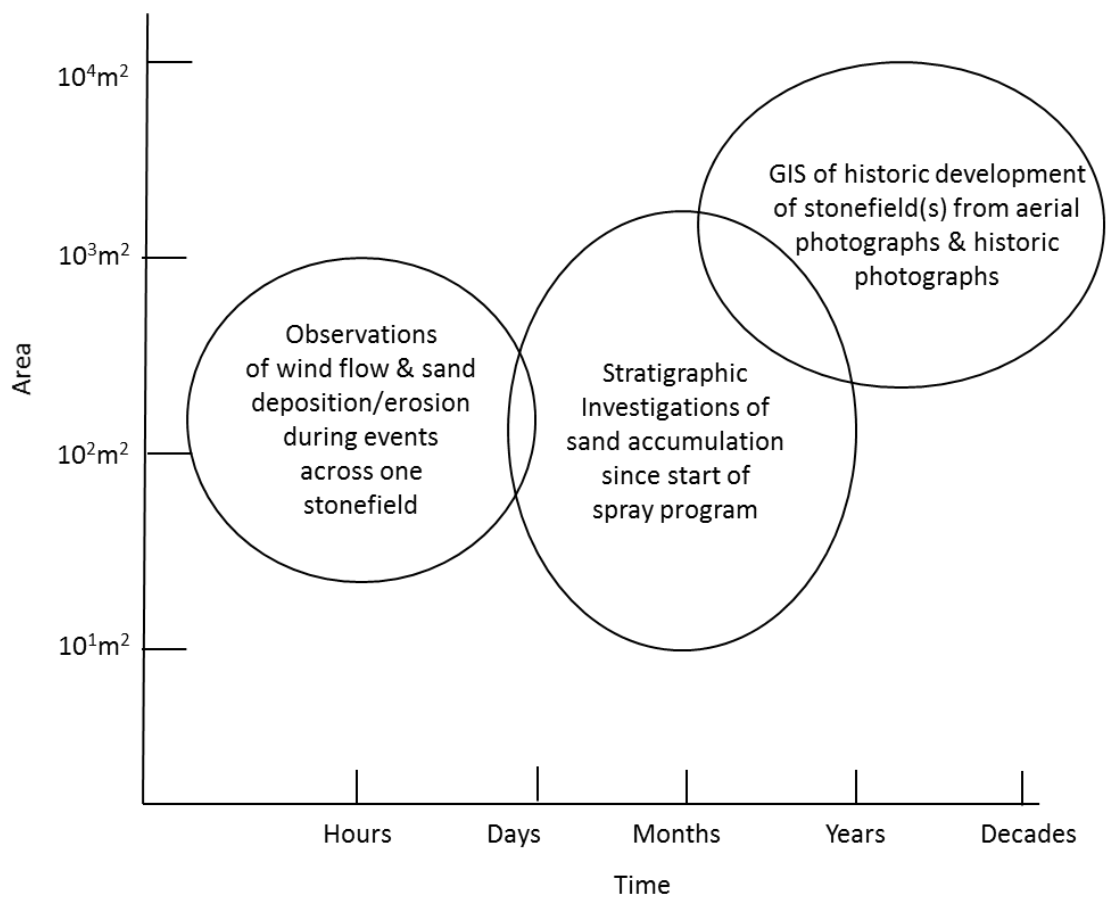


Figure 1.3: Temporal and spatial scales of investigations used in this study.

1.4 Thesis structure

Chapter One has provided an overview of the context of this study through a general literature review. Dynamic restoration has become increasingly popular in coastal dune management as coastal managers aim to protect the biodiversity of coastal dunes systems. Dynamic restoration often involves the destabilisation of coastal dune forms through devegetation. The implications of these destabilisation efforts have, however, not been considered for downwind ecosystems, which may be buried by increased sedimentation. Mason Bay is the world's largest *A. arenaria* eradication programme and therefore provides the opportunity to study the effects of foredune destabilisation on the downwind deflation surface known as the stonefield and associated plant communities.

Chapter Two describes the development of the stonefield in response to the invasion of *A. arenaria* and its subsequent removal. A brief review of the literature focuses on *A. arenaria* associated landform changes and the geomorphic interlinking in transgressive dune systems. The landforms from a series of eight aerial photographs beginning in 1958, will be mapped in GIS with a focus on the changes in shape and area of the stonefield. In reference to the aerial photographs, the landform changes will be discussed in association with the invasion of *A. arenaria* and its removal in 2002.

Chapter Three establishes whether sand is accumulating in the stonefield and investigates the possible patterns and processes occurring in the stonefield. Sand accumulation is measured over the period of months using a series of erosion pins and volume changes in *F. spiralis* nabkha. This chapter investigates whether the upwind destabilisation efforts are causing an increase in sand accumulation in the stonefield between June 2014 and March 2015.

Chapter Four measures the importance of event-scale sedimentation patterns in the stonefield. A sediment budget analysis is used to determine the proportion of sand deposited in the stonefield during wind events. Wind speed and direction is measured on the seaward and landward margins to analyse whether there is a velocity gradient occurring within the stonefield. This chapter aims to support the recorded sedimentation processes measured in Chapter Three.

Chapter Five analyses the distribution of two native stonefield plant communities (sand binding species and non-sand binding species) and their relationship to the observed sedimentation patterns. An experiment on the effect of sand accumulation will be carried out on the native cushion species *Raoulia hookeri*, related to the subspecies found in the stonefield to understand the tolerance levels of this ‘at risk’ species. The aim of this chapter is to assess the implications of the observed and possible increased, sedimentation patterns on the native stonefield plant communities.

Chapter Six is a summary of the main findings and conclusions of the study. Future study directions will be outlined and discussed in relation to the main findings.

Chapter 2

Evolution of the Mason Bay stonefield in conjunction with the invasion and recent removal of *Ammophila arenaria*

2.1 Introduction

Coastal transgressive dunes are dynamic landforms which become reshaped by geomorphological and ecological processes (Hesp, 2013; Doing, 1985). They evolve primarily as a result of varying sediment supply, climate such as wind and precipitation and the effectiveness of sand binding vegetation (Hesp, 2013; Carter *et al.*, 1990; Kiljin, 1990). These symbiotic relationships and their feedbacks are responsible for the formation of various landforms that are characteristic of transgressive dune systems. Examples of characteristic landforms include: foredunes, blowouts, parabolic dunes, deflation surfaces and sand sheets (Luna *et al.*, 2011; Tsoar and Blumberg, 2002; Hesp and Thom, 1990).

Transgressive dune systems are highly connected. Landforms in transgressive dune systems can be seen to influence the development of downwind landforms (Hesp and Thom, 1990). For example, coastal transgressive dunes may change the near surface wind velocity (such as topographic acceleration) and direction, thus affecting sediment transport downwind (Anderson and Walker, 2006). The foredune is seen as one of the most influential landforms that may exert significant control over the evolution of a transgressive dune system (Hesp, 2013). Blowouts in a foredune developing into new parabolic dunes immediately downwind are an example of this influence (Hesp, 2002; Tsoar and Blumberg, 2002). Carter *et al.*, (1990) attributed the rapid growth of deflation surfaces on the Oregon coast to the elimination of sediment input from the beach due to the high linear foredunes. Ultimately, the evolution and future development of transgressive dunes is linked to the landforms that can affect the sediment supply and wind energy.

A number of studies have observed a link between *Ammophila arenaria* invasion and significant landform changes in transgressive dune systems (Hart *et al.*, 2012; Wiedemann and Pickart, 1996; Arens *et al.*, 1995). *A. arenaria*, is able to thrive under high rates of sand burial. Under such conditions vertical growth and biomass proceed unimpeded, resulting in increased sand capture and dune elevation (Zarnetske *et al.*, 2012). One of the most significant impacts of *A. arenaria* invasion appears to be the loss of connectivity in transgressive dunes. This is where high continuous foredunes have developed, restricting the sediment exchange between the beach and the backdune systems (Wiedemann and Pickart, 1996). This loss of connectivity can be attributed to the development of deflation surfaces, elongation of parabolic dunes and dune stabilisation (Hart *et al.*, 2012; Carter *et al.*, 1990). The reduced sediment supply has in turn reduced the natural dynamic of sand burial and erosion leading to stabilisation and loss of biodiversity in dune systems globally (Arens *et al.*, 2013a; Maun, 2009; Wiedemann and Pickart, 1996). It appears, however, that few studies have investigated the impact of *A. arenaria* on the transgressive dune systems that lie downwind (Hart *et al.*, 2012; Wiedemann and Pickart, 1996).

A. arenaria eradication programmes have begun in a few transgressive dune systems in an effort to protect or re-establish the dynamics and the mobility of transgressive dunes (Konlechner *et al.*, 2014; Arens *et al.*, 2013b; Pickart, 2013; Hilton *et al.*, 2009). Hesp and Hilton (2013) predicted that destabilisation of dune landforms would create increased sediment inputs into downwind environments. Efforts to date, suggest that any remobilised landforms could threaten downwind landforms via sand inundation in the lee of parabolic dunes, creating an advancing front, or during strong wind events (Arens *et al.*, 2013b; Arens *et al.*, 2004). Strong wind events carry finer grained sediments up to 200 m downwind of a parabolic dune crest (Arens *et al.*, 2004). In the Doughboy Bay dune system, on Stewart Island, devegetated foredunes have started to erode, increasing downwind sand supply and transgressive dune development. Increased sedimentation is accumulating downwind creating an advancing slip face that is encroaching into the hinterland environment (Konlechner *et al.*, 2014; Hesp and Hilton, 2013).

Previous research (Hart *et al.*, 2012; Peterson *et al.*, 2011) argues that the development of the foredune and parabolic dunes at Mason Bay resulted from the invasion of *A. arenaria* in the early 1950s. A large deflation surface has formed landward of these features, generally known as the 'stonefield'. This study therefore hypothesised that the stonefield's evolution has been indirectly influenced by the invasion of *A. arenaria*. This chapter describes the historic

development of the Mason Bay stonefield in relation to the invasion and subsequent removal of *A. arenaria* through the following research questions:

- i) How has the stonefield evolved since the invasion of *A. arenaria* in 1958?
- ii) Have changes in the stonefield shape and location occurred since the removal of *A. arenaria* began in 2002?

2.2 Method

2.2.1 Aerial photography

Aerial photographs help to describe the dynamics of dune systems on a broader systems scale (Hernández-Calvento *et al.*, 2014; Hart *et al.*, 2012; Hayes and Kirkpatrick, 2012; Tsoar and Blumberg, 2002). The aerial photographic record of the Mason Bay transgressive dune system started in 1958, soon after *A. arenaria* colonisation. Eight aerial images between 1958 and 2013 were analysed to determine the evolution of the stonefield (Table 2.1).

Table 2.1: Aerial photographs and satellite images were sourced from New Zealand Aerial Mapping (NZAM), private collections (PC) and Google Earth (GE).

Date		Scale	Colour	Resolution	Quality	Source	Run Number
Dec	1958	1:3000	B & W	Grainy	Poor	NZAM	C/10 1054
Feb	1978	1:3000	Colour	Fine	Good	NZAM	K/7 5244
	1989	1:3000	Colour	Fine	Good	PC	-
	1998	1:3000	Colour	Fine	Good	PC	-
	2000	1:4000	Colour	Fine	Excellent	PC	-
Jul	2002	1:4000	Colour	Fine	Excellent	GE	-
	2011	1:4000	Colour	Fine	Good	GE	-
	2013	1:4000	Colour	Fine	Excellent	GE	-

The images were orthorectified in the GIS programme ArcMap 10.2. A portion of the Mason Bay transgressive dune system was mapped (refer to grey rectangle in Figure 2.1), for two main reasons: (i) it encompassed the central stonefield area from the beach through to the hinterland dune environment, and (ii) it extended to the limits of the aerial photographs available (Figure 2.1). The outline of the central stonefield and the foredune was mapped for each of the images,

starting with the 2013 image and working sequentially backwards. The stonefield lies to the east of the parabolic depositional lobes and was characterised by the rough texture of the stony lag deposit (Figure 2.2).

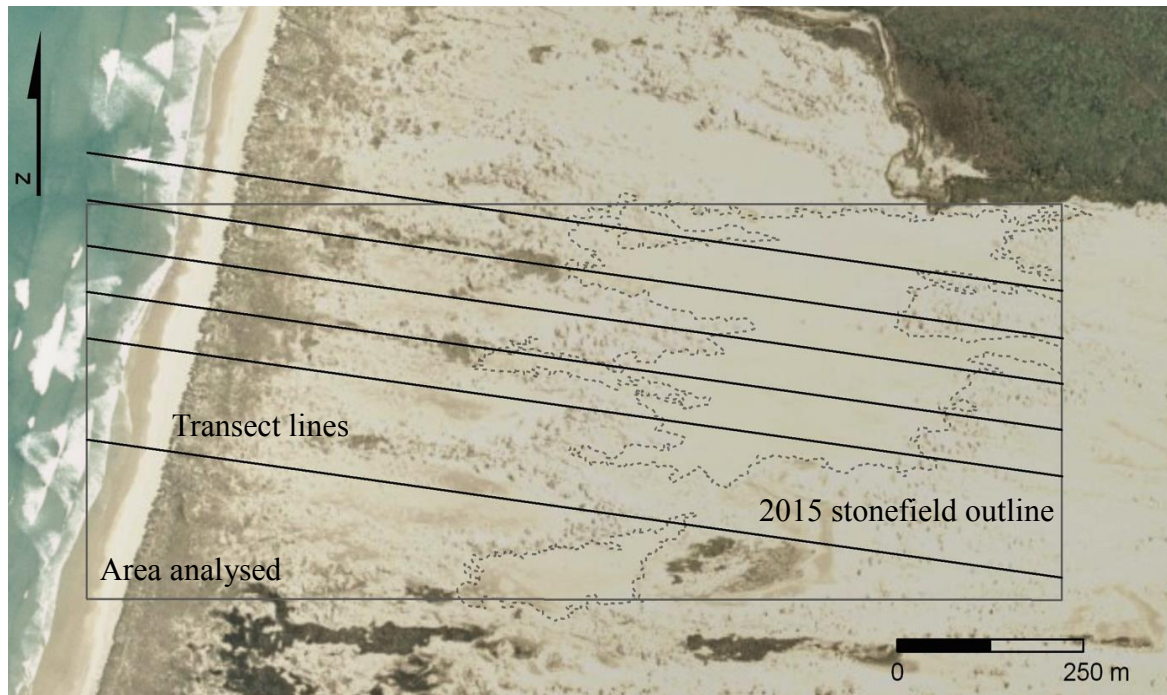


Figure 2.1: Mason Bay central transgressive dune system. The rectangle is the area analysed for each aerial photograph (area = 675612m^2 , width = 514m, length = 1313 m). The horizontal lines outline the six transects used to measure the movement of stonefield. They are running in the direction of parabolic central axis. The dashed lines represent the outline of the 2015 stonefield.

2.2.2 Mapping the current stonefield

Changes between the most recent aerial image (2013) and the current (2015) stonefield were measured by a GPS survey. A hand-held Garmin 62CS GPS unit was used, with a horizontal accuracy of $\pm 3\text{m}$. The 2015 stonefield outline was mapped over the 2013 aerial image, providing a spatial reference for assurance that aerial images were correctly orthorectified. The 2015 stonefield outline was also used to ensure the central stonefield landforms delineated in the 2013 aerial photographs were spatially referenced correctly.

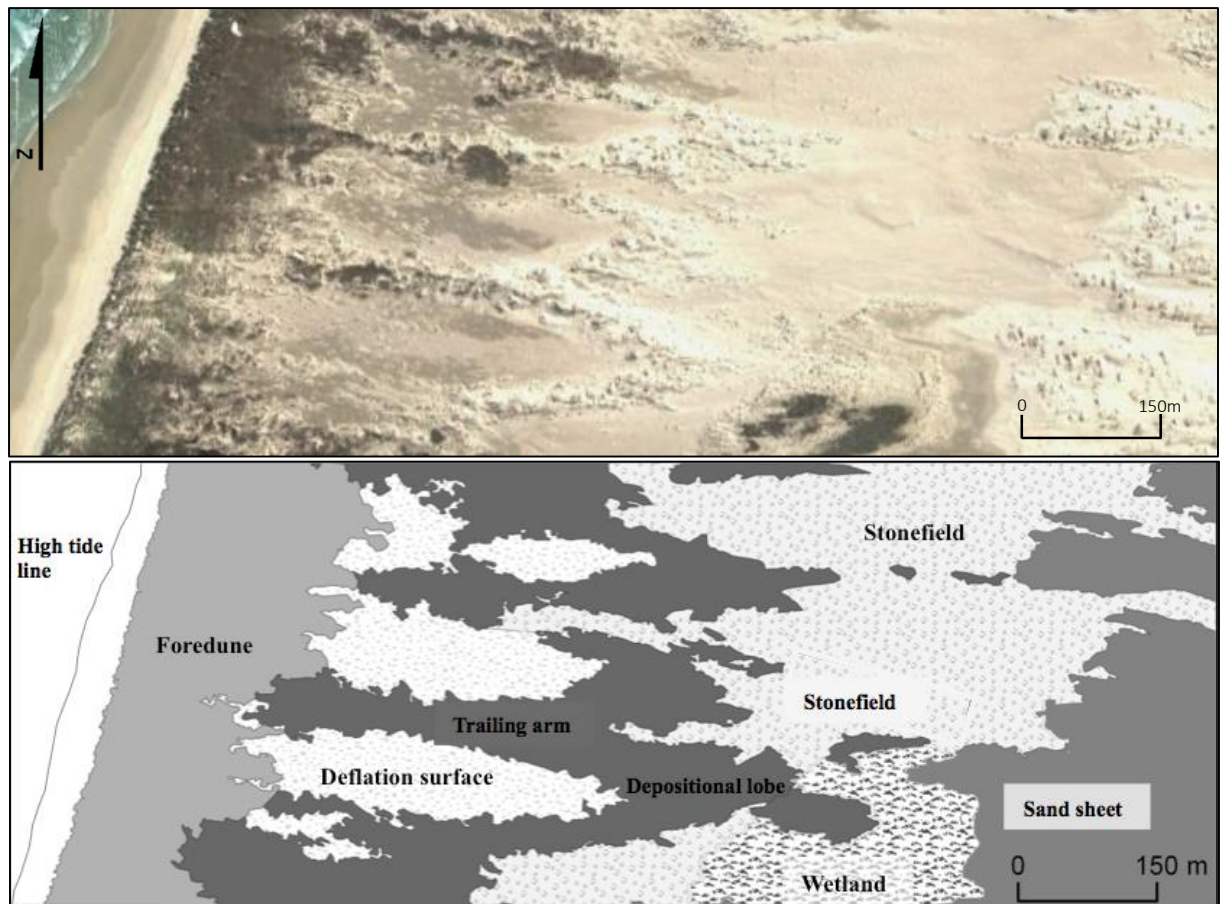


Figure 2.2: Landforms within the Mason Bay central transgressive dune system. a) 2013 satellite image of the central dunes. b) Outline of the landforms in 2013. The long walled parabolic dunes encompass the trailing arms and the depositional lobes.

2.2.3 Limitations of aerial photography

The delineation of landforms from aerial photographs can have limitations, such as observer bias (Hugenholtz *et al.*, 2012) and decay in image reliability over the years (Swetnam *et al.*, 1999). Older oblique images were used to extend the photographic record from as early as 1929. Aerial photographic records were limited which often resulted in large time gaps, particularly between the older photographs i.e., 20 years between 1958 -1978.

2.2.4 Analysis of stonefield land form changes

The following quantitative measurements were taken for each aerial photograph comparison: area (m^2) of the entire stonefield landform, movement (m) and direction ($^\circ$) of the entire stonefield landform, and the movement of the stonefield's landward and seaward margins (m and $^\circ$). Distance and direction components for the seaward and landward margins of the

stonefield were calculated using six transects randomly located through the central dunes (Figure 2.2). Transects were aligned to the central axis of the parabolic dunes (097°) as these indicate the pattern of sedimentation and dune form migration in the Mason Bay central dune complex (Hart *et al.*, 2012). Similarly, the movement and direction of the entire stonefield landform was calculated from the centroid point which represents the geometrically calculated 2D centre of the stonefield (calculations made in ArcMap 10.2). Hart *et al.*, (2012) observed that the elongation of the parabolic dunes and growth of the foredune occurred simultaneously. Therefore the relationship between the growth of the foredune and the growth of the stonefield was analysed using a linear regression analysis between in the statistical program R.

2.3 Results

In 1958 the foredune environment comprised of scattered nabkha described by Cockayne (1909b) as “haystack like dunes”, probably formed in conjunction with *Ficinia spiralis*. The present day foredune is seen to be a largely *A. arenaria* vegetated, continuous feature up to 15m high situated between the beach and parabolic dunes. Running eastwards, inland from the foredune the long walled parabolic dunes were mapped. The parabolic deflation surfaces were distinguishable from the central stonefield by their location in the centre of the parabolic dunes. The sand sheet was defined as the large sand sheet like form, on the landward margin of the stonefield.

2.3.1 Stonefield evolution before *A. arenaria* control (between 1958 and 2000)

The stonefield was present in 1958 (Figure 2.3a). At this time it had a texture similar to the 2011 and 2013 aerial photographs. Two plausible stonefield outlines were delineated in the 1958 aerial photograph, the larger of which was adopted for the purposes of this study (refer to the solid and dashed lines indicated in Figure 2.3a). The stonefield in 1958 was a continuous feature running through the Mason Bay transgressive dune field. The stonefield was located closer to the sea, than today (Figure 2.4). No ground images were available for 1958, however the 1929 oblique image (Figure 2.5), looking south across the Mason Bay transgressive dunes, appears to show a stonefield closer to the sea than the current stonefield. Since 1958 that stonefield has moved progressively inland, as can be seen by the movement of the stonefield centre (Figure 2.6b).

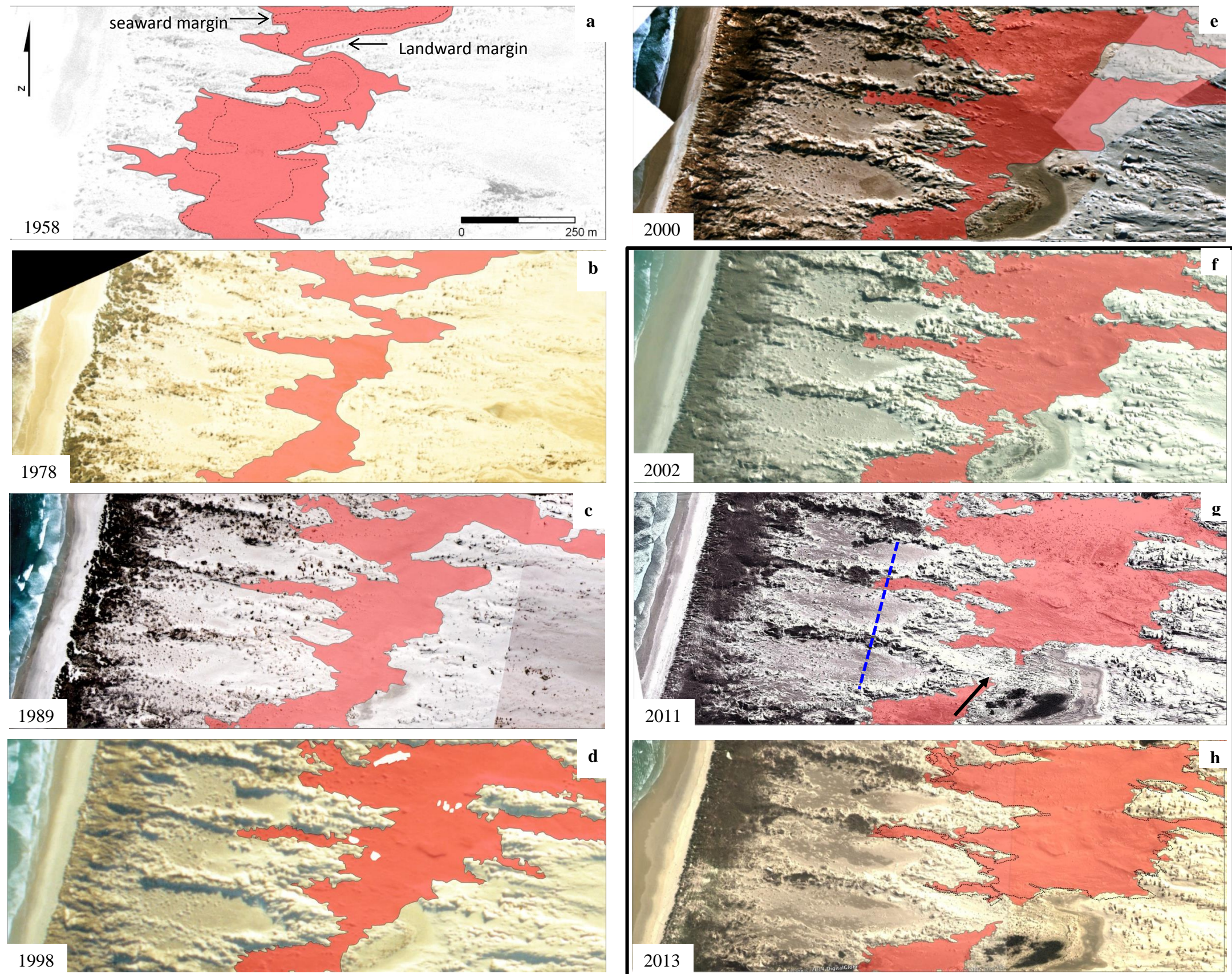


Figure 2.3: Aerial photographs of a section of the Mason Bay dune system, from 1958 to 2013, with an interpretation of the extent of deflation surface (red). In the 1958 image the dashed lines indicate the smaller of the stonefield outlines. In the 2013 image the dashed line is the outline of the 2015 stonefield (surveyed by GPS). The aerial images outlined in black are after the removal *A. arenaria* commenced in 2002. The blue dashed line in the 2011 image outlines the western margin of the spray efforts. The black arrow in the 2011 image indicates where the depositional lobe has extended into the stonefield.

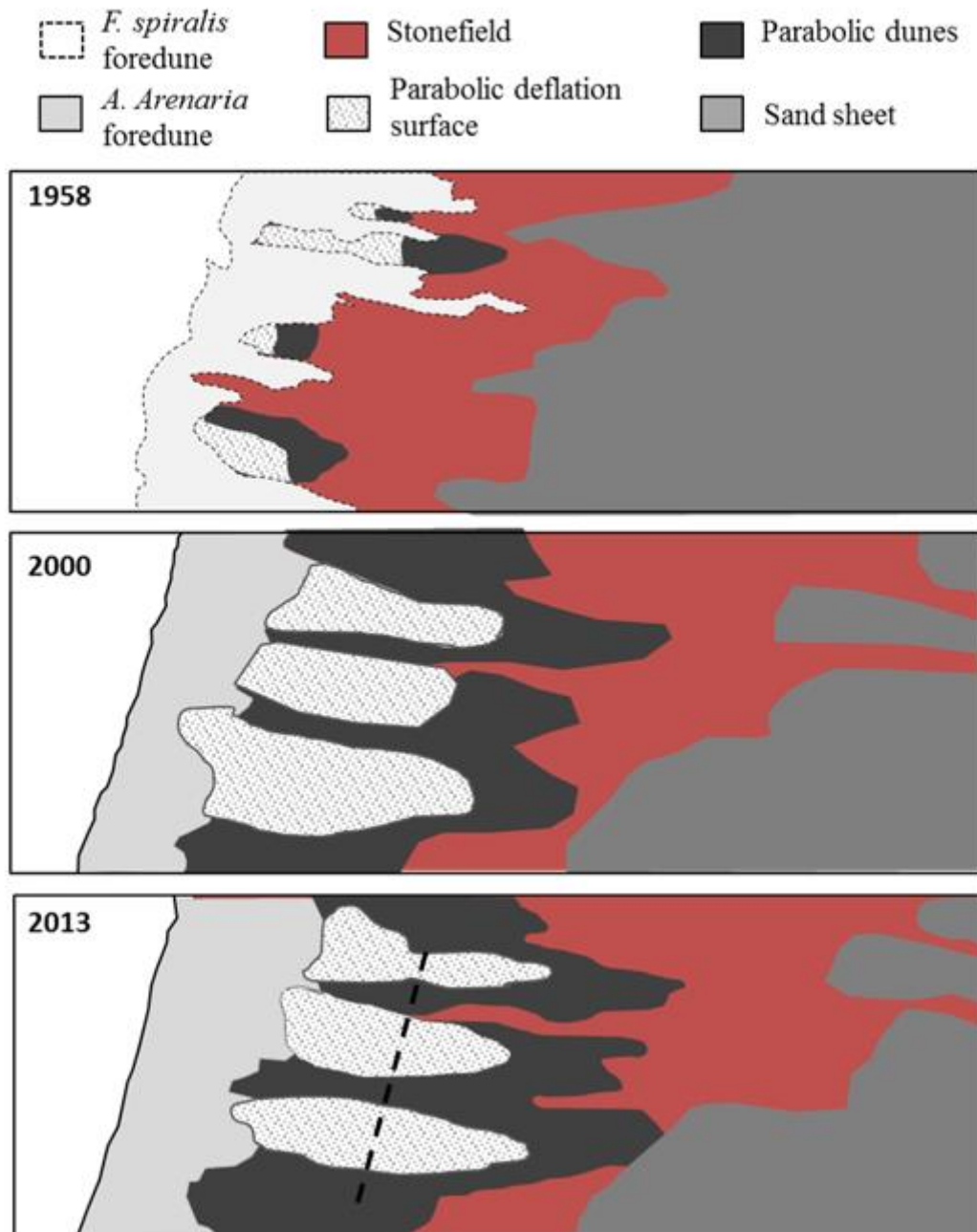


Figure 2.4: Outline of the key landforms through the two key stages of the stonefield's evolution. The invasion of *A. arenaria* into the Mason Bay transgressive dune system took place prior to 1958. 2000 saw the maximum level of *A. arenaria* invasion, just prior to start of the eradication programme in 2002. 2013 is the current stonefield, the dashed line indicates the western extent of the eradication programme.



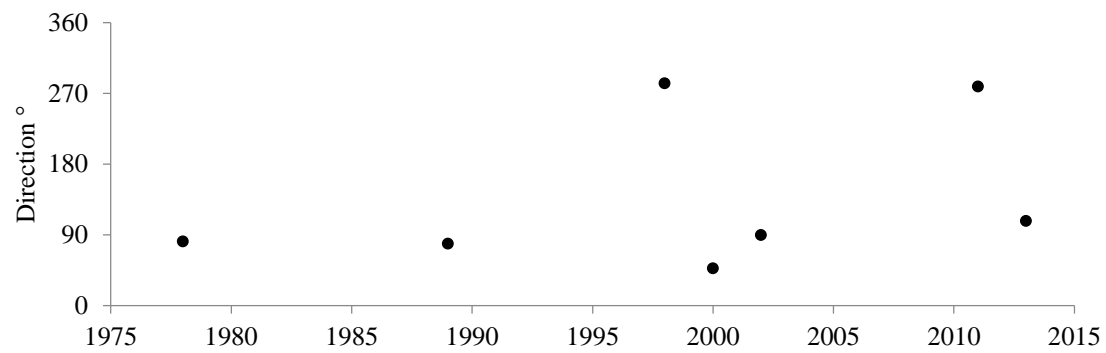
Figure 2.5: Mason Bay transgressive dune system in 1929. This photo is looking southwest towards the Earnest Islands. A stonefield is discernable in the center of the image. Source: Stewart Island Museum.

Changes in the shape and location of the stonefield were observed in relation to the invasion of *A. arenaria* after 1958. *A. arenaria* established itself in the foredune environment and created large shadow dunes. The *A. arenaria* shadow dunes began to join in 1978 forming a large continuous foredune. This in turn created a barrier between the beach and the backdune environment (Figure 2.3a-e).

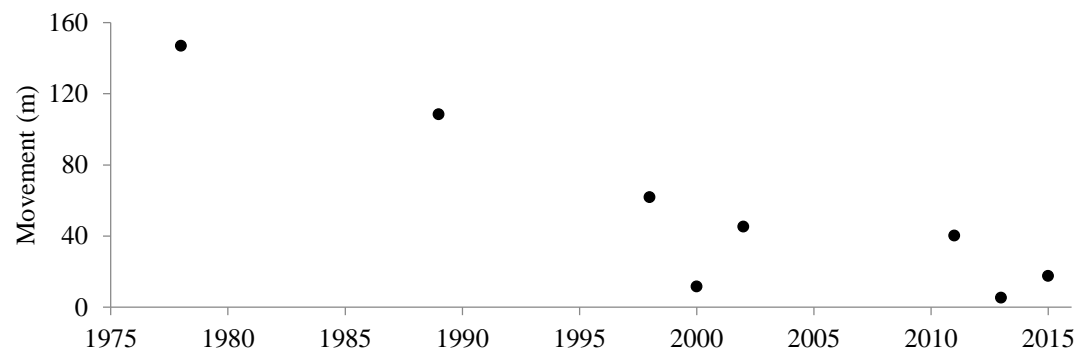
The depositional lobes of the parabolic dunes elongated into the stonefield shifting the seaward margin of the stonefield inland (Figures 2.4 and Figure 2.6c). Initially, between 1958 and 1978, the seaward margin was moving inland and the landward margin was considered stable limiting the growth of the stonefield (Figure 2.6d). The seaward margin continued to move inland as the parabolic dunes continued to elongate up until 1998. Between 1998 and 2000 the parabolic depositional lobes were colonised by *A. arenaria* halting their elongation into the stonefield (refer to arrow indicating *A. arenaria* colonisation of depositional lobes in Figure 2.7a).

The landward margin began to move inland after 1978 at a greater rate than the seaward margin (Figure 2.6d). This was caused by the erosion of the sand sheet. The inland movement of the landward margin created a wider and much larger stonefield and greatly increased the stonefield area (Figures 2.4 and Figure 2.8). In 2000 the inland distance of the landward margin was less than previous years as *A. arenaria* had begun to colonise the sand sheet.

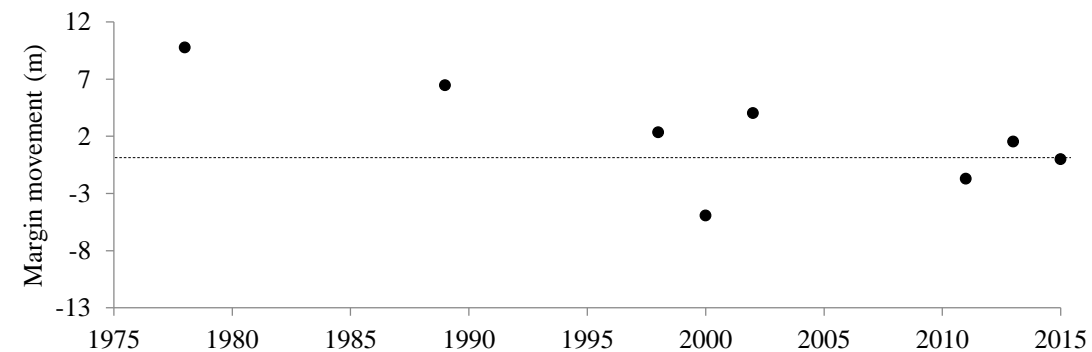
a) Direction of stonefield movement



b) Centre of stonefield movement



c) Seaward margin movement



d) Landward margin movement

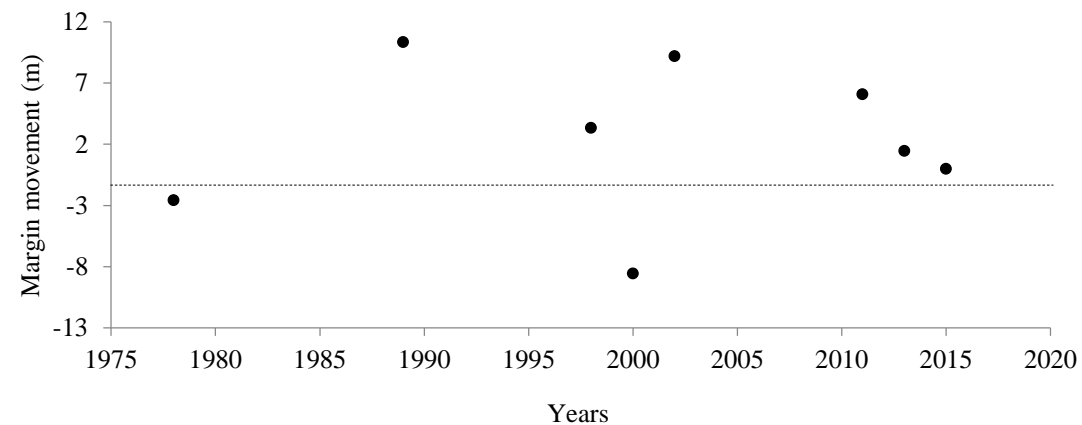


Figure 2.6: Spatial and temporal changes in the morphology of the Mason Bay central stonefield derived from the aerial photographic analysis and GPS data.

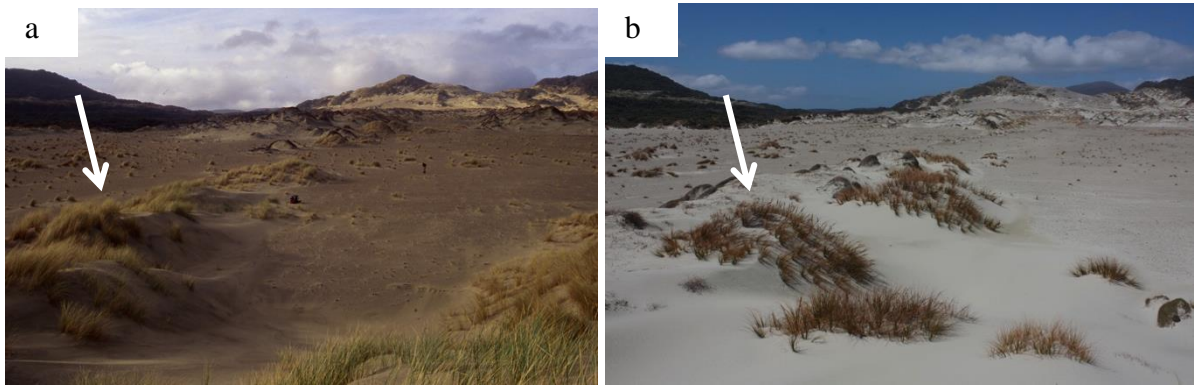


Figure 2.7: Oblique images of the parabolic depositional lobes extending into the stonefield. a) Parabolic depositional lobe in 1998, white arrow indicated *A. arenaria* colonisation (source Mike Hilton). b) *F. spiralis* has since colonised the leeward side of the depositional lobes, which has slowed but not prevented this erosion parabolic, white arrow indicates *F. spiralis* colonisation.

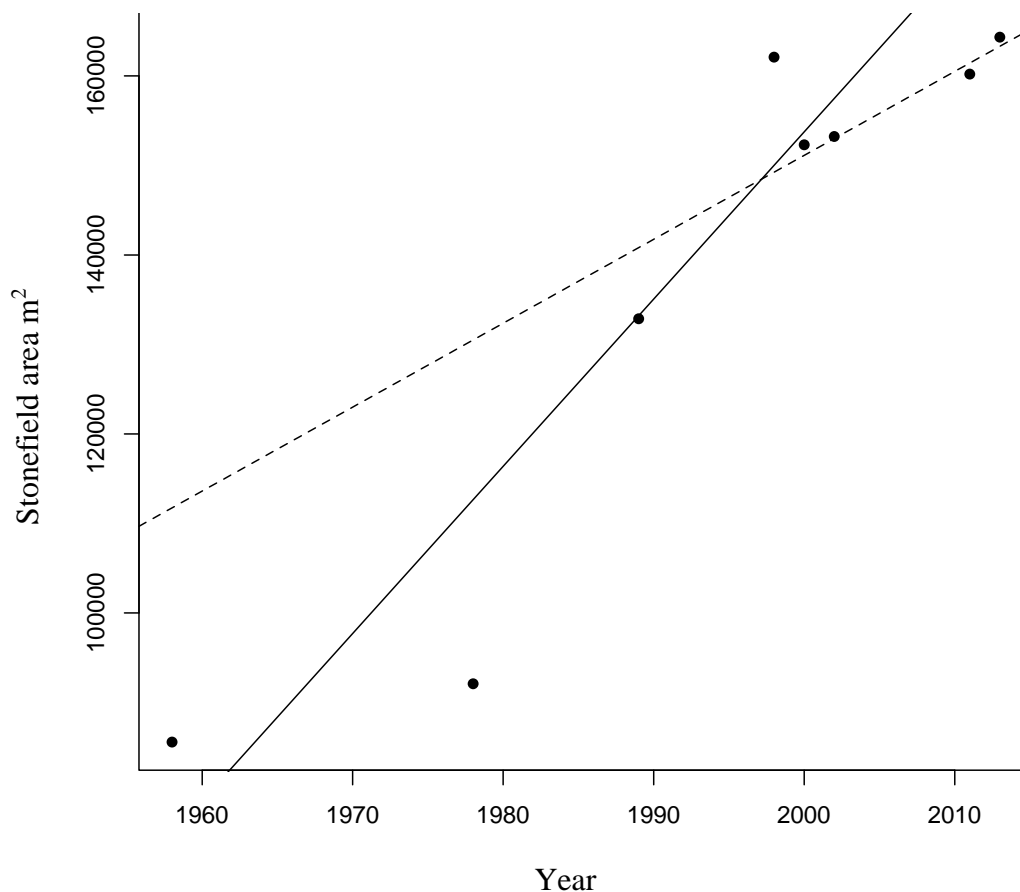


Figure 2.8: Plot of the stonefield area (m^2) each year between 1958 and 2013. The solid line is the regression of the stonefield areas prior to *A. arenaria* removal between 1958 – 2000 (p.value = 0.028, $r^2 = 0.81$, $df = 2$). The dashed line is the regression of the stonefield areas post *A. arenaria* removal 2002 – 2013 (p.value = 0.131, $r^2 = 0.92$, $df = 1$)

2.3.2 A. arenaria eradication programme (between 2002 and 2015)

The eradication of *A. arenaria* commenced in 2002, east (inland) of the current stonefield. This resulted in the sand sheet starting to erode, causing the landward margin of the stonefield to retreat inland (Figures 2.3f-h and Figure 2.6d). The parabolic dunes and depositional lobes were not sprayed until 2006. Therefore, the seaward margin was relatively stable until 2011, when the deposition lobes of the parabolic dunes (now substantially devegetated) started to erode. As a result the width and area of the stonefield grew between 2002 and 2013 (Figure 2.3f-h and Figure 2.4).

The seaward margin of the stonefield began to move eastwards after 2011 as the *A. arenaria* rhizome began to decay allowing for the aeolian erosion to occur on the parabolic depositional lobes. *F. spiralis* has since colonised the leeward side of the depositional lobes, which has slowed but not prevented this erosion (Figure 2.7b). On the southern margin of the stonefield the parabolic depositional lobe has elongated inland dividing the stonefield (Figure 2.3g arrow indicates the depositional lobe dividing the once continuous stonefield feature). The location of the stonefield appears to have remained constant since 2000 (Figure 2.8b), whereas the area of the stonefield has increased as the landward margin has advanced to the east at a greater rate than the seaward margin (Figures 2.4 and 2.6b).

In 1998 *A. arenaria* nabkha could be found throughout the stonefield (Figure 2.9a). Since the removal of the *A. arenaria*, the surface of the stonefield has not changed. However, *F. spiralis* nabkha have replaced *A. arenaria* nabkha (Figure 2.9b). This suggests that there have been no major changes, such as increased sand deposition, within the stonefield since the start of *A. arenaria* removal in 2002.

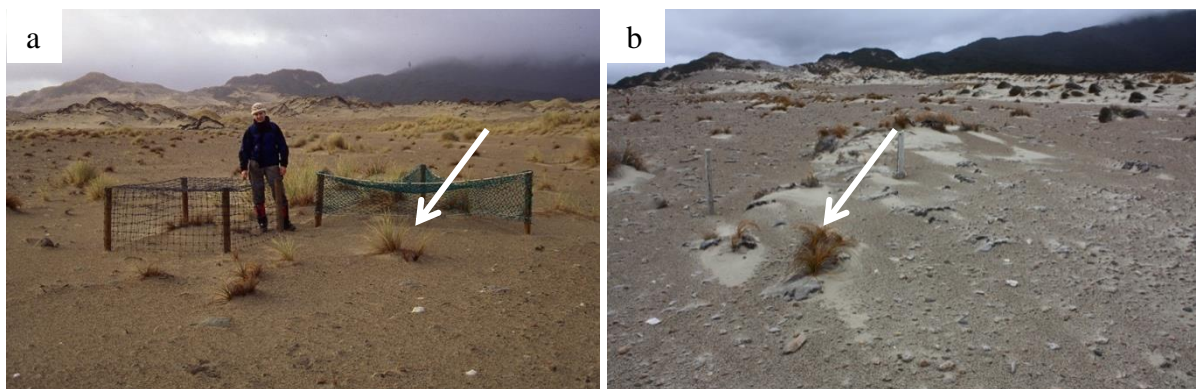


Figure 2.9: Oblique images looking landwards through the stonefield. a) Stonefield in 1998, white arrow indicates *A. arenaria* nabkha. b) Stonefield in 2015, white arrow indicated *F. spiralis* nabkha.

2.3.3 Relationship between the stonefield and foredune growth.

In the initial phase of the stonefield's development, when *A. arenaria* was invading, there was a strong relationship between the foredune area and the stonefield area (p.value of 0.02) (Figure 2.10). In the second phase of the stonefield's development, after the start of the *A. arenaria* eradication programme, the relationship between foredune area and stonefield area had decreased (p.value of 0.67).

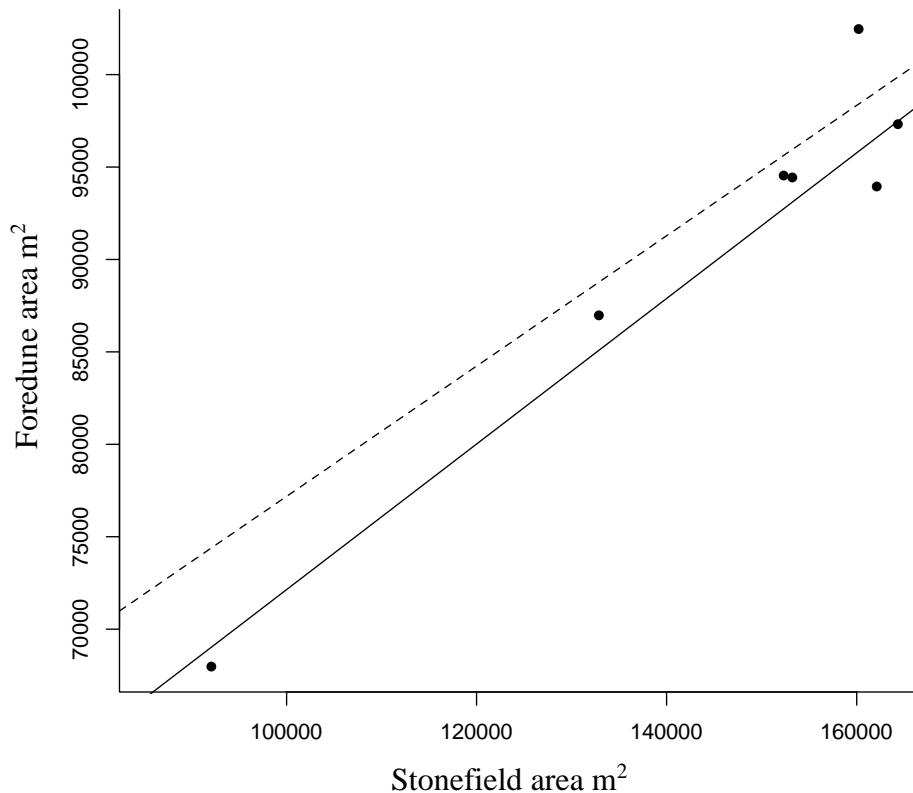


Figure 2.10: Linear regression analysis between the stonefield area and the area of the foredune. The solid line is the regression of the stonefield areas and the foredune areas prior to *A. arenaria* removal between 1978-2000 ($r^2 = 0.95$, $df = 2$). The dashed line is the regression of the stonefield areas and the foredune areas after *A. arenaria* removal between 2002-2013 ($r^2 = 0.24$, $df = 1$).

2.4 Discussion

Prior to the invasion of *A. arenaria* the Mason Bay central stonefield was a continuous landform, located 270m (western margins) closer to the sea. Both landward and seaward margins of the stonefield moved eastwards between 1958 and 2000. This migration coincided with the invasion of *A. arenaria* and the development of a continuous foredune. A recent study on the effects of the Mason Bay foredune on sand transport (Peterson *et al.*, 2011) found that sand transport decayed exponentially across the *A. arenaria* dominated foredune. Only 2% of the total sand flux was transported east (inland) of the foredune. The development of a continuous *A. arenaria* foredune effectively severed sand transport into the backdunes. A positive correlation between the growth of the foredune and the growth of the stonefield during the invasion of *A. arenaria* (1958-2000) was found. The growth of the continuous foredune appears to have severed the sediment exchange between the back dunes and beach: altering the evolution of the Mason Bay landforms.

The stonefield expanded between 1958 and 1998 as *A. arenaria* progressively invaded the foredunes and parabolic dunes. The expansion of the stonefield occurred as the landward margin eroded and a stony lag developed. This process occurred at a greater rate than the eastern migration of the seaward margin, resulting in an increased surface area of the stonefield. It is plausible that erosion of the sand sheet can be linked to the reduced sand supply to the sand sheet, however it is not possible to establish a cause-effect relationship.

Herbicides are an effective tool in killing *A. arenaria* (Konlechner *et al.*, 2014). However, the roots and decaying plant matter continue to affect the sand transport potential, slowing the rate of erosion thus causing a response lag (Hesp and Hilton, 2013; Pickart, 2013). A response lag is the period before the reaction to perturbation is evident and occurs due to changes in vegetation and geomorphic temporal response (Hesp and Martinez, 2007). The long-walled parabolic dune landforms have remained relatively intact, as they have not yet been completely sprayed with herbicide (Figure 2.3g blue line indicates the western limit of the herbicide applications and maintenance). This indicates that there have been no significant large influxes of sediment into the stonefield above what could be considered normal. The colonisation of the depositional lobes by *F. spiralis* has also meant that a portion of the eroding sand is being trapped in the lee of the depositional lobes creating an advancing front into the stonefield. Furthermore, since the start of *A. arenaria* eradication there has been no change to the surface

of the stonefield area which promotes the view that there has been little change to the sand inputs into or out of the stonefield.

A. arenaria invasion has caused significant changes to the Mason Bay transgressive dune system. The high connectedness of the Mason Bay coastal dunes has meant that landform changes downwind of the stonefield have influenced the stonefield evolution. There were two evolution phases of the stonefield, the first being the invasion of *A. arenaria* into the dune system and the second was after the start of the *A. arenaria* eradication programme

- i. The development of the large continuous foredune in relation to *A. arenaria* invasion was attributed to the stonefields growth between 1958 and 1998. It was suggested that the severing of the sand supply to the backdunes caused the parabolic dunes to elongate moving the stonefield inland. The erosion of the eastern margin of the stonefield was greater than the western margins in land movement creating, a larger stonefield area.
- ii. The destabilisation of the sand sheet in 2002 may have resulted in the eastern margin of the stonefield moving further inland, while the parabolic dunes remained relatively stable. This landward movement increased the surface area of the stonefield in the initial stages of the *A. arenaria* eradication program.
- iii. In 2006 the parabolic depositional lobes and the eastern half of the trailing arms were sprayed with herbicide. There was a lag in the erosional response of these landforms which was attributed to remnant *A. arenaria* rhizome (Hilton and Konlechner, 2010). In the 2011 the parabolic depositional lobes began to elongate into the stonefield. *F. spiralis* was shown to have colonised the deflation surfaces trapping eroded sand and forming an advancing front into the stonefield.

This study poses the next question in the development of the stonefield: what is the fate of the stonefield as the parabolic features become unstable and sediment transport into the stonefield increases?

Chapter 3

Short-term sedimentation patterns within the stonefield

3.1 Introduction

The remobilisation of dunes to restore dune mobility and dynamics is often achieved through vegetation removal (Konlechner *et al.*, 2014; Provoost *et al.*, 2011). Devegetation of dune forms increases sand erosion and deposition potential within a transgressive dune system (Hesp and Hilton, 2013; Martinez *et al.*, 2013; Walker *et al.*, 2013; Arens and Geelen, 2006; Arens *et al.*, 2004). Studies quantifying the effects of remobilisation have focused directly on the dune forms that were previously stabilised (e.g. Pickart, 2013; Walker *et al.*, 2013; Hilton *et al.*, 2009; Arens *et al.*, 2004). It was found that dune forms often adapted aerodynamically by flattening and moving downwind, encroaching on hinterland environments. With the exception of studies on the encroachment of dune forms as they move downwind, the effect of increased sand mobility on downwind environments has been little studied (Hesp and Hilton, 2013; Rhind *et al.*, 2013).

Transport and deposition of sand into the backdune system differs both temporally and spatially. Temporal patterns in sand deposition are dependent on sand availability and climatic conditions, such as wind and rain, over time. Spatial patterns in sand deposition and transport depend on surface moisture, wind conditions and vegetation (Hesp and Thom, 1990; Carter *et al.*, 1990; Elser, 1970). Sand is deposited when the wind drops below the transport threshold (6 m/s) (Sherman and Hotta, 1990), or when sand transporting winds encounter a rough surface such as vegetation (Hesp, 1981). An increase in sand deposition, with distance inland, across the stonefield would indicate that either more sand was available inland or that vegetation was influencing sand deposition. An understanding in the spatial patterns of sand accumulation and erosion (henceforth sedimentation patterns) will increase understanding of where sand from destabilised parabolic dune forms is accumulating.

The presence of vegetation acts as an obstacle that disrupts the airflow, causing deceleration and thereby promoting localised sand accumulation (Mounteny and Russel, 2006; Hesp, 1981). The biophysical feedback between vegetation and sand is an important factor when determining patterns of sedimentation in a given area. Areas of increased sand accumulation in coastal dunes are commonly related to the presence of sand binding vegetation, often forming nabkha (isolated dunes formed by sand deposition around plants) (Cooke *et al.*, 1993; Hesp, 1981). The morphological characteristics of nabkha i.e., long axis length, short axis and dune height, are a function of sand supply, wind, vegetation density and the growth habit of the plants they form around (Lange *et al.*, 2013; Zarnetske *et al.*, 2012; Cooke *et al.*, 1993) (Figure 3.1). Increased sand inputs into the stonefield environment could be trapped by sand binding species, creating a positive biophysical feedback loop between sand accumulation and vegetation growth (Figure 3.1). A positive biophysical loop is illustrated by the increased growth of sand binding plants as they are nourished by sand, therefore increasing their sand trapping efficiency and the size of the nabkha (Zarnetske *et al.*, 2012; Cooke *et al.*, 1993; Hesp and Thom, 1990). *Ficinia spiralis* is a primary sand colonising species capable of vertical and lateral growth and, therefore, capable of nabkha formation (Sykes and Wilson, 1990).

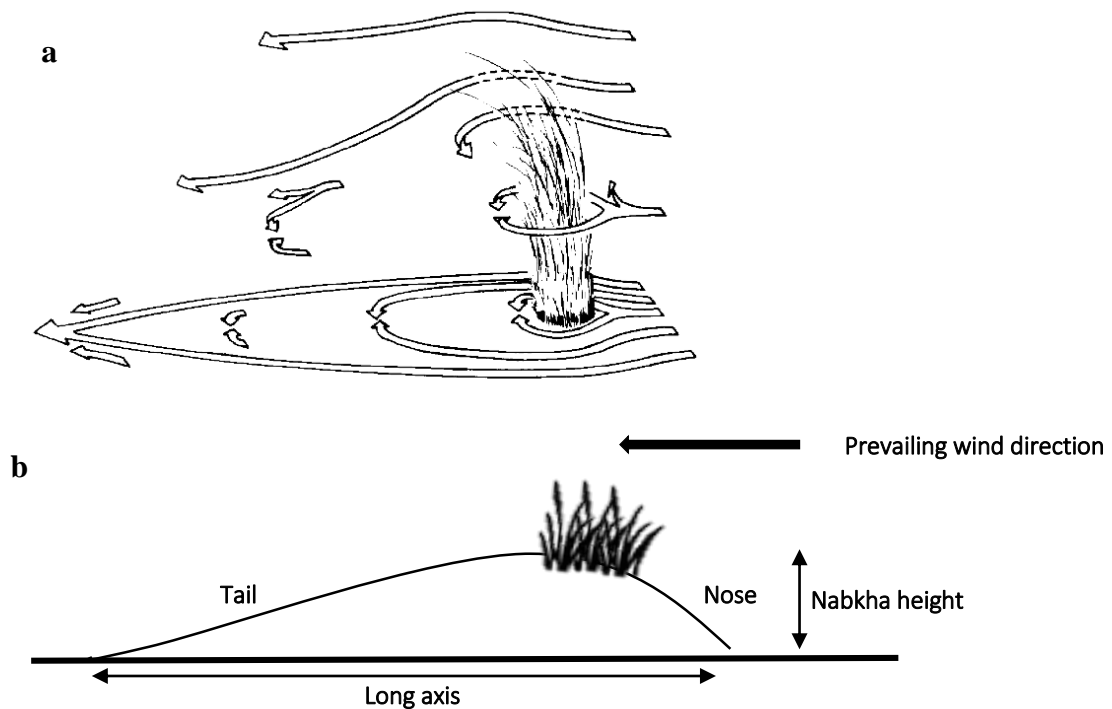


Figure 3.1: The formation of nabkha around isolated sand binding species such as *Ficinia spiralis*. a) Arrows show the air flow around vegetation. Sand deposition occurs along the centerline where the opposing vortices meet. b) The depositional form of nabkha in relation to the prevailing wind. Adapted from Hesp, 1981 and Lang *et al.*, 2013.

Patterns of erosion in the stonefield would indicate that sand from the destabilised parabolic dunes is passing through the stonefield into the sand sheet. Aeolian erosion occurs when the wind speed reaches above the 6m/s threshold (Sherman and Hotta, 1990). Erosion in the stonefield would suggest that the destabilisation efforts were not directly impacting the stonefield and its associated plant communities through burial. Differential rates of sand deposition and erosion through space and time interact to create a mosaic of different physical habitats characteristic of mobile dunes (Nordstrom, 2008). Measuring the spatial patterns of sedimentation in the stonefield will provide an understanding of the effect downwind destabilisation is having on the stonefield.

Chapter Two has shown that the parabolic depositional lobes in the Mason Bay dune system are encroaching into the stonefield along the seaward margin since *Ammophila arenaria*. The aim of this chapter is to assess whether sand liberated from the recent and ongoing destabilisation is accumulating in the stonefield. This chapter addresses two questions:

- i) Has sand accumulated in the stonefield over the study period?
- ii) Are the observed patterns of sedimentation in the stonefield related to the distribution of *Ficinia spiralis* nabkha? That is, is the primary sand colonising species present in the stonefield responding positively to the increased rate of sand deposition?

3.2 Method

A study site was located in the central stonefield, within which sedimentation patterns were observed. The study site was located directly downwind of a devegetated parabolic deflation surface on the southern end of the stonefield. The study site spanned the length of the stonefield (200m) and was angled Southeast (SE) to reflect the dominant onshore wind direction observed in the angle of the parabolic trailing arms (Figure 3.2b).

Temporal and spatial patterns of sand accumulation were investigated using a series of methods. Firstly a survey of sedimentation patterns was carried out using a suite of erosion pins in the study area. Sedimentation patterns in relation to *F. spiralis* were then established by a survey of *F. spiralis* nabkha volume and height changes within the study area. In order to look at the recent past burial patterns within the stonefield a series of soil pits were dug to examine the soil

profile for recent burial patterns. These methods aimed to determine whether sand was accumulating in the stonefield over the short-term period of months to years (Figure 1.3).

3.2.1 Stonefield area survey

An extensive ground survey was carried out in the Mason Bay stonefield (Figure 3.2a, b). The study site was divided into 100, 10m² quadrats. Within each 10m², five quadrats of 1m² were located to ensure an accurate representation of each 10m² area (Figure 3.2c). In each quadrat the presence of *F. spiralis* was recorded as the presence of vegetation as *F. spiralis* is the primary sand colonising species present in the stonefield.

Sand accumulation and erosion was measured in each 1m² quadrat using erosion pins. Erosion pins measure the change in the sand surface elevation relative to the first measurement providing a measurement of the sand accretion and erosion on the dune surface (e.g. Levin *et al.*, 2006; Arens *et al.*, 2004; Visser *et al.*, 2004; Burkinshaw and Rust, 1993). One erosion pin was placed in the center of each 1m² quadrat and the height was recorded during the study, with an accuracy of approximately 1mm (Figure 3.2c). Using an array of erosion pins across the stonefield, spatial patterns of sedimentation could be measured and compared to observed *F. spiralis* plants.

Erosion pins are representative of only a small area surrounding the pin (Arens *et al.*, 2004); therefore elevation changes in the sand surface were measured against the erosion pins, then averaged to obtain a single sedimentation value for each 10m² quadrant. Erosion pins were measured at the commencement of the study in June 2014, then again after eight months (February 2015) and nine months (March 2015). Measurements were taken at eight months as the opportunity arose to measure sedimentation patterns over a one month period. The erosion pins were surveyed using a Leica total station to spatially reference the recorded sedimentation patterns within the study site.

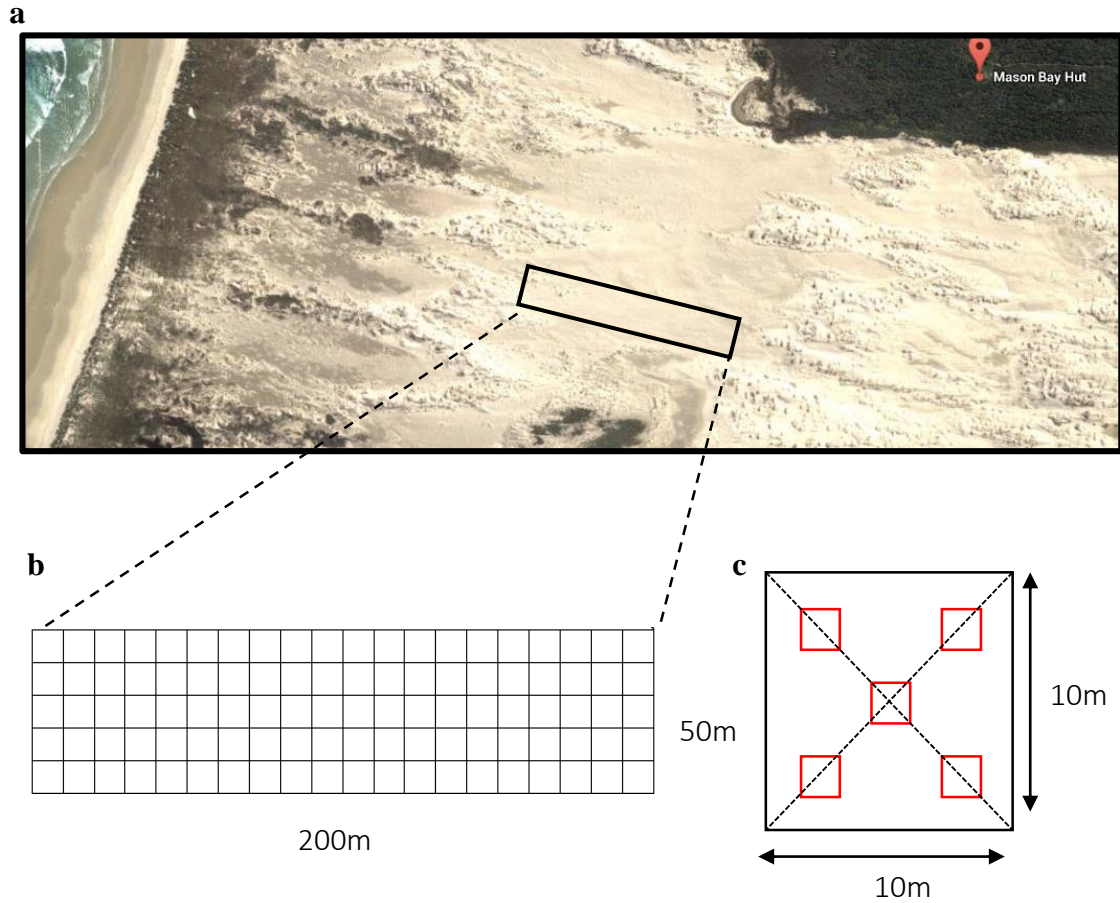


Figure 3.2: Ground survey in Mason Bay central stonefield. a) Ground survey in the Mason Bay Central stonefield. b) Area of survey 200m x 50m running (west to east), divided into 100 quadrants of 10m². c) Location of five 1m² quadrats within each 10m² quadrant. The size of the quadrats has been exaggerated to make them visible in this diagram.

3.2.2 *Ficinia spiralis* nabkha development

Within the Mason Bay stonefield there is a scattering of *F. spiralis* plants that have formed small nabkha (Figure 3.3a). *F. spiralis* can establish on almost any substrate, but only flourishes conditional of sand addition. As the growth of nabkha reflects sedimentation patterns (Lang *et al.*, 2013; Cooke *et al.*, 1993), *F. spiralis* nabkha were used as a method of measuring sediment inputs into the stonefield.

A total of 18 nabkha were selected at approximately 10m intervals, along the east-west central axis of the survey area (Figure 3.3b). *F. spiralis* nabkha were surveyed using a Leica total station to create a DEM (Digital Elevation Model). The total station was set up over a nail in the northern seaward post for each survey and the baseline aligned with the southern seaward corner post. This allowed each nabkha survey to be checked against the known location and

height of the survey area posts. Surveys of the nabkha were carried out in August 2014 and March 2015, the longest time frame possible. Photographs of the nabkha were taken after each survey and the direction of the nabkha tails was recorded. The dynamic nature of the tails meant they were often switching in relation to current wind direction (Figure 3.3a).

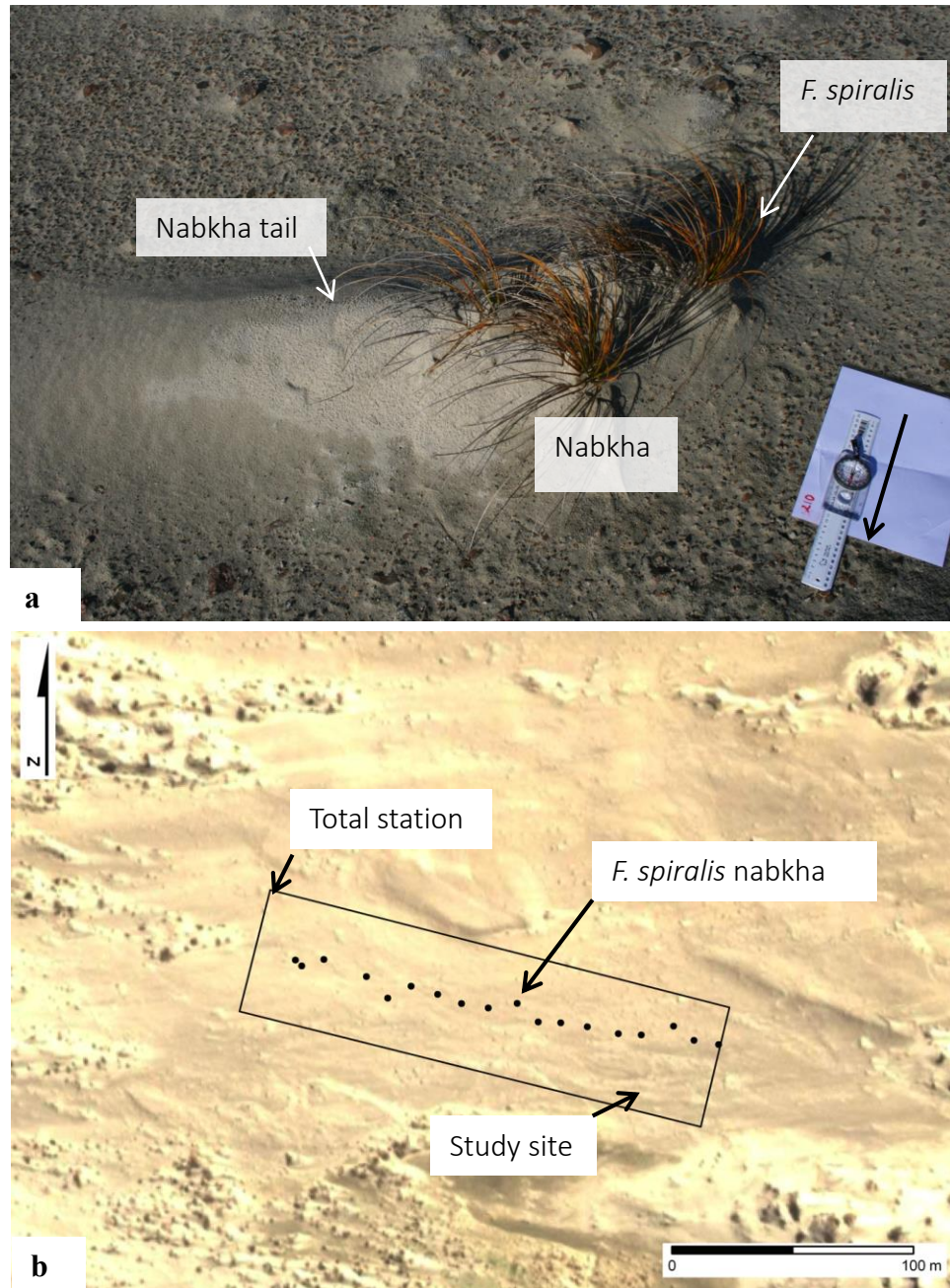


Figure 3.3: a) *Ficinia spiralis* nabkha. Note the distinct tail in the lee of the *F. spiralis*. b) Location of the 18 surveyed *F. spiralis* nabkha within the study site (black rectangle). The prevailing westerly winds blow right to left in the top image and left to right in the lower images.

3.2.3 Soil profiles

Soil profiles have been used to identify buried soils (paleosols) in many settings (Havholm *et al.*, 2004). Soil profiles were dug to examine the history of sand accumulation in the stonefield and to link the observed short-term changes in the stonefield (the focus of this chapter) with changes recorded in the historic photograph analysis (Chapter Two). A distinct organic layer was visible in the profiles, distinguished by colour (dark) and texture (mottled). This layer comprised plant stems and roots of *Raoulia* spp., pebbles and gravel, (similar in size to those seen on the stonefield surface) (Figure 3.4). The depth of sand above the organic layer was measured to calculate the extent of burial. Soil profiles were measured in the study site, on the edges of the parabolic depositional lobes and on the landward margin of the stonefield, soil profile sites were located downwind of the depositional lobes.

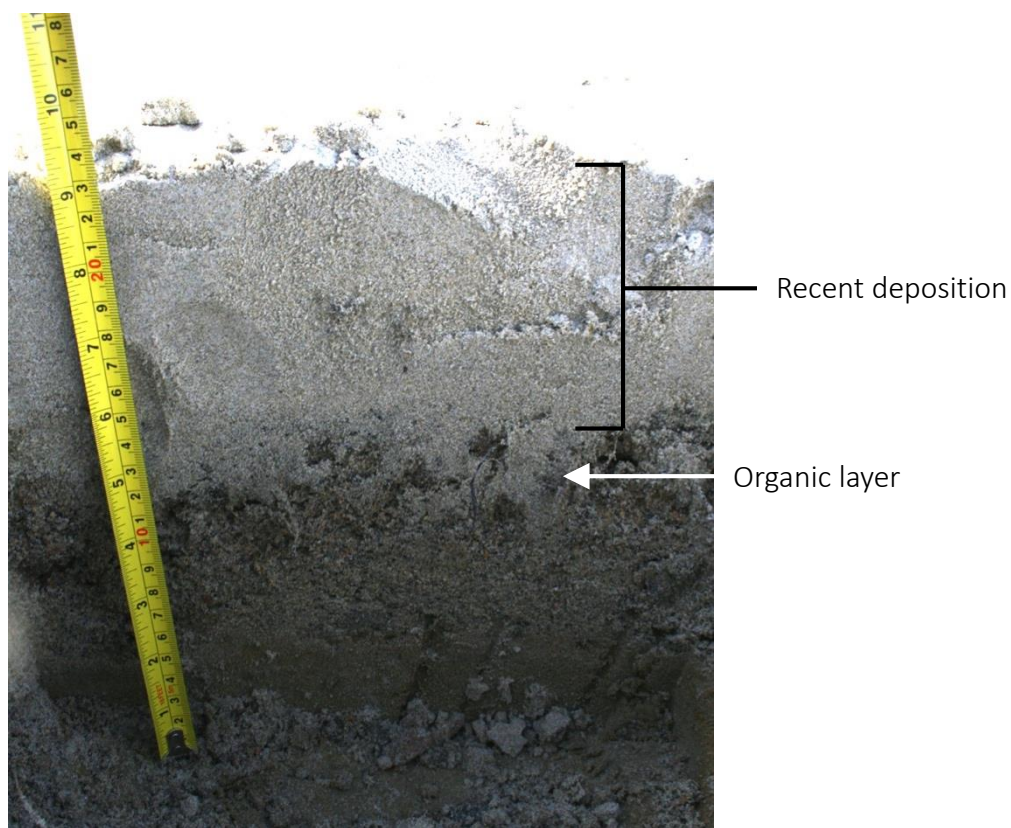


Figure 3.4: Stratigraphic layers of a soil pit dug downwind of a depositional lobe of a parabolic dune. The distinct roots and darker appearance identify the organic layer. The width of the sand layer above the organic layer was recorded and compared spatially between the soil profiles.

3.2.4 Data Analysis

The nabkha proved to be very dynamic, with significant variation in the orientation of the tails (Figure 3.3a). This resulted in some erosion pins being either buried or exposed because of movements in the tails of the nabkha, rather than sustained erosion or deposition. It was not possible, because of the remoteness of the study area, to measure the erosion pins after periods of similar wind direction. Those erosion pins affected by vegetation, e.g., in the lee of *F. spiralis* nabkha or directly located in plants, were excluded from the sedimentation analysis to ensure that any overall sedimentation trends were revealed.

A linear regression analysis was conducted in the statistical programme R to determine the relationship between the average sedimentation per 10m² quadrant and their distance from the parabolic depositional lobe. This was completed for both the nine month and one month periods. A contour map of the recorded sedimentation in each 10m² quadrant was created to document the spatial patterns across the study site and the relationship between the recorded *F. spiralis* plants. The mean sedimentation over the nine month and one month periods were compared using a paired t-test.

The morphological features net volumetric change and maximum height changes of *F. spiralis* nabkha were measured to determine whether sand was accumulating in the stonefield. The net volumetric change was calculated by comparing the volume of each nabkha survey (August 2014 and March 2015 surveys) in SURFER. Kriging was chosen as the best-fit model and spacing was set at 0.01 when analysing the nabkha DEMs (Andrews *et al.*, 2002). The change in nabkha height was determined by calculating the difference between the maximum heights of each nabkha survey.

Spatial patterns in nabkha growth were determined by conducting a linear regression analysis between the morphological changes (change in nabkha volume and height) and the nabkhas distance from the parabolic depositional lobe. The size of a nabkha reflects the sediment availability in the recent past, over the last 3-5 years, or since the depositional lobes of the parabolic dunes were revegetated. Therefore a linear regression analysis was conducted between the nabkha volume and distance from the foredune to measure any spatial patterns in recent sediment availability.

Sand accumulation and erosion can also be influenced by climate variables such as wind speed and direction (Sherman and Hotta, 1990). The wind direction and wind speed during the study period were examined to determine whether the observed patterns of sedimentation during the study period were influenced by abnormal climatic conditions. The nearest climate station to Mason Bay is the South West Cape, Stewart Island weather station (47.28°S, 167.46°E). The average wind speed (m/s per day) during the period of the study were compared to the long term wind record (1991-2012), to determine whether the wind patterns were consistent with previous years or an anomaly.

3.3 Results

3.3.1 Sedimentation patterns recorded by the erosion pins

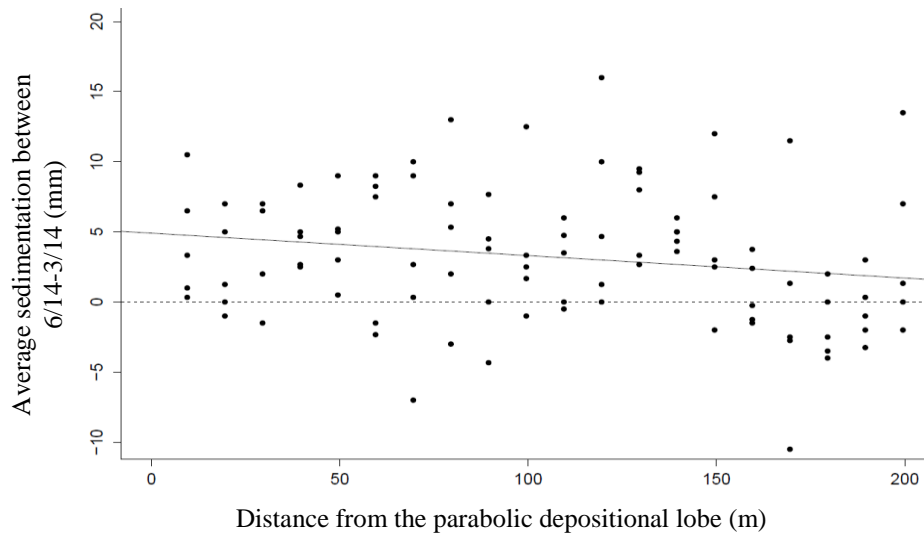
During the nine month study period sand accumulated in the stonefield, with an average accumulation over the entire stonefield area of 3.22mm (0.36mm per month). The maximum accumulation was 16mm (standard error (SE) 0.008) over nine months. This was calculated after the erosion pins affected by vegetation were removed. The average accumulation of sand for all erosion pins, including pins affected by vegetation, was 2.76mm. Sedimentation over one month was also positive with an average accumulation of 2.14mm (the average of all erosion pins was 1.5mm), with a maximum accumulation of 10.33mm (SE 0.005). Sand accumulation during this one month period (between February and March 2015) accounted for 66% of the (average) accumulation recorded over the nine months.

The linear regression analysis indicated that there was no significant relationship between distance from the source of sand and accumulation ($r^2 = 0.028$); however, the p.value of 0.053 suggests that there may be a small negative relationship between distance and sand accumulation (Figure 3.5a). Between February and March there was also no significant relationship between sedimentation patterns and distance inland noted (Figure 3.5b).

The spatial pattern of sand accumulation and erosion within the study site is shown in the contour map (Figure 3.6). *F. spiralis* plants recorded in the quadrats are indicated by the black triangles in the contour maps to determine whether the spatial sedimentation patterns observed within the study area were centred around *F. spiralis* plants. Some distinct areas of erosion and accretion could be seen centred around *F. spiralis* plants. However, no general pattern of

accretion or erosion around these plants was discernible from the contour maps, i.e., the pattern of accumulation seems independent of the presence of *F. spiralis*. Areas of the stonefield accumulated up to 16mm and others that eroded up to -11mm over the period of a month. However, these were not observed over the nine month period (Figure 3.6). This indicated that sand is coming and going from the stonefield and the results are highly dependent on when the sample is taken.

a) Sedimentation patterns over nine months



b) Sedimentation patterns over one month

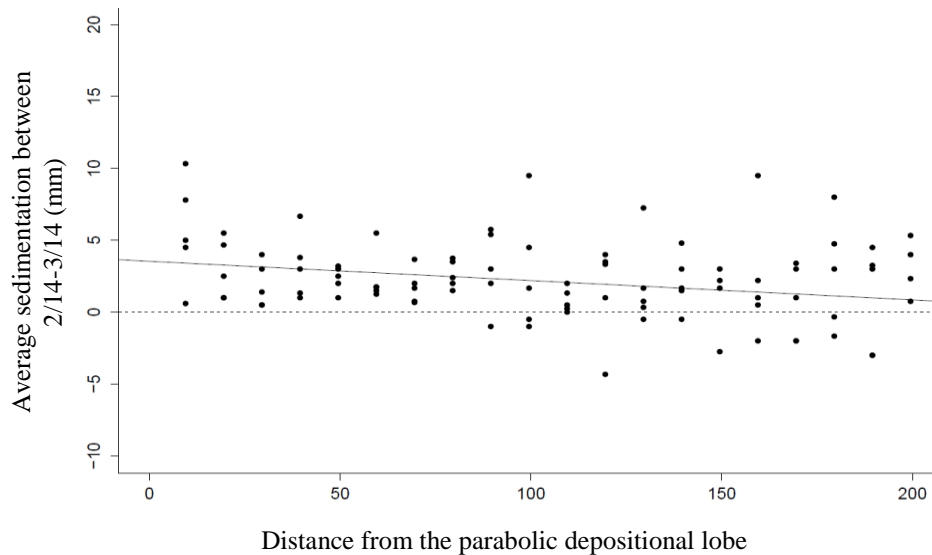


Figure 3.5: The average accretion and erosion (mm) for each 10m² quadrant (average of the five 1m² quadrats). The negative values represent sand erosion and the positive values represent accretion. The solid black line is the regression line and the dashed line represents 0. a) Average between June 2014 and February 2015 (df = 97). b) Average between January 2015 and February 2015 (p.value = 0.01, $r^2 = 0.056$, df = 67).

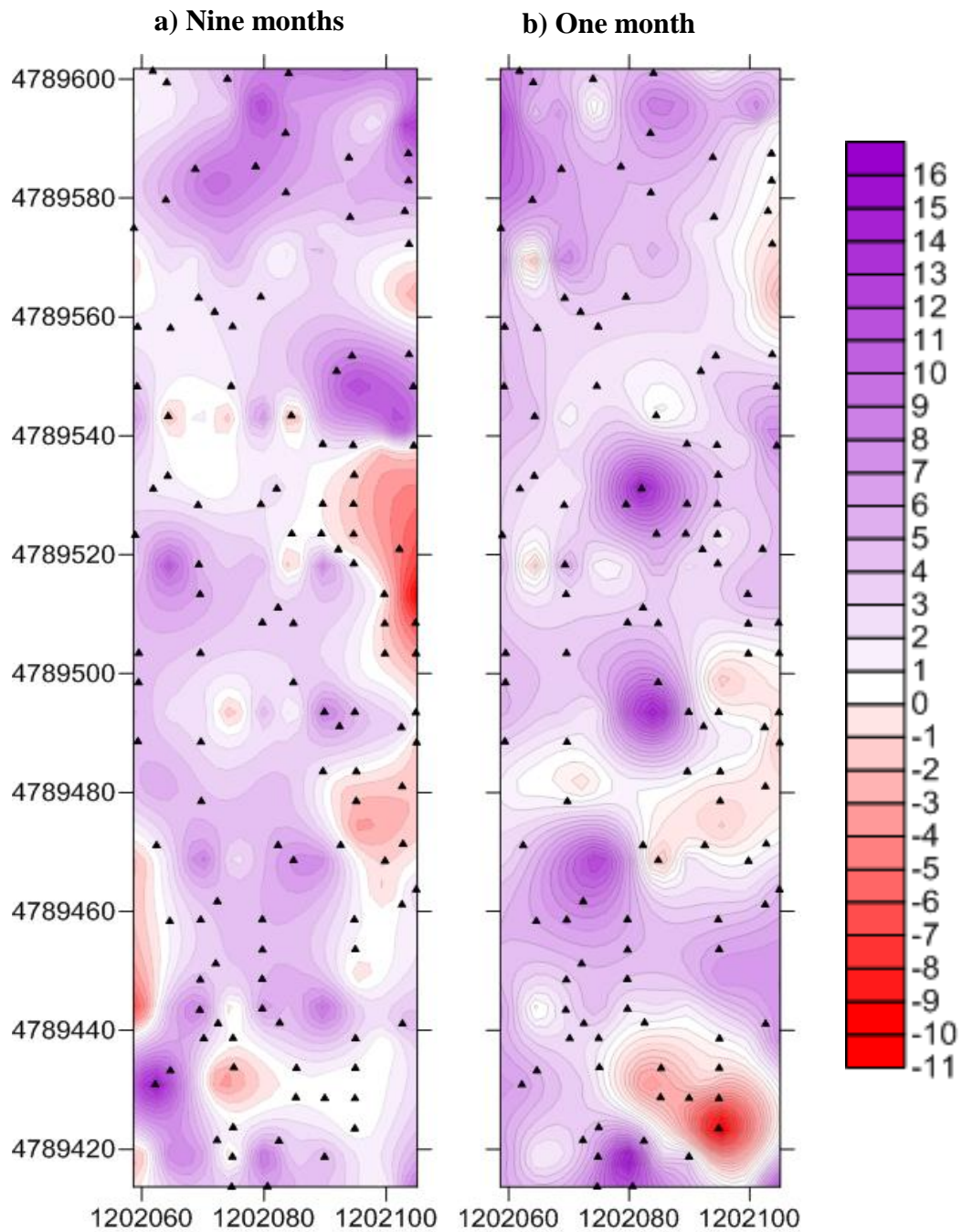


Figure 3.6: Contour maps showing the average accretion or erosion of sand per 10m by 10m quadrat. a) Sedimentation between 6/2014 and 3/2015, b) sedimentation between 2/2015 and 3/2015. Black triangles indicate the location of *F. spiralis* plants that were in March 2015.

3.3.2 Patterns in *F. spiralis* nabkha size and development

The 18 measured *F. spiralis* nabkha measured increased in volume across the study site (p.value<0.01) (Figure 3.7). This indicates that in the recent past more sand has been accumulating around nabkha in the inland (eastern) half of the stonefield. There was a negative relationship between distance from the parabolic depositional lobe and net volume change in *F. spiralis* nabkha across the stonefield between August 2014 and March 2015 (p.value of 0.01, SE 0.001) (Figure 3.8a). The average net volume change in nabkha was only 0.29m³ this was considered insignificant and the nabkha were considered stable during the study period (Figure 3.8a). There was positive correlation between the maximum height change and distance from the foredune, where a decrease in height loss moving inland was noted (p.value of 0.01). The maximum height change in the nabkha was on average -0.66mm (SE 0.0001), this was considered too low to infer any relationship. (Figure 3.8b).

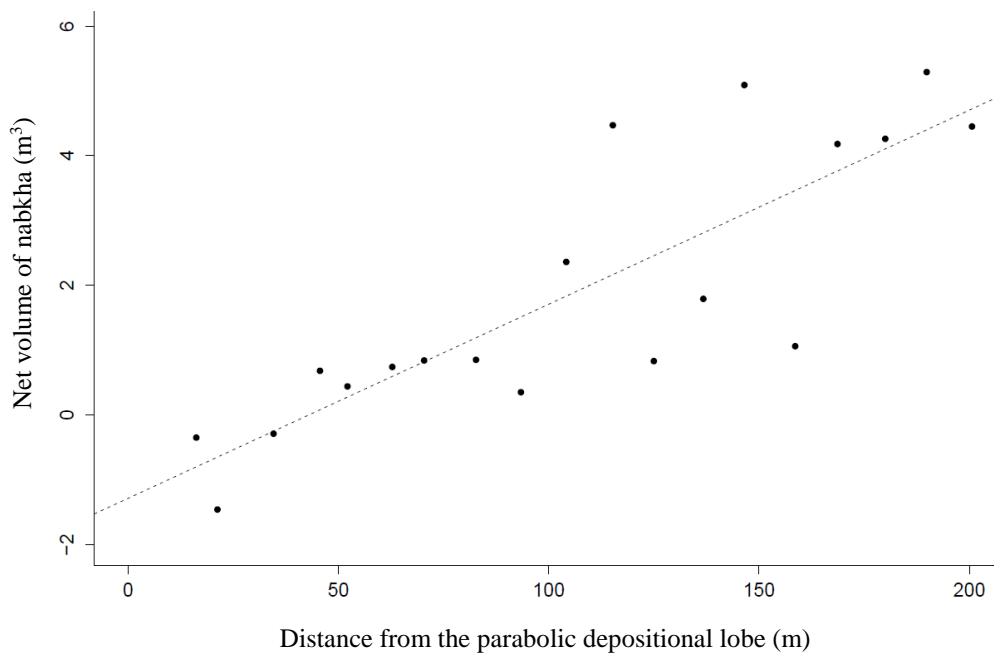


Figure 3.7: Net volume of the *F. spiralis* nabkha versus distance from the parabolic depositional lobe, (r^2 of 0.692, $df = 17$, $SE < 0.00$).

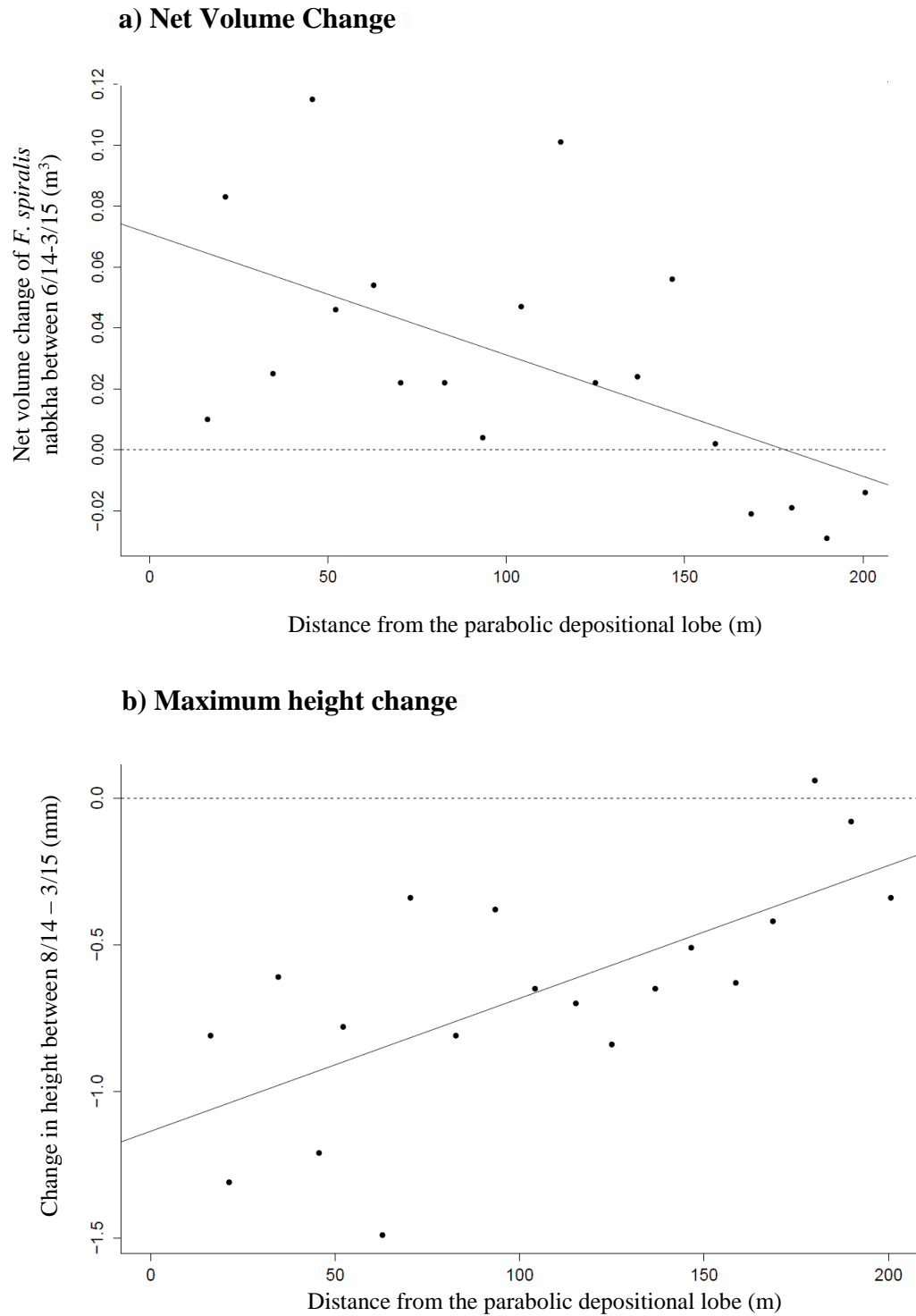


Figure 3.8: a) *F. spiralis* nabkha net volume change (m^3) between August 2014 and February 2015. The dashed line equals 0. ($r^2 = 0.294$, $df = 17$, $SE < 0.00$). b) *F. spiralis* nabkha maximum height change (mm) between August 2014 and February 2015. The dashed line equals 0. ($r^2 = 0.434$, $df = 17$, $SE < 0.00$).

3.3.3 Spatial distribution of recent burial patterns

The average depth of the organic layer along the eastern (downwind) edge of the parabolic depositional lobes was 98mm (see soil profiles 1 to 9, Figure 3.10). A maximum burial of 155mm was observed at one site (soil profile 2 Figure 3.10). The dune surface in the lee of the depositional lobes was bare sand. From the results shown in Chapter Two it can be understood that the parabolic depositional lobes have elongated by approximately three meters in the last five years, therefore, there has been an approximate average deposition of 78mm in the lee of the parabolic dunes in the last five years.

The soil profiles displayed in the study area show a thin veneer of sand (5mm) on top of the stony surface. Vegetation such as *Raoulia hookeri* var. *hookeri* and *colobanthus muelleri* along with large stones were widespread across the surface indicating that there has been no significant burial occurring in the centre of the stonefield study site in recent history compared to in the lee of the depositional lobes. It was observed that to the lee of the large deflation plateau on the northern margin of the study area the stonefield surface was buried 15mm (see soil profile 4 Figure 3.9).

The soil profiles along the landward (eastern) edge of the study area and stonefield show burial up to 36mm (soil profiles seven and eight Figure 3.9, and soil profiles 11 and 12 Figure 3.10). The surface of the stonefield at the landward locations was bare sand with pea sized gravel. Soil profile nine, was an exception, where only 15mm burial was observed. No vegetation was growing on the surface of the stonefield at this location (soil profile nine, Figure 3.9). Soil profile 10 along the southern margin of the study site showed a high level of deposition (80mm) in the lee of the dune parallel to the southern margin (Figure 3.10).



Figure 3.9: Soil profiles measured in August 2014 in the Mason Bay stonefield study site. The grey tone is the depth of burial (mm) with the dune surface at 0mm. The soil profiles correspond to the pits (black dots) located on the right hand side of each set of profiles.

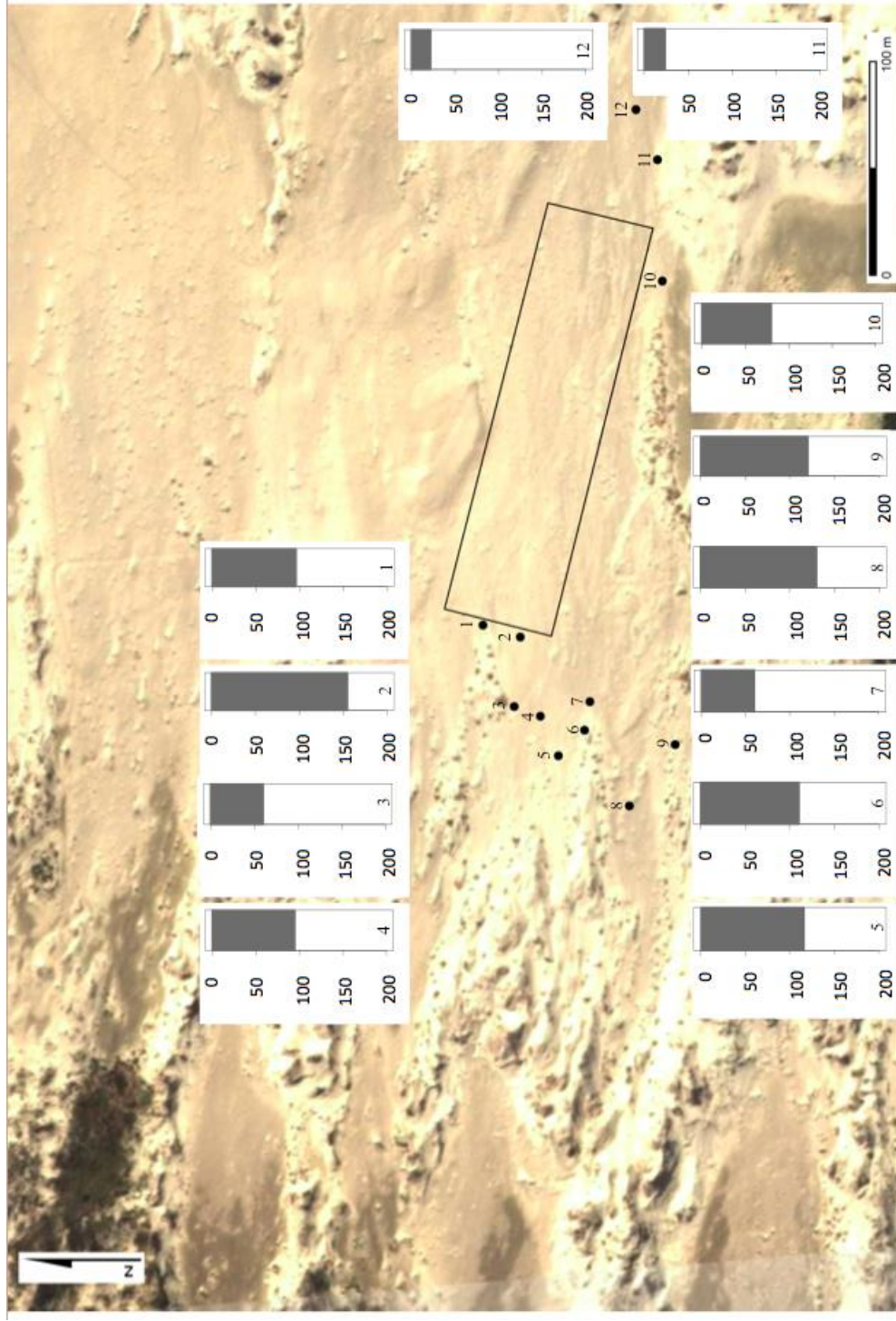


Figure 3.10: Soil profiles measured in August 2014 in the Mason Bay stonefield study site. The grey tone is the depth of burial (mm) with the dune surface at 0mm. The soil profiles numbers correspond with the number and location of each soil pit (black dot).

3.3.4 Wind regime during the study period

The average wind direction during the study period at South West Cape was 255.08° , similar to the average direction of the long term South West Cape wind record 251.40° (1991 – 2012) (Figure 3.11). The average daily wind speed during the study period was 9.84m/s similar to the daily average wind speed recorded between 1991 and 2012. This suggests that sedimentation patterns measured during the study period were not influenced by abnormal wind conditions.

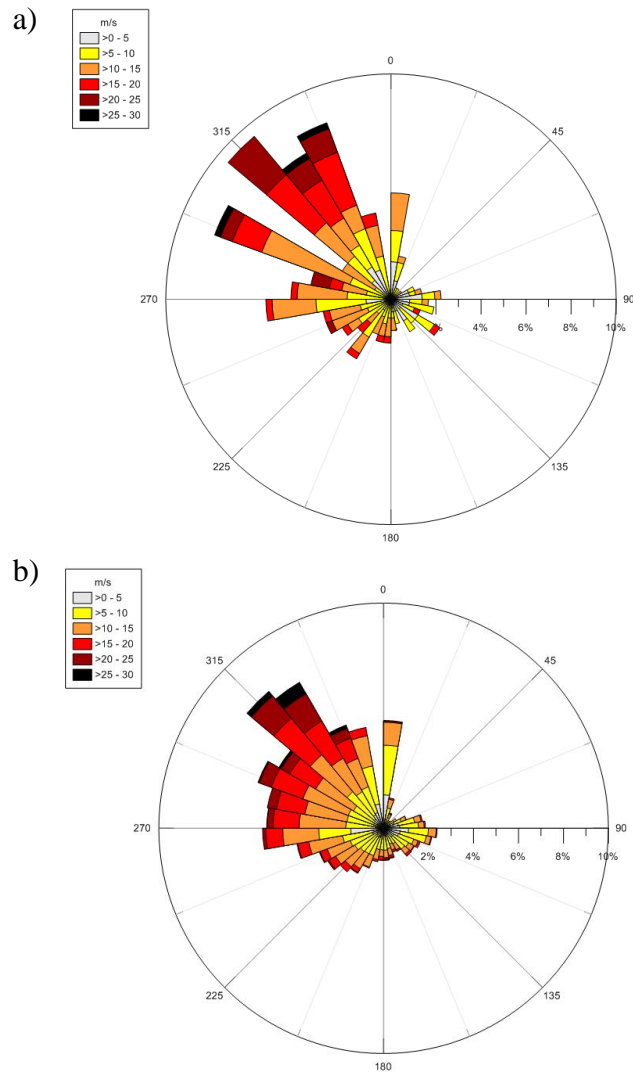


Figure 3.11: Wind roses for the South West Cape Weather station, Stewart Island. a) Wind regime during the study period (May 2014 – April 2015). b) Wind regime during the period 1991 – 2012.

3.4 Discussion

Over the nine month study period there was a general trend of sand accumulation in the stonefield with an average accumulation of 0.36mm per month (total 3.22mm over the study period). No strong spatial trends were recorded in relation to either a landward gradient or the spatial distribution of the native sand binding sedge *F. spiralis*. Within the stonefield *F. spiralis* plants had formed discrete isolated nabkha before the commencement of this study, however the maximum net volume only increase was 0.12m³ over seven months, and the maximum height of the nabkha decreased, on average, by -0.66mm. This was considered insignificant compared to previously recorded *F. spiralis* nabkha growth of 2-3m over a seven to five year period recorded by Hilton *et al.*, (2009) at nearby Doughboy Bay in a foredune environment. The volume and height of the studied nabkha did not change much during the study period and were considered stable. Mounteny and Russell (2006) found that *A. arenaria* nabkha in southern Iceland that attained and maintained a maximum height reflected a system that was sediment supply limited. A system that was not sand supply limited would have facilitated the growth of *F. spiralis* nabkha through increased sand deposition, eliciting a positive growth response (Hesp, 1981).

There was no observed trend in nabkha growth across the study area, however, the net volume of nabkha increased with distance inland. It was hypothesised that nabkha growth would be greater closer to the depositional lobes as *F. spiralis* plants would be exposed to a greater supply of sand eroded from the recently revegetated parabolic dunes. However, the significant relationship between increasing distance inland and nabkha size suggests that in the recent past there has been more sand available to *F. spiralis* plants further inland than from the eroding depositional lobes. Increased sand inputs further downwind could be caused by sand transported in active saltation/suspension in periods of high winds (Arens *et al.*, 2004). Arens *et al.*, (2004) attributed sand transport via suspension to minor deposition 200m downwind of an inland parabolic dune crest after vegetation removal. However, previous remobilisation efforts have found that a significant proportion of mobilised sand is deposited in the lee of the destabilised land form such as the parabolic dunes (Konlechner *et al.*, 2014; Arens *et al.*, 2013b). The soil profiles measured around the depositional lobes indicated that there has been significant burial (as seen by the encroaching depositional lobes noted in Chapter Two). The deposition of sand in these areas is probably related to reduced wind speeds in the lee of the parabolic dunes, as described in general by Robertson-Rintoul, (1990). Chapter Two also noted that *F. spiralis* was

colonising the depositional lobes, and possibly reducing the sand supply into the stonefield and the nabkha closer to the seaward margin.

The average sand accumulation in the study site over nine months (3.22mm) was not too dissimilar to the average sand accumulation over the one month period between February and March 2015 (2.14mm). Walker *et al.*, (2013), over the period of a year, noted that there were seasonal patterns to volume changes in a dune system after recent destabilisation. Due to limited access to Mason Bay restricting the number of erosion pin measurements taken, seasonality was not discernable from the recorded data.

On the landward margin of the study area the stony fraction looked to be buried and the surface was bare sand with small pea sized gravel. The buried stone fraction was similar to the lag deposit seen in the stonefield. From data analysis in Chapter Two it was observed that the backdunes have been eroding since the removal of *A. arenaria*. Therefore, it was considered that the stony lag deposit had not been fully exposed, rather than accumulation occurring along the landward margin of the stonefield. One of the soil profiles from the landward edge, however, did have a surface similar in texture to the stonefield, except the surface was not colonised by the characteristic stonefield plant species (*R. hookeri* var. *hookeri* or *C. muelleri*). This suggests that the stony surface has recently been exposed, and colonisation by the stonefield communities has yet to take place.

This short term study of spatial and temporal sedimentation patterns in the stonefield indicated that a small portion of sand is accumulating in the stonefield with no significant spatial patterns observed in relation to distance from the destabilised parabolic dune or *F. spiralis* distribution. The increase in *F. spiralis* nabkha size (but not height) moving inland suggests that there is a spatial element to sediment availability which was not detected over the nine month study period. Some sand deposition however is occurring close to the parabolic depositional lobes, suggesting that the stonefield is at risk from the elongation of the parabolic depositional lobes into the stonefield. In the last 5 years there has been approximately 780mm of sand accumulated in the lee of the parabolic dunes. Presently there is no significant sand accumulation occurring across the rest of the stonefield, beyond 4.5m from the depositional lobes.

Chapter 4

Event-scale stonefield sedimentation

4.1 Introduction

Coastal dune systems represent the integration of a suite of geomorphic processes and sedimentary responses over varying temporal and spatial scales (Sherman, 1995). The spatial and temporal patterns of wind speed and direction are important determinants in patterns of sand transport and deposition (Sherman and Hotta, 1990). The recent and ongoing destabilisation associated with *Ammophila arenaria* eradication will increase the potential sediment supply to the stonefield, by understanding the wind patterns within the stonefield it is hoped that coastal managers will gain a sense of where recently released sand is being deposited.

The previous chapter established that within the stonefield the net sand accumulation was low across the entire stonefield during the short term study period (nine months). Landform changes in coastal dunes over time are the sum of event-scale changes. Event-scale often establishes the local sediment transport patterns key to understanding landform developments (Sherman, 1995). This chapter examines the contribution of event-scale sedimentation in the stonefield to identify whether sand accumulation is a future threat to the stonefield plant communities. Specifically, it aims to assess patterns of sand transport and sedimentation during discrete weather events.

The sand transporting power of wind is the most effective factor in sand mobility (Tsoar, 2000). Spatial and temporal variability in wind speed results in spatial and temporal patterns in sand transport. The threshold velocity for transporting sand is 6m/s (Bagnold, 1941). The wind direction determines which way sand is transported (Sherman and Hotta, 1990). In coastal dune systems the wind speed and direction are used to determine the sand drift potential, this calculates the sand transport potential for each wind direction (e.g. Jewell and Nicoll, 2011). This chapter establishes a high drift potential using the Fryberger method, therefore, aeolian processes will determine the transport and deposition of sediment within the stonefield. The

study of spatial and temporal patterns of wind flow through the Mason Bay stonefield will help to predict sand transport and deposition within the stonefield at the event-scale, over periods of minutes to hours (Walker *et al.*, 2013).

The nature of the dune surface is an important factor in determining sand transport and deposition in dune systems. Surface roughness of a dune influences the sand drift potential by changing the threshold velocity. Vegetation cover and sediment size are two common variables increasing the bed shear stress and the surface roughness in coastal dunes (Olson, 1958; Hesp, 1981). This means that a greater wind velocity is required to transport sand. The roughness height is the height at which the wind velocity decreases due to vegetation or sediment size (Hesp, 1981). Roughness height on vegetated surfaces can be attributed to the vegetation characteristics (Olson, 1958). Wakes *et al.*, (2010) found that the roughness height of *A. arenaria* dominated foredunes was 0.24, compared to the parabolic deflation surfaces (similar to the Mason Bay stonefield) that were characterised by sand and gravel with a roughness height of 0.05. The greater the roughness height the greater wind velocity required to transport sand. Therefore the rate and direction of sediment transport reflects the wind speed and direction as well as the nature of the dune surface (Anderson and Walker, 2006).

Wind direction and speed can also be influenced by the topography of the dune system (Bauer *et al.*, 1990). Dune landforms cause topographic steering, topographic acceleration and deceleration. For example, foredunes cause topographical acceleration of wind velocities with localised flow steering as the wind moves over the landform (Hart *et al.*, 2012; Anderson and Walker, 2006; Hesp *et al.*, 2005). As the wind moves over the foredune into the backdune localised deceleration occurs in the lee of the foredune. As the wind accelerates over landforms the sand transport increases, however as the wind decelerates and drops below threshold velocity sand is deposited. Demonstrating how the spatial variability of wind causes erosion and deposition in different areas (Sherman *et al.*, 1990). Within transgressive dune systems there is an array of dune features and vegetated areas altering the wind speed and direction as the wind moves through the system.

The wind speed and direction and simultaneous sand transport need to be measured to accurately measure the event-scale sedimentation. Recent field studies coupled quantitative sand transport studies with an analysis of wind to create a more realistic approach to understanding local sedimentation patterns (Pearce and Walker, 2005; Sherman and Hotta,

1990). Measuring these factors together in the field enables studies to include the measurement of local sand supply and transport limiting factors. By measuring these factors simultaneously in the stonefield the sand transport and deposition from the recently revegetated parabolic dunes can be calculated and related to the observed wind speed and direction accurately representing the sand transported from the parabolic dunes, into the stonefield and potentially through the stonefield.

The wind regime in the Mason Bay transgressive central dune system is dominated by strong onshore westerly winds (occurred 15% of the time between 2011 and 2014 Figure 4.1). The average westerly wind speed was 9m/s. During this period the wind was above the widely accepted sand transport threshold for an ideal surface (horizontal, dry, unobstructed and unvegetated; Sherman and Hotta 1990) 42% of the time for all wind directions.

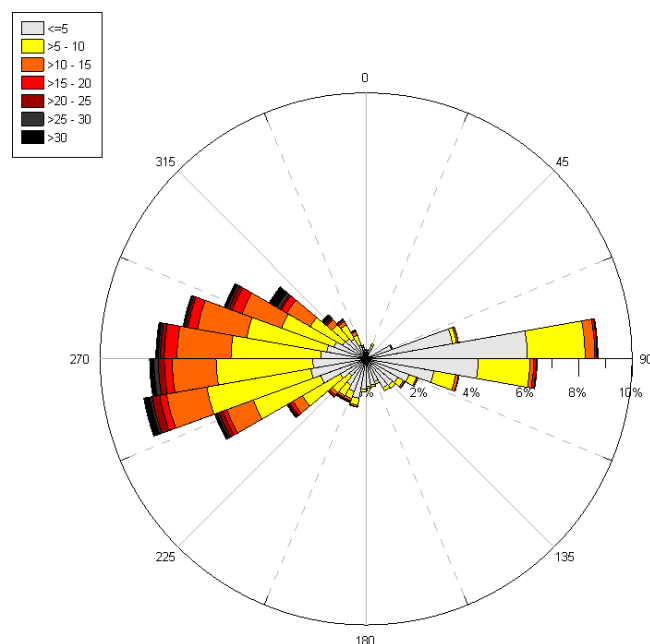


Figure 4.1: June 2011 till March 2014 wind record from the Mason Bay foredune anemometer (green dot in Figure 4.2).

This experiment was set up to assess whether the small positive sand budget measured over nine months, in Chapter Two, was a result of local wind patterns. A sediment budget analysis was conducted, in which the sand deposition or erosion is calculated within the study area by

comparing the sediment inputs and outputs. The following research questions were investigated:

- i) To calculate a sediment budget for the study site allowing for consideration of sand inputs and outputs.
- ii) Determine the dominant sand transport direction within the Mason Bay Stonefield.

4.2 Method

The event-scale sedimentation and wind patterns in the stonefield study area were investigated through a sediment budget experiment and simultaneously a wind analysis. The wind analysis was conducted to measure whether there was any spatial variability in wind direction and speed. The sediment budget experiment measured the sand transport into and out of the study site during the discrete wind events.

The importance of the measured event scale sedimentation patterns in the long-term history of the Mason Bay dune system was determined through the calculation of the potential sand drift using the Fryberger method. This model has been used to assess wind energy, sand transport potential and dune form in various environments (Jewell and Nicoll, 2011; Pearce and Walker, 2005; Bullard, 1997). Calculating the potential sand drift potential will also inform the study as to whether sand will be transported from the recently revegetated parabolic landforms into the stonefield.

4.2.1 Study site

The sediment budget analysis was carried out in August 2014 and March 2015 in the central stonefield study area. The orientation of the sediment budget plot was corrected to 067° , which aligned the long axis of the plot with the prevailing wind direction prior to the experiment (red rectangle in Figure 4.2). This was to ensure that the sand transporting winds and all sedimentation would occur along the long axis of the study site to accurately record sand inputs and outputs. The original study site was orientated to the direction of the parabolic trailing arms (112°) (black rectangle in Figure 4.2).

The seaward edge of the corrected sediment budget plot was located just downwind of the devegetated depositional lobes of the parabolic dunes described in Chapter Two (Figure 4.2). The devegetation of the parabolic dunes has increased the available sand for downwind transportation. The landward margin of the corrected study area was in front of a deflation ridge. The surface of the study area was a surface lag deposit comprised of larger stone fraction, a scattering of *Ficinia spiralis* nabkha, *Raoulia hookeri* var. *hookeri* and associated stonefield plant species.

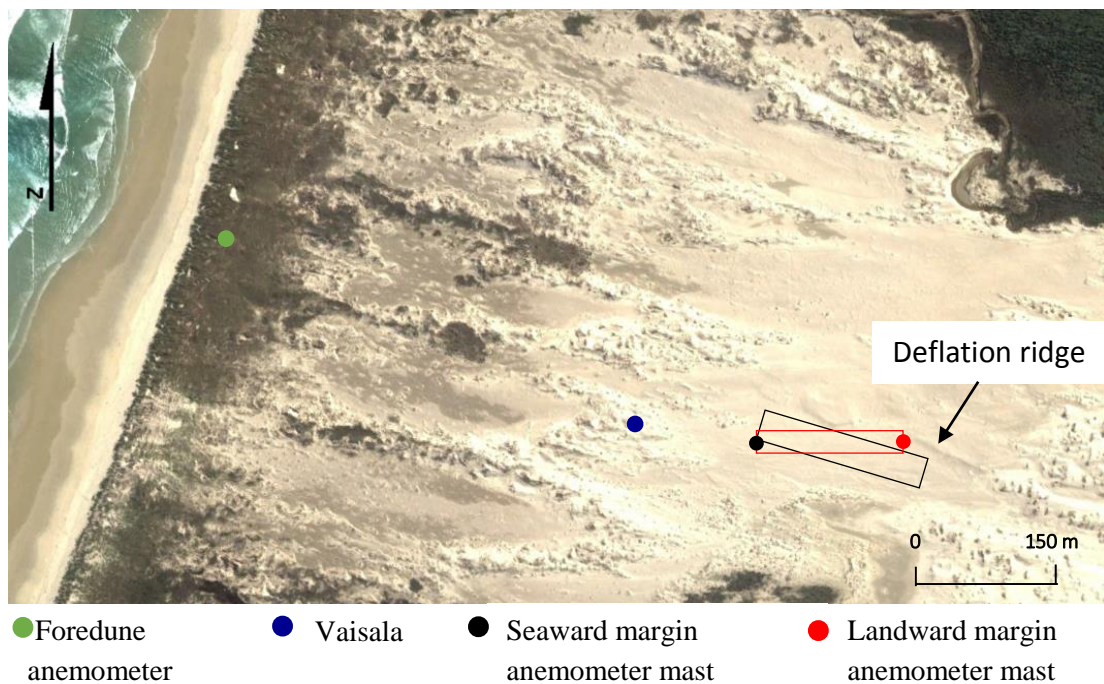


Figure 4.2: The anemometer layout in the stonefield study site. At the seaward (black dot) and landward (red dot) margin four anemometers were erected on a vertical mast. The red rectangle is the reoriented sediment budget plot and the black rectangle is the original study area.

4.2.2 Wind analysis

Anemometer masts were erected at each end of the sediment budget plot to measure wind speed and direction. Each mast contained four 2D sonic anemometers (Gill ‘Windonics’) in a vertical array, logarithmically spaced (black and red dots in Figure 4.2 and Figure 4.3b). These masts were offset from the traps to prevent any interference in sand. The anemometers were connected to a CR1000 Campbell data logger and wind speed and direction and speed were recorded at 1-second intervals (in m/s). The vertical array of anemometers were used to (i) ensure the wind direction was the same at both ends during the sediment budget experiment so that an accurate

calculation of sand entering and leaving the study site was being recorded; and (ii) examine any increase or decline in wind speed across the stonefield.

Dune landforms topographically steer the wind, and therefore to understand the degree of steering occurring in the stonefield the wind speed in the stonefield was compared to the regional wind using a Vaisala 2D anemometer. The Vaisala was erected at a height of six meters on the top of the high depositional lobe (blue dot in Figure 4.2), approximately 20m above the level of the stonefield. The Vaisala recorded the regional wind direction and speed (m/s) at 1-second intervals. The foredune permanent anemometer (RM Young marine) was also used to determine the regional wind direction (orange dot Figure 4.2). It was originally hoped that the foredune Yong anemometer could be used to aid in the analysis of the topographical steering of wind through the dune complex to the stonefield. During the August study period the foredune anemometer encountered technical difficulties so was unable to be used, but was running during the March study period.

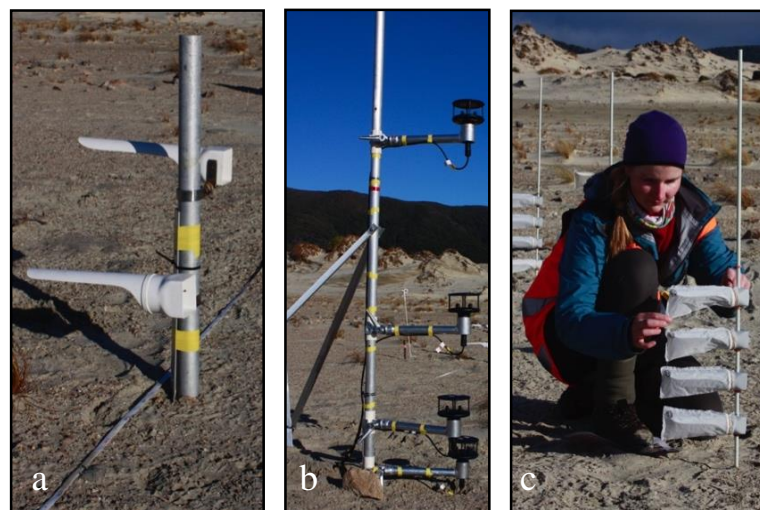


Figure 4.3: a) Fixed sand traps (without sand bags). b) Wind anemometer mast. c) Swing traps with bags.

4.2.3 Sediment budget analysis

To calculate the sediment inputs and outputs an array of sand traps were deployed over five to ten minute intervals in an identical formation at either end of the sediment budget plot (Figure 4.4a). Two types of traps were used; swing and fixed traps. The swing traps were designed by Mike Hilton of the University of Otago and are self-orientating into the wind allowing for a more accurate sediment capture (Figure 4.3c). The fixed traps hold a larger amount of sand so

they could, therefore, be deployed over a longer period of time if required, but do not move in relation to changing wind conditions (Figure 4.3b).

The configuration of fixed and swing sand traps was set to capture sand entering and leaving the study area. The main mode of sediment transport observed through the stonefield environment was streamers of saltating sand close to the bed, therefore, the lowest of the vertical array of swinging sand traps were located as close to the bed as possible (60mm above the ground). The wind experienced during both experiments involved low rates of sand flux, so to measure as much sand transport as possible the sand traps were all located below 460mm.

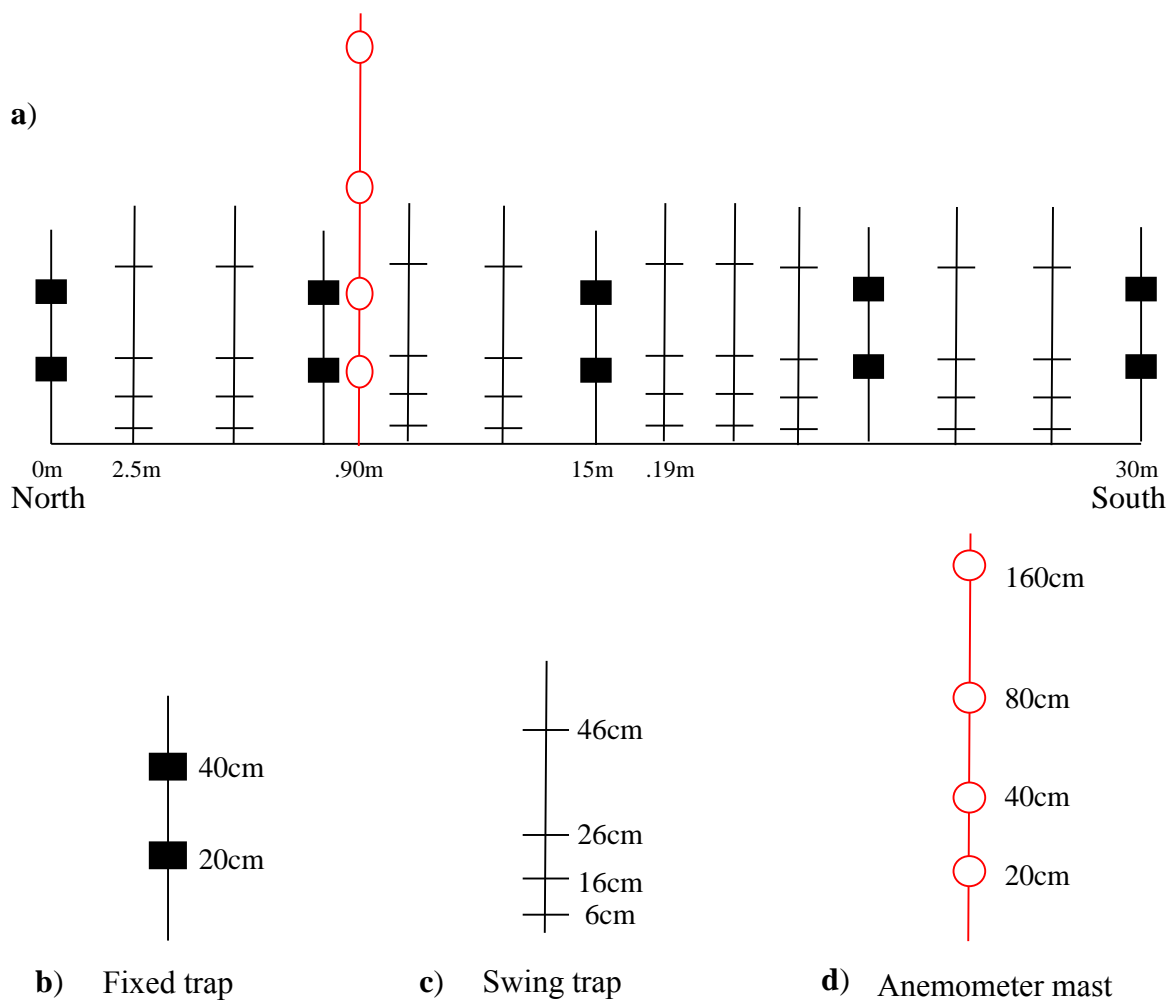


Figure 4.4: The anemometer and sand trap layout. a) Layout of fixed and swing sand traps, and anemometer mast. The layout is repeated at the landward and seaward edge of the study site, facing west. b) The configuration of fixed traps at 40 and 20cm from the ground. c) Configuration of swing traps at 46, 26, 16, 6cm from the ground. d) Configuration of the anemometers on the mast 20, 40, 80, 160cm.

The wind speed only averaged 7.4m/s (recorded from the highest landward wind sonic 1.6m above the ground), with a maximum gust of 9.65m/s, during the August study. In March the wind averaged 5.8m/s, with a maximum gust of 11.89m/s. Despite being above the transport threshold (6m/s) this was insufficient to transport significant quantities of sand to permit accurate analysis of the proportion of sand accumulating (or not) in the stonefield. There was also a small portion of sand that accumulated in the sand traps between each experiment period, despite coverings designed to prevent this. Therefore the sediment budget analysis was not included in the results of this study.

4.2.4 Analysis

4.2.4.1 Sediment budget analysis

The sand captured in each sand trap was weighed and summed for each trial, to represent sand inputs (seaward margin) and outputs (landward margin). The total sand captured at the seaward margin was then compared to the total sand captured at the landward margin. The difference between the margins determined how much sand was either deposited or eroded from inside the sediment budget plot. The wind direction from the top anemometer of each anemometer mast were compared to ensure the wind was moving through the long axis of the sediment budget plot (that is, the anemometers recorded the same wind direction at each end).

4.2.4.2 Wind analysis

The regional wind (Vaisala) and wind in the stonefield (recorded from the highest anemometer on each stonefield mast) was compared to determine whether there was any wind steering as the wind passed through the stonefield. As the Vaisala was not operating in March the foredune anemometer was used instead. To compare the wind direction and the speed between the three anemometers, the wind direction for the Vaisala and the foredune anemometer over the two study periods (August 2014 and March 2015) were analysed. From the Vaisala and foredune wind records 17 periods of stable wind direction (three to five minutes of unidirectional wind) were selected during the two study periods. The timestamp for the start and end of each stable wind period was recorded and the same periods were extrapolated from the top anemometer for both the landward and seaward anemometer masts. The average wind speed and direction was calculated for each of the 17 extrapolated periods, for each of the anemometers. These averages were then compared for each event in a scatter plot. If there were no steering occurring across the sediment budget plot, the stonefield anemometers would record the same wind direction.

4.2.4.3 Digital terrain model

A digital terrain model (DTM) was created in SURFER using the data from the topographic survey. Two profiles were extracted from the DTM; (i) through the center of the study site used in Chapter Three beginning on the parabolic depositional lobe (black dashed line through the black rectangle in Figure 4.5); and (ii) between the anemometer masts through the sediment budget plot (red line through the red rectangle in Figure 4.5). The digital elevation model (DEM) provides a basis for interpreting the observed wind speeds across the stonefield.

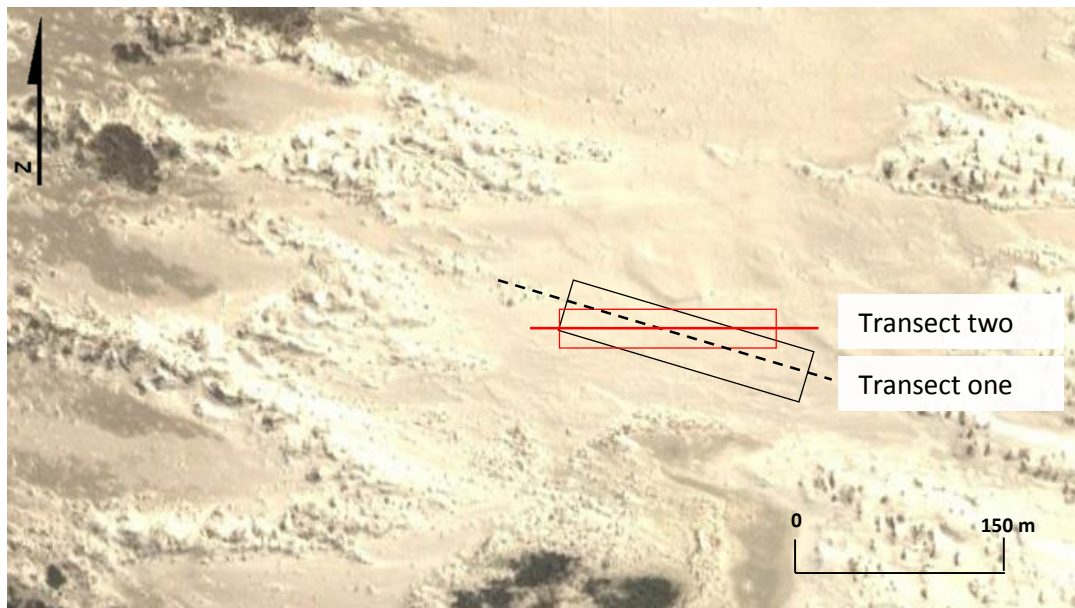


Figure 4.5: The two profiles to be extracted from the digital terrain model (DTM). The first is through the center of the study site (black dashed line through the black rectangle), the second is between the anemometer masts (red line through the red rectangle).

4.2.4.4 Fryberger Model

Fryberger's model is an accessible method for analysing meteorological data to assess the wind energy, sand transport potential and predominant sand transport direction (Fryberger, 1978 and 1979). This model was used to predict the dominant direction sand enters the stonefield and the importance of the measured even-scale sedimentation patterns. With hindsight, this model should have been calculated earlier in the study to orient the study area. The accessibility of this model has meant that many coastal dune systems have been categorised by Fryberger's classification (Table 4.1), providing an excellent opportunity to compare the wind energy environment of Mason Bay to global coastal systems.

Table 4.1: Fryberger's (1979) classification of wind energy environments using total drift potential (DP) and directional variability (RDP/DP) ratio. Adapted by Bullard (1997) to m/s.

Values of drift potential calculated using wind speeds in m/s	RDP/DP	Wind-energy environment
<27	<0.3	Low-energy environment, obtuse bimodal
27-54	0.3-0.8	Intermediate-energy environment, obtuse to acute bimodal
>54	>0.8	High-energy environment, narrow unimodal

A long-term wind record from the foredune anemometer (orange dot Figure 4.1c), between June 2011 and August 2014 was available to calculate the sand drift potential within Mason Bay dune complex. This information was used to infer the potential sand drift and direction into the stonefield. The sand “drift potential” (DP) was calculated using Fryberger's model adjusted by Pearce and Walker (2005) (Fryberger, 1978 and 1979). The Fryberger model combines frequency and magnitude of effective winds, and characterises the amount and directional variability of the driving force in aeolian dune morphodynamics (Pearce and Walker, 2005). The equation to calculate DP is:

$$DP \propto V^2(V - V_t)t \quad (1)$$

Where DP is the amount of sand drift expressed in vector units (VU); V the mean wind velocity in meters per second at 10m height for each wind class in each directional class (Pearce and Walker, 2005), V_t the threshold velocity at 10m height 6 m/s (Bagnold, 1941); and the frequency of transporting winds in each direction t expressed as a percentage of the total period of analysis. The $V^2(V - V_t)$ portion of Eq. (1) is the ‘weighting factor’, in which strong winds are given high weightings and weaker winds lower weightings. The value of $V^2(V - V_t)$ is divided by 100 to lower the magnitude of the weighting factors and simplify the plotting of sand roses (Fryberger, 1979). The DP was calculated for each of the 16 compass directions by adding the VU for each speed class above the threshold (6m/s) in each direction class. The compass direction classes were equal class ranges (i.e. North 350-011°), this method is similar to

previous investigations (Pearce and Walker, 2005). The DP for all the wind directions was used to calculate the resultant drift direction (RDD) and the resultant drift potential (RDP) through a vector analysis. The RDP/DP was calculated to measure the directional consistency of winds capable of moving aeolian material (Table 4.1). The DP for each wind class was plotted on an angular histogram with an arrow indicating the RDD and RDP.

The height of the foredune weather station was two meters so all the wind speeds had to be corrected to 10m in height using the logarithmic law (Arya, 1988).

$$V_R = V_Z \frac{\ln(Z_R/Z_0)}{\ln(Z/Z_0)} \quad (2)$$

Where V_Z is the wind speed (knots) at elevation z (2m), V_R is wind speed at a 10-m reference elevation, Z_R is 10m, and Z_0 is the roughness height (assumed to be 0.01; Archer and Jacobson, 2003). V_R was then corrected to m/s (1 knot = 0.5144 m/s).

4.3 Results

4.3.1 Spatial wind analysis

Wind direction was compared over a stable three to five minute wind direction for the August studies showed that the Vaisala (measuring regional wind at 6m height) recorded a slight variation in wind direction of 020° degrees towards the south (Figure 4.6). The foredune anemometer recorded similar wind directions to the top stonefield anemometers during the March wind events, when the Vaisala was not deployed (Figure 4.6 and Figure 4.7a). Both the landward and seaward top anemometers recorded the same wind direction for each event (black dot and red diamond overlapping Figure 4.7a). A regression analysis of the recorded wind speeds at the seaward and landward edge of the stonefield showed a significant correlation (p.value of 0.001), indicating wind is moving down the long axis of the study plot (Figure 4.8). The wind directions recorded during the 17 wind events in the stonefield ranged between 260° and 301°.

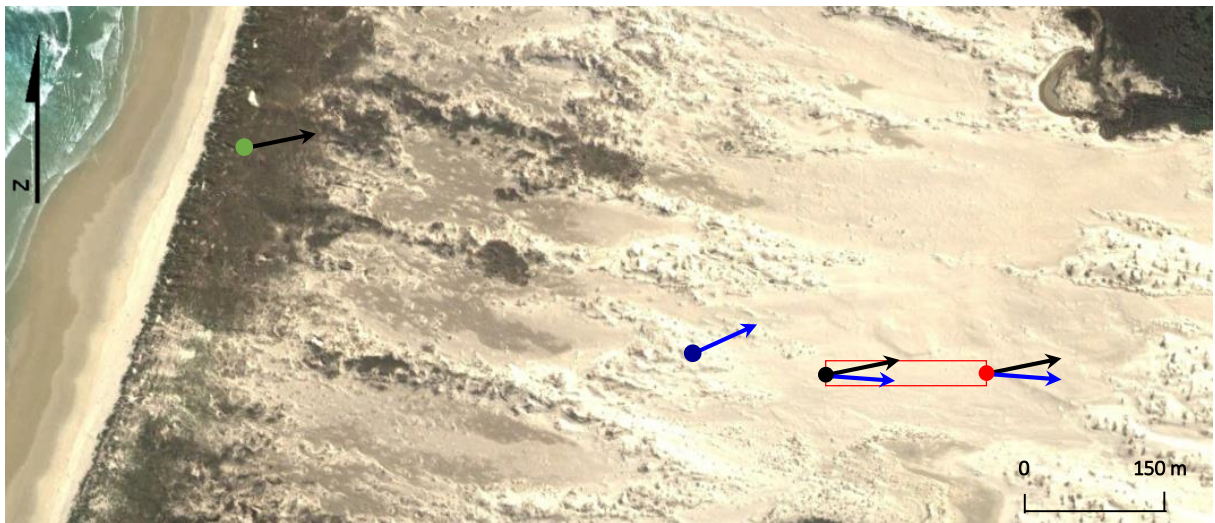


Figure 4.6: Summary vector diagram of the average wind direction for the August (blue arrows N=12) and March (black arrows, N=5) study periods at each of the four anemometer locations

The regional (Vaisala) and foredune wind speeds were greater than those recorded by the stonefield anemometers (Figure 4.7b). In the stonefield the wind speeds recorded at the landward margin were often greater or equal to the wind speed recorded at the seaward edge during each wind event (Figure 4.7b). Regression analysis of the seaward and landward margins showed a significant positive relationship between the winds speeds recorded at either end of the stonefield (p.value of 0.00) (Figure 4.9). This strongly suggested that there was no loss in wind speed across the stonefield moving inland. There were periods of stronger wind velocities (above 4m/s) in which the wind velocity on the landward margin was greater than the seaward margin (Figure 4.7b). Suggesting the inland portion of the stonefield is more exposed than the seaward margins. It appears as though the depositional lobes of the parabolic dunes are sheltering the eastern margins of the stonefield.

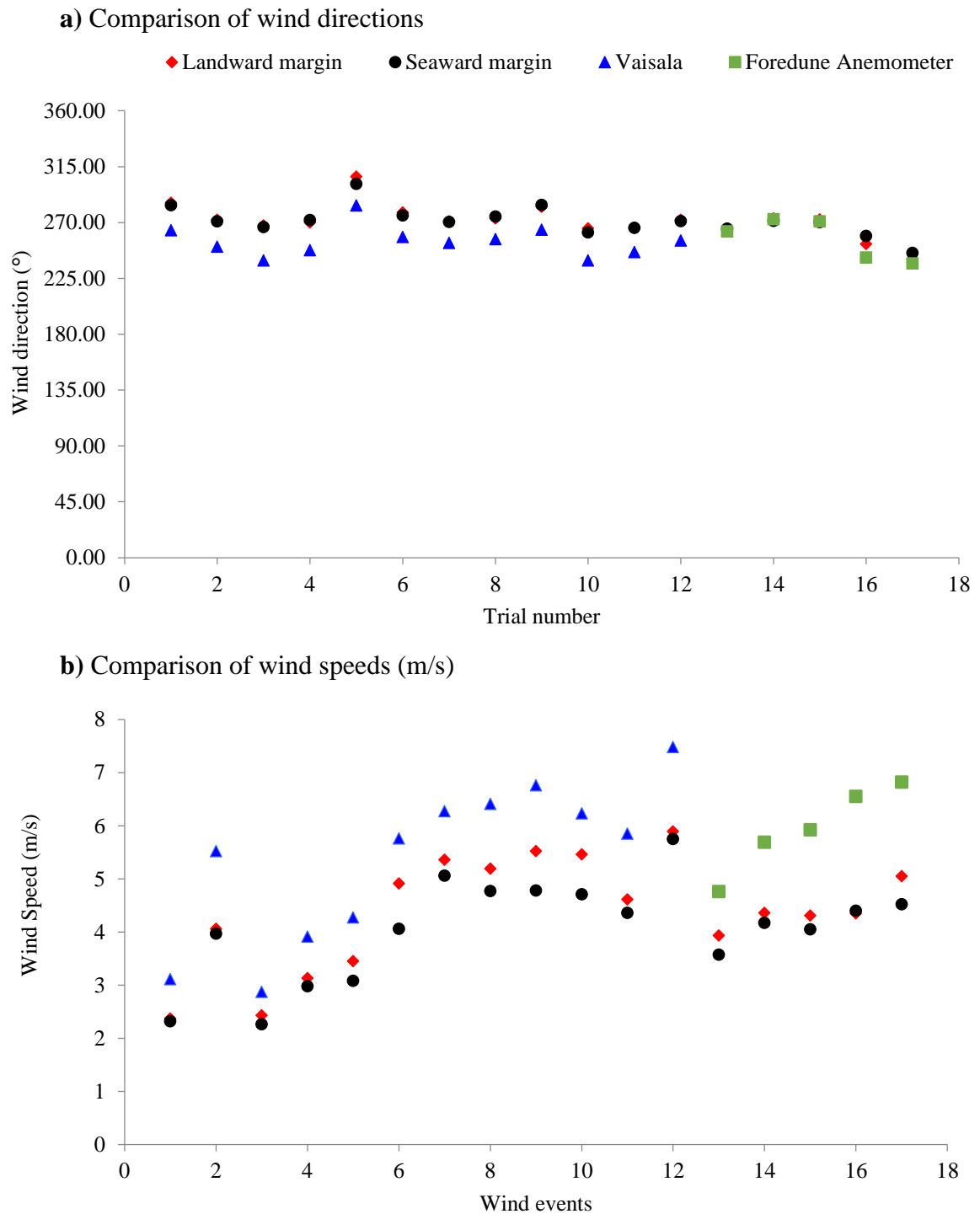


Figure 4.7: Comparisons of wind direction (a) and wind speed (b) between the landward and seaward stonefield, regional (Vaisala) and fore-dune anemometers. Each represents a three to five minute section of the wind record when either the regional or fore-dune anemometers were at a constant direction (17, three to five minute sections were analysed). The wind events were recorded in August 2014 (N=12) and March 2015 (N=5).

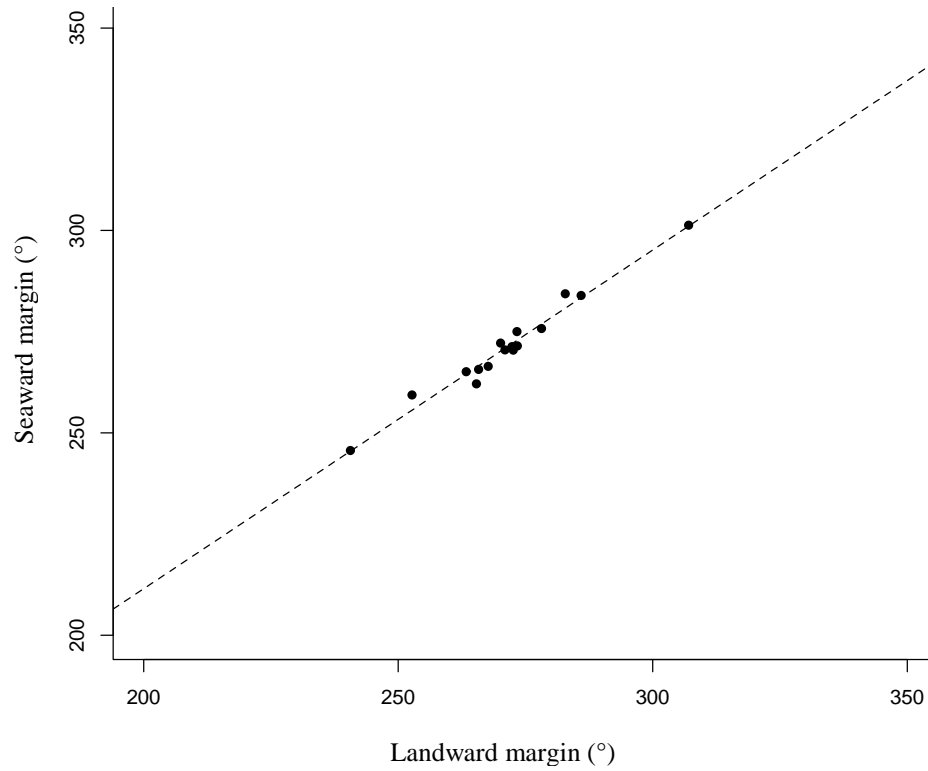


Figure 4.8: Regression analysis of wind direction (°) at the landward and seaward margins of the study area for 17 trials ($r^2 = 0.969$, $df=15$).

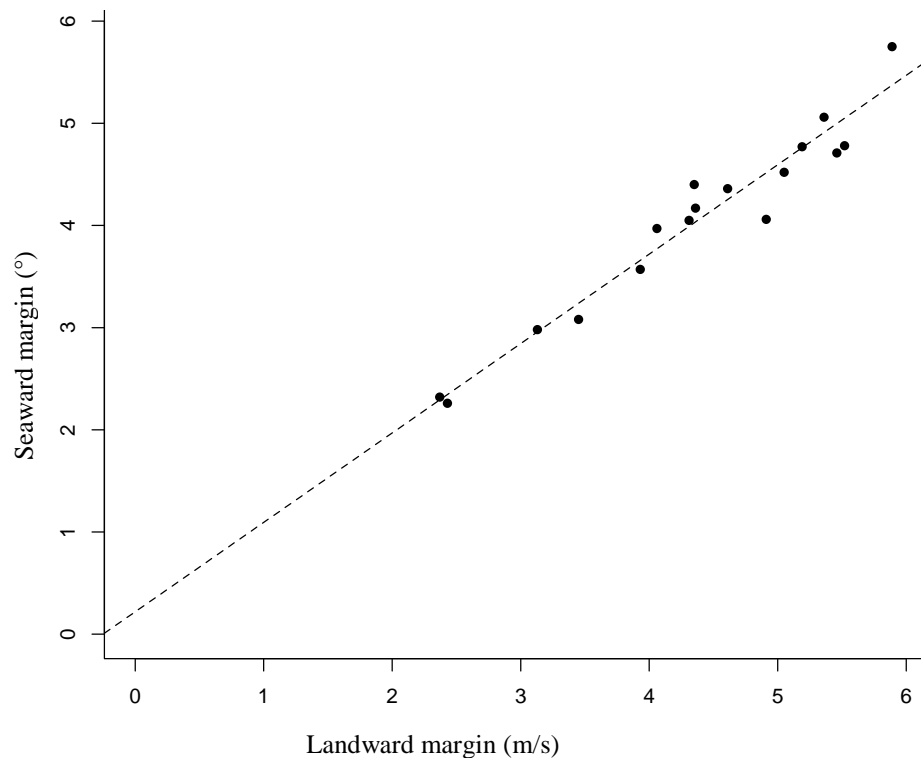


Figure 4.9: Regression analysis of wind speed (m/s) at the landward and seaward margins of the study area for 17 trials ($r^2 = 0.941$, $df=15$).

4.3.2 Stonefield digital terrain model

The elevation of the stonefield containing the study areas slopes towards the east. The eastern margin is 5.45m higher than the western margin (representing a 2.7m elevation gain per 100m) (Figure 4.11). Small hummocks are evident near the seaward end of the plot, these are the devegetated parabolic deflation lobes. Between the seaward and landward anemometer masts through the sediment budget site there was an elevation increase of 3.5m (Figure 4.12).

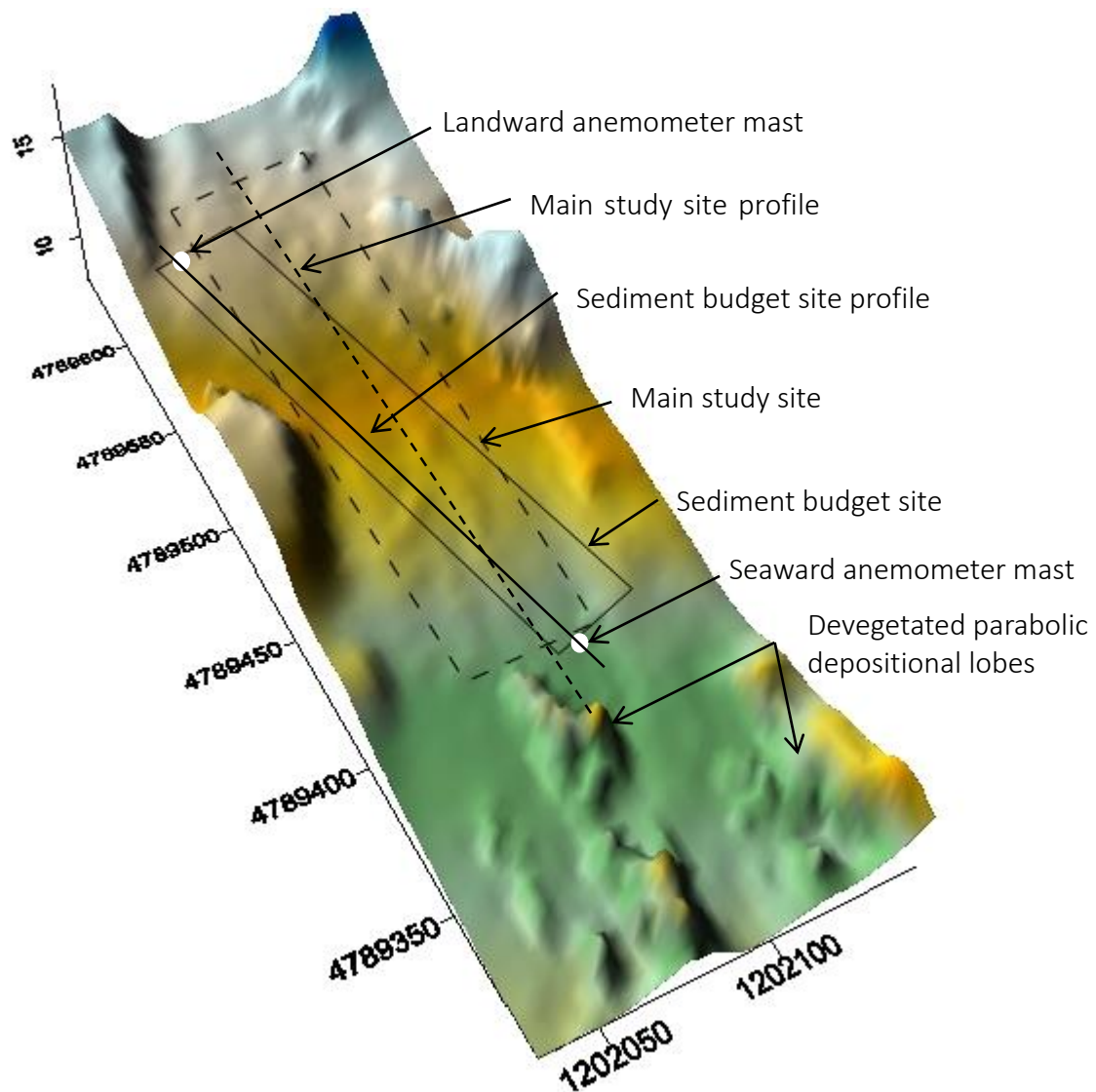


Figure 4.10: Digital terrain model of the study areas in the stonefield. The dashed rectangle is the outline of the main study site. The solid rectangle is the outline of the sediment budget plot. The white dots are the locations of the landward and seaward anemometer masts. The coordinate system is in meters.

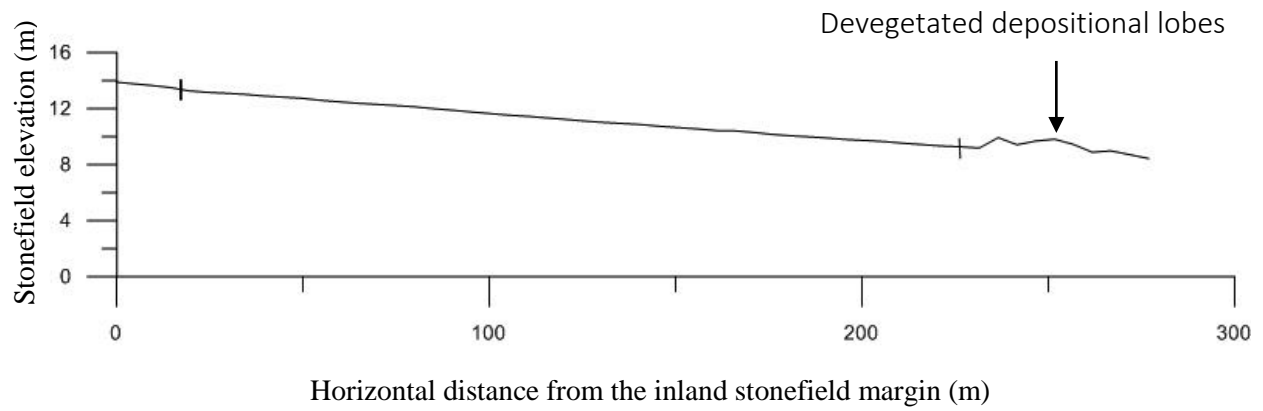


Figure 4.11: Cross section through the short term sedimentation study area heading eastwards. The intersecting lines indicate the start and finish of the study area.

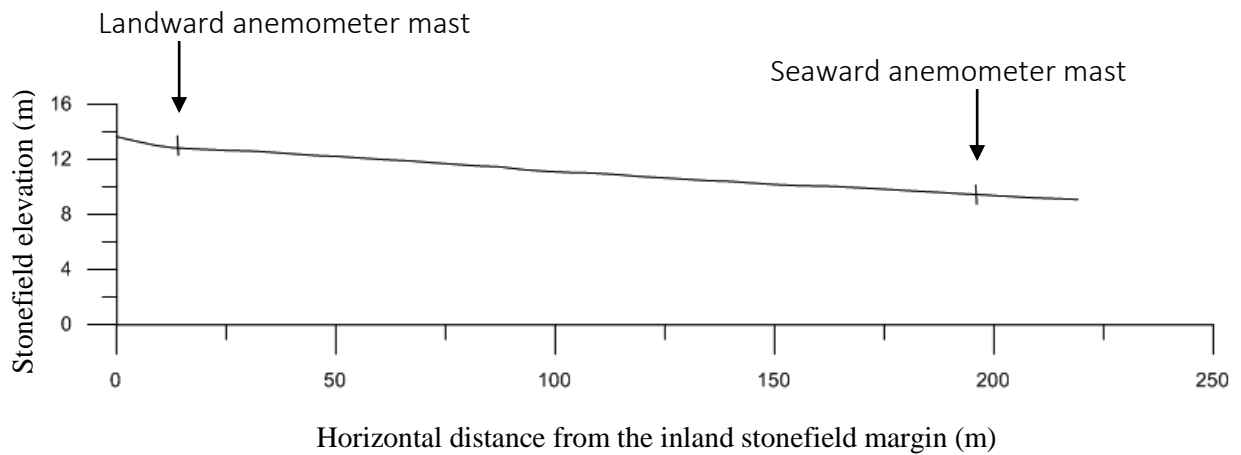


Figure 4.12: Cross section through the sediment budget plot heading landwards. The intersecting lines outline the start and finish of the sediment budget site.

4.3.3 Mason Bay sand drift potential

The sand drift potential calculated using the Fryberger equation (Eq. (1)), indicates that the Mason Bay environment is a high energy wind environment ($DP > 54$). In Mason Bay the drift consistency of winds capable of moving sand the RDP/DP was 0.82 which according to the Fryberger (1979) classification of wind energy environments was narrow unimodal meaning the wind energy predominates from a narrow Westerly direction (Figure 4.13). The resultant drift direction (RDD) is onshore at 094.8° which is reflected in the orientation of the existing parabolic dunes at Mason Bay.

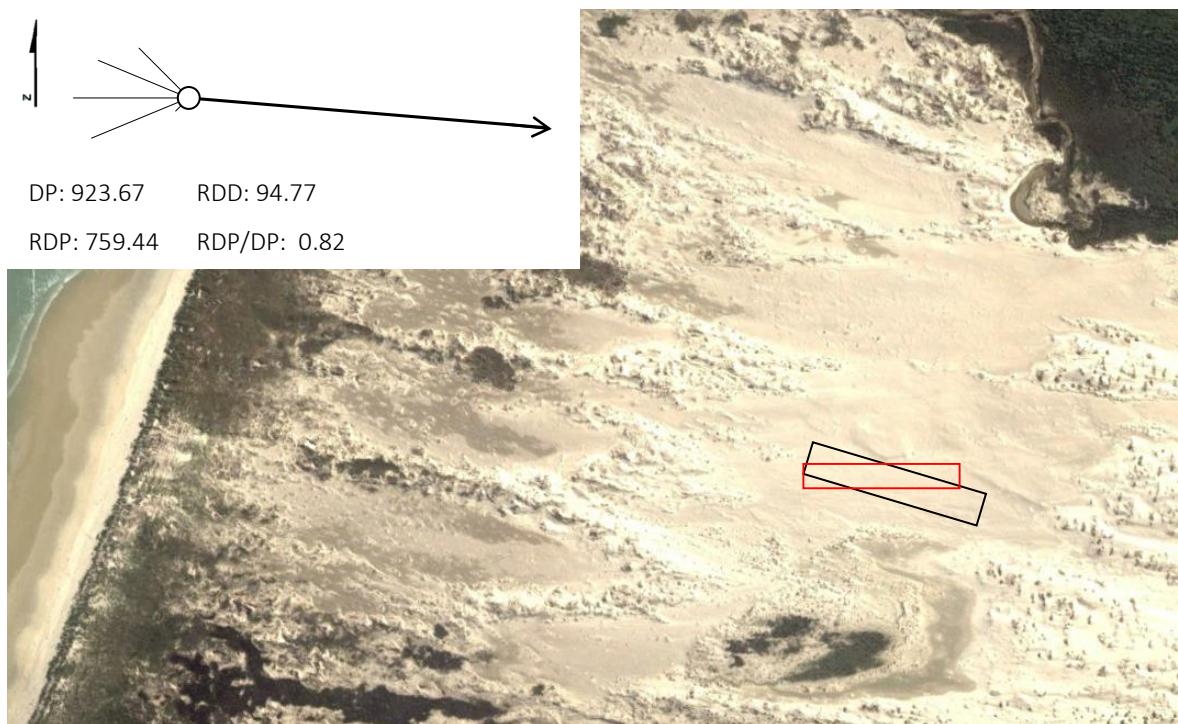


Figure 4.13: Sand drift rose calculated via the Fryberger model (Eq. (1)), with wind values from the Mason Bay foredune anemometer between 2011 and 2014. The rose represents the Drift Potential (DP) for 16 equal compass directions. The bold line indicates the Resultant Drift Direction (RDD) and the Resultant Drift Potential (RDP). The aerial photograph is from 2013 Google Earth image. The black rectangle represents the study area and the red rectangle represents the outline area in which the sediment budget analysis was carried out.

4.4 Discussion

The Fryberger model indicated that Mason Bay has a high sand drift potential. The wind regime at Mason Bay was classified as narrow unimodal, where the sand transporting winds are from one narrow direction (Fryberger 1979). In Mason Bay the sand transporting events are predominantly onshore (southwest to northwest), which would mean sand is transported landwards through the stonefield. It should be noted that not all competent winds are geomorphically effective. The Fryberger model needs to be supported by research into the influence of localised supply and transport limiting factors in the dune system (Pearce and Walker 2005). The sediment budget analysis would have complemented and supported the Fryberger model, but inconveniently the wind speeds during the study periods were insufficient for transporting enough sand to make comparisons. To understand the importance of wind regimes in the transport of sediment across the stonefield in relation to event forced sedimentation patterns the sediment budget analysis will need to be completed. The sediment budget analysis incorporates the effects of the regional sediment inputs and surface roughness during event-scale sedimentation.

The analysis of wind speed and direction through the stonefield at Mason Bay during discrete wind events established that there is no decline in wind speed across the stonefield. The top anemometer at the landward edge of the stonefield often recorded higher wind velocities than the top anemometer at the seaward edge. The stonefield increases in elevation by approximately 3.5 meters across the sediment budget plot between the landward and seaward anemometers. As one moves inland across the stonefield away from the shadowing effects of the parabolic depositional lobes, and increase in elevation, the stonefield is exposed to higher wind velocities. This exposure, in conjunction with the sparse vegetation cover, may be helping to limit sand deposition in the stonefield. This study was limited by low wind speeds in the stonefield (which did not exceed 9m/s). To test whether acceleration is occurring within the stonefield during increased wind speeds, further studies over a wider array of wind speeds should be conducted.

Surface roughness influences the sand deposition in the stonefield, as it modifies the near surface velocity, reducing the bed shear stress causing sand deposition (Sherman and Hotta, 1990). The rough boundary layer in the stonefield is created by the stony lag deposit and vegetation, both sand binding species and other species i.e. *Raoulia hookeri* var. *hookeri*. The small positive sediment budget observed in Chapter Three could be a result of sand entrainment

in the rough boundary layer. The lack of gradient in the wind across the stonefield suggests that any future accumulation will be linked to the sand trapping efficiency and growth response of sand binding species, like *F. spiralis*. Sand binders trap sand and grow in response, increasing their trapping efficiency and, therefore, increasing sand accumulation (Zarnetske *et al.*, 2012).

This chapter examined the contribution of event-scale sedimentation in the stonefield during prevailing South Westerly wind events to assess the patterns of sedimentation during weather events and determine whether sand is accumulating in the stonefield during such events. Despite Mason Bay dune system having a high sand drift potential and unimodal onshore sand drift, the lack of wind speed deceleration across the stonefield indicates that there is little potential for sand deposition to occur in the stonefield. This study indicates to coastal managers that sand binding species will be the principal cause of sand deposition in the stonefield if sand inputs increase.

Chapter 5

The impact of sedimentation on the native dune species *Raoulia hookeri* var. *hookeri* and *Ficinia spiralis*.

5.1 Introduction

Dynamic restoration restores dune mobility, wherein the erosional and depositional processes create a variety of landscapes to support a range of plant communities. (Konlechner *et al.*, 2014; Walker *et al.*, 2013; Mori, 2011). As the restored dune systems respond, what are the short-term implications for pre-existing native plant communities persisting downwind of these once stabilised dune forms? It has been noted in previous restoration projects that there is often a decrease in species diversity and the remobilised dunes came at the expense of down-wind wetlands and other ecosystems (Hesp and Hilton, 2013). It is expected that after dynamic dune restoration, the processes of plant dispersal and colonisation will result in an increasingly “natural” distribution of plant species (Konlechner *et al.*, 2014).

Plant community composition in coastal dunes reflects the micro environmental conditions created by biotic and abiotic factors. Plants have adapted to the great variety of microhabitats in coastal dunes, increasing biotic diversity and the resilience and integrity of coastal dune ecosystems (Roman and Nordstrom, 1988). The variety of habitats within coastal dunes reflects changes in climate, sand burial, salt and other plant species interactions. These habitats can be altered by abiotic disturbances such as changes in sand burial rates or erosion leading to allogeneic succession of the plant communities (Maun, 2009; Perumal and Maun, 2006).

Sand burial is a key abiotic factor influencing the distribution of plant communities in coastal dune systems. Sand burial alters the microenvironment surrounding the plant in relation to factors such as soil moisture, temperature, and light (Figure 5.1) (Maun, 1998; Baldwin and Maun, 1983). Sand burial also controls the success of germination and seedling establishment

(Maun, 1994). Plant and community responses to sand burial are rate dependent, and above a certain critical level, plants are negatively affected (Skyes and Wilson, 1990). Sand burial filters out species as the level of burial exceeds their levels of tolerance.

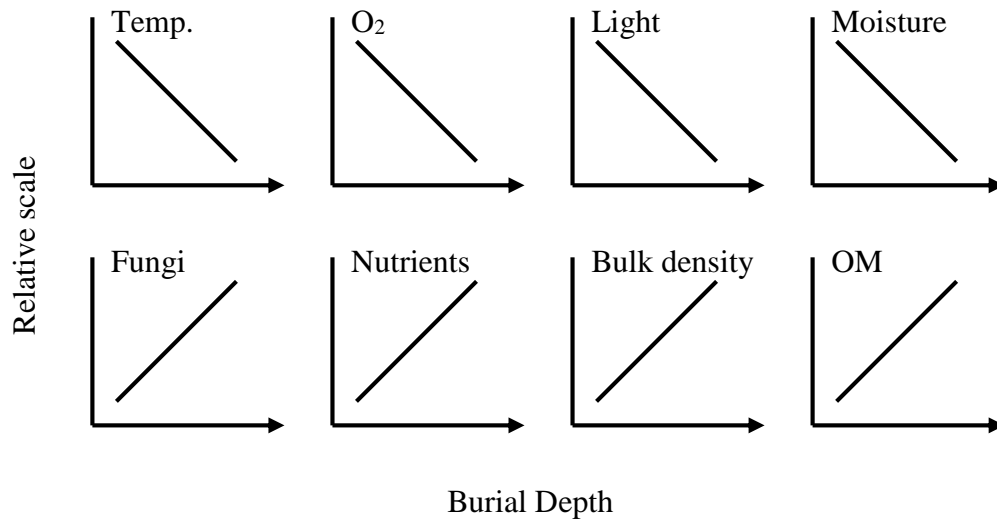


Figure 5.1: Changes in temperature, moisture, bulk density, organic matter (OM) and other environmental factors at different burial depths (adapted from Maun, 1998 and Maun, 2009).

Certain dune species favor higher rates of sand accretion. *Ficinia spiralis*, (Musaya and de Lange, 2010), is a sand binding sedge that used to be throughout New Zealand coasts. Sand binding plants are characterised by rapidly growing underground stems, which possess the ability to root near the tips of the branches and to put forth new shoots as fast as the old ones are buried (Cockayne, 1982). *F. spiralis* is most commonly associated with exposed and mobile environments, generally appearing when there is a rapid increase in blown sand, thus initiating dune-building processes (Cockayne, 1990b). Previous studies have shown that the growth of *F. spiralis* seedlings is stimulated by moderate rates of sand accumulation of approximately 10-20cm per year (Bergin and Kimberly, 1999; Sykes and Wilson, 1990), and that *F. spiralis* is also sensitive to erosion of sand around its roots and buried rhizomes (Elser 1970). *Ammophila arenaria* displaced *F. spiralis* from the Mason Bay dune system as it can tolerate higher rates of sand burial (Hilton *et al.*, 2009).

Raoulia hookeri var. *hookeri* is also found in coastal dunes, however, in contrast to *F. spiralis* it is a low lying cushion plant associated with coastal deflation surfaces in the Mason Bay dune

system. *R. hookeri* var. *hookeri* was considered to be representative of the non-sand binding plant community in stonefield. Non-sand binders are plants which do not elicit any positive biophysical feedback between sand accumulation and plant growth. *R. hookeri* var. *hookeri* is an endemic New Zealand cushion species that forms dense mats or cushions with very small, close set leaves (Dawson *et al.*, 1993). *R. hookeri* var. *hookeri* is commonly associated with higher elevations, sand and infertile soils (Ullmann *et al.*, 2007; Sommerville *et al.*, 1982). In the coastal environment *R. hookeri* var. *hookeri* is found to inhabit back dune deflation surfaces (Hilton *et al.*, 2005). Deflation areas, such as the stonefield, share environmental similarities with alpine areas where cushion plants are abundant, as there are strong winds, unstable substrates and high solar radiation (Korner, 2003). *Raoulia* species' mode of dispersal is wind and some species were found to have a dispersal distance greater than 10m (Spence, 1990). Studies have focused on the distribution of *Raoulia* species in the alpine zone (Smissen *et al.*, 2003), in braided rivers (Ullmann *et al.*, 2007), and following colonisation after sand mining (Partridge, 1992). There is little research on the coastal distribution of *R. hookeri* var. *hookeri*.

As the Mason Bay dunes become mobile, it is predicted that sand deposition will increase in the Mason Bay stonefield. An increase in sand deposition would be considered a natural disturbance, however what are the implications for the existing native plant communities inhabiting this unique deflation environment? The response of *F. spiralis* in the stonefield is an indicator of the future stonefield communities if sand accumulates. The response of *R. hookeri* var. *hookeri* to different rates of sand burial is unknown but important for understanding its coastal distribution and conservation. It is hoped that through this study the relationship between the sedimentation patterns and the response of sand-binding and intolerant species will provide an indication of the future of the stonefield habitat.

This chapter assesses the impact of the sedimentation patterns observed in Chapter Three and Four on the plant communities inhabiting the stonefield. In the study area there are two distinct plant communities; the non-sand binding species and the sand binders. *R. hookeri* var. *hookeri* is used in this thesis as a representative non-sand binding species and *F. spiralis* as a sand binding species. In this chapter the following questions are addressed:

- i) Is there a correlation between the observed sedimentation patterns and *R. hookeri* var. *hookeri* surface area patterns?

- ii) Is there a correlation between the observed sedimentation patterns and *F. spiralis* surface area patterns?
- iii) How does sand burial directly affect the growth of a related taxon within the *R. hookeri* complex?

5.2 Method

To analyse the response of stonefield plant communities to changing patterns in sand accumulation and erosion, two species were used as indicator species. This study hypothesised that *F. spiralis* would be positively associated with sand accumulation and *R. hookeri* var. *hookeri* negatively associated. Little is understood in regards to tolerance of the non-sand binding species in habiting the stonefield, therefore a burial experiment of a related taxon within the *R. hookeri* complex was carried out.

5.2.1 Relationship between *F. spiralis* and *R. hookeri* var. *hookeri* surface area and sedimentation patterns

Using the same study area as in Chapter Three, the surface area of *R. hookeri* var. *hookeri* and *F. spiralis* was calculated for each 10m² quadrant using five 1m² quadrats (Chapter Three). A vertical photograph of each 1m² quadrat was taken in June 2014. Using ImageJ 10.2 the perimeter of all individuals of each species was outlined and the total surface area per quadrat was calculated (Park *et al.*, 2012). The average surface area of the five quadrats for the two species was calculated to represent the 10m² quadrant. Species presence was also noted in each of the 1m² quadrats to survey the different species inhabiting the stonefield.

The average sedimentation (sand accumulation or erosion (mm)) for each 10m² over nine months was calculated by averaging sedimentation recorded by erosion pins in the center of each 1m² quadrat (Chapter Three). This determined whether there was any relationship between patterns of sedimentation and the surface area of *R. hookeri* var. *hookeri* and *F. spiralis* across the stonefield.

5.2.2 *Raoulia hookeri* burial experiment.

The response of *R. hookeri* var. *hookeri* to burial has not yet been studied, therefore a controlled experiment was carried out looking at both direct sand burial and incremental burial over a four-week period. *R. hookeri* var. *hookeri* species found in Mason Bay are not grown

commercially and for the purpose of this study, plants from Mason Bay, Stewart Island could not be cultivated, so commercially available *R. hookeri* was used instead. The *R. hookeri* var. *hookeri* plants found in the stonefield differed morphologically from those used in the burial experiment *R. hookeri* (Figure 5.2). The leaves of Mason Bay *R. hookeri* var. *hookeri* are smaller and stems were more tightly packed (Figure 5.2b) than the commercially available *R. hookeri* plants, which were greener with larger leaves and less tightly packed stems (Figure 5.2a). Originally 21 *R. hookeri* plants were sourced from Ribbonwood nurseries (Dunedin), however these plants contracted a fungal infection in the greenhouse and were too large for a controlled burial experiment. The next set of *R. hookeri* plants was sourced from Moa nurseries (Dunedin). These plants were on average 70mm in diameter (Figure 5.2a).

Each plant was individually potted in commercially available fertilised potting mix in 100mm diameter pots and kept in a covered area outside. The experiment ran from April until June 2014. There were six burial treatments and one control treatment and for each treatment there were three plants (Table 5.1). Five wooden pins were inserted into each plant in a cross formation. The pins were marked with the burial depths and the height of the plant at the start of the study. The pins were used to ensure an even cover during sand burial. Sand from nearby St Kilda beach, which was considered to be of the same grain size as s and from Mason Bay, Stewart Island, was collected and washed to remove salt.

Plants received one of two sand treatments; direct burial (all sand added at once) and incremental burial (a set amount added each week over 4 weeks). Incremental burial was used to reflect sand burial from continual sand transportation. Plants were buried to one of 3 depths; 5, 10 and 20mm. The depths used were based on preliminary recorded burial depths in stonefield study area over three months (max 11mm). It was assumed *R. hookeri* would be unable to survive the 20mm burial treatment. The 10mm burial treatment approximated the upper limit of what was observed in the study area. To conserve accuracy 5mm was the lowest burial depth possible.

At the end of each week for five weeks from the start of the burial experiment the number of stems emerging above the sand level was recorded. At the end of the experiment (three months since the start of burial) the vertical growth of the plants was measured. To compare the height growth between the controls and the burial treatment a final height measurement was taken three months after the last burial treatment. A three month period was used on the basis that the

growth of plants which have emerged through sand burial treatments would have returned to similar levels as the control after three months (Maun 2009)

Table 5.1: The six *R. hookeri* burial treatments. Three direct burial and three incremental burial depths. There were three replicates for each burial treatment.

Control	5mm	10mm	20mm
No Burial	Direct application	Direct application	Direct application
	Incremental application: 1.25mm applied every 7 days (over 4 weeks)	Incremental application: 2.5mm applied every 7 days (over 4 weeks)	Incremental application: 5mm applied every 7 days (over 4 weeks)

5.2.3 Analysis

The proportion of species in the stonefield was calculated from the number of quadrats in which each species was present. The species present in the stonefield were then divided into the two plant community types, non-sand binding and sand binding. The surface area of the two plant species *R. hookeri* var. *hookeri* and *F. spiralis* and the sedimentation patterns were correlated with a standard major axis regression. The standard major axis regression is a model II linear regression, used because both the response and explanatory variables of the model have error associated with their measurements (Legendre and Legendre, 2012). Standard major axis regression can be used on variables that are not in the same dimension. The measured values for *F. spiralis* surface area were wide ranging so the x and y axis were log transformed for analysis and for the sake of comparison the *R. hooker* var. *hookeri* x and y axis were also log transformed.

The effects of different burial regimes on *R. hookeri* were compared on a scatter plot including both direct burial and incremental burial treatments. This allowed for comparisons to be drawn between the responses of *R. hookeri* to the two sand application methods. The total vertical growth for each burial was also compared to determine whether burial influenced the growth

of the plants. A multiple analysis of variance (ANOVA) was used to determine whether there was any statistical difference in the treatment means.



Figure 5.2: a) *R. hookeri* species from Moa nurseries (Dunedin). b) *R. hookeri* var. *hookeri* found in the Mason Bay stonefield. c) *R. hookeri* var. *hookeri* plant in the Mason Bay stonefield.

5.3 Results

5.3.1 Stonefield plant communities

The plant species recorded within the study site fitted into two main categories; sand binding species and non-sand binding species. The proportion of quadrats each species inhabited is represented in Table 5.2. Sand binding species found within stonefield were *F. spiralis*, *Poa billardierei* and *Ammophila arenaria*. *A. arenaria* has been sprayed within the central stonefield since the start of the eradication program (2002) so was only represented by seedlings missed by the spray program. *F. spiralis* was the most common sand binding species within the stonefield (present in 29.2% of quadrats). The maximum *R. hookeri* var. *hookeri* cover was 17.62% per 10m² compared to the maximum *F. spiralis* cover of 8.84% per 10m².

The non-sand binding species found, thought to be at risk of burial, were *R. hookeri* var. *hookeri*, *Colobanthus muelleri*, *Coprosma acerosa*, *Myosotis pygmaea* var. *pygmaea*, *Luzula celata*, *Carex flagellifera*, *Gentianella saxosa* and *Isolepis nodosa*. *R. hookeri* var. *hookeri* was the most common species (present in 94.4% of all quadrats).

Table 5.2: Species found in the stonefield, and the percentage of quadrats in which they were found.

Plant species	Percent of quadrats occurrences (N=500)
Non-sand binding plant species	
<i>Raoulia hookeri</i> var. <i>hookeri</i>	94.4
<i>Colobanthus muelleri</i>	75.2
<i>Coprosma acerosa</i>	12.6
<i>Myosotis pygmaea</i>	1.6
<i>Luzula celata</i>	1.4
<i>Carex flagellifera</i>	0.6
<i>Gentianella saxosa</i>	0.2
<i>Isolepis nodosa</i>	0.2
Sand binding plant species	
<i>Ficinia spiralis</i>	29.2
<i>Poa billardierei</i>	15.4
<i>Ammophila arenaria</i>	4.4

5.3.2 *R. hookeri* var. *hookeri* and *F. spiralis* surface area patterns

The average surface area of *R. hookeri* var. *hookeri* was 595cm² per 10m² with a maximum surface area of 1764cm² per 10m². There was a negative relationship between *R. hookeri* var. *hookeri* surface area and distance from the seaward edge of the survey site (p.value < 0.001, $r^2 = 0.1338$, SE 0.47, df = 96). The average surface area of *F. spiralis* was 120cm² with a maximum surface area of 884 cm². There was no relationship between *F. spiralis* surface area and distance inland (p.value 0.83, df = 59).

Sedimentation was measured as the average change in surface height over nine months (mm) within each 10m² quadrant. There was an average sand accumulation of 3.22mm during the nine month study observed in Chapter Three and a maximum accretion of 13.5 mm. This meant that there was a maximum accretion rate of approximately 1.5 mm per month. There was a slight correlation between the observed sedimentation patterns recorded in the stonefield and *R. hookeri* var. *hookeri* surface area (p.value < 0.05) (Figure 5.3). There was no correlation found between the *F. spiralis* surface area and the observed sedimentation patterns (Figure 5.4).

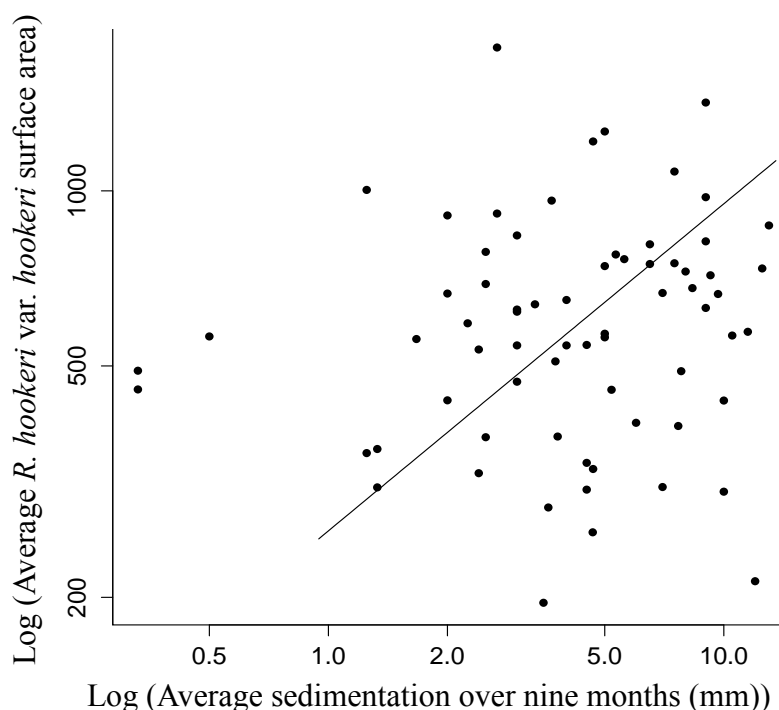


Figure 5.3: Standardised major axis regression between the log transformed average sedimentation over nine months (mm) and average *R. hookeri* var. *hookeri* surface area (cm²) per 10m² ($r^2 = 0.01$, df = 67).

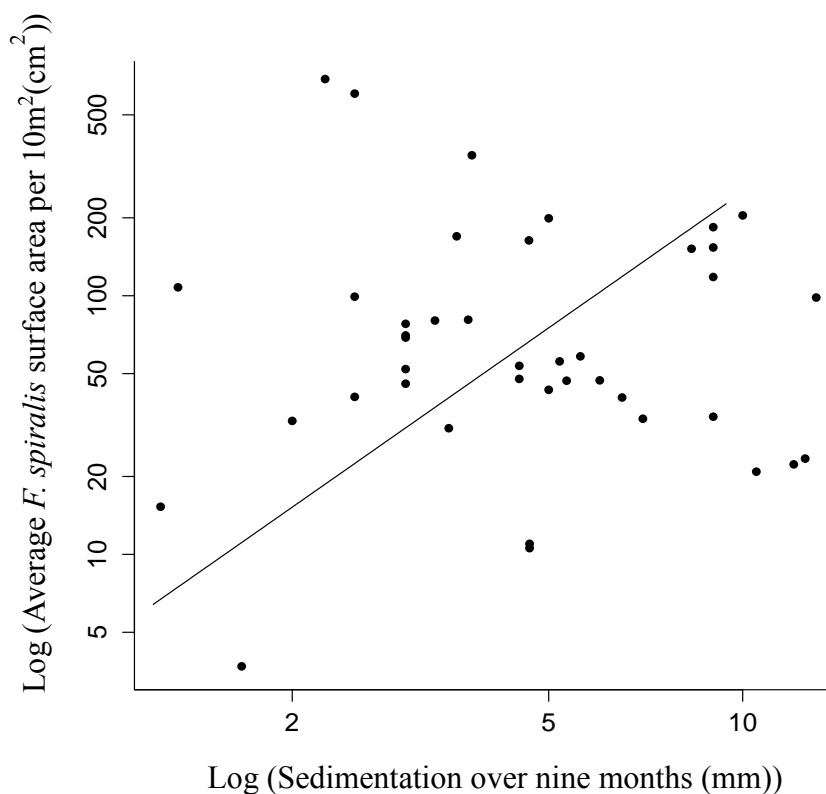


Figure 5.4: Standardised major axis regression between the log transformed average sedimentation over nine months (mm) and average *F. spiralis* surface area per 10m² (cm²) ($r^2 = 0.001$, $df = 39$, $p\text{-value} < 0.05$).

5.3.3 *R. hookeri* burial experiment

R. hookeri stems had emerged through the sand in all treatments (both direct and incremental burial) by the end of five weeks (Figure 5.5). In the 20 mm direct burial treatment, stems took longer to emerge and in one of the pots, despite having five stems visible after four weeks, in the fifth week all stems were dead and no new stems had emerged. The incremental burial (10mm each week for four weeks) allowed *R. hookeri* stems to emerge before the next sand application (Figure 5.6a). In the 10mm burial treatments the direct burial also reduced the number of stems breaking through, however one of incremental burial trials had the least number of visible stems in the first three weeks out of all the 10mm trials (Figure 5.6b). The 5mm direct and indirect burial treatments were not sufficient to suppress the vertical growth of *R. hookeri* (Figure 5.6c).



Figure 5.5: Burial trial after two weeks of incremental burial, at a depth of 1.25mm per week.

The vertical growth of *R. hookeri* stems after 3 months for the 10mm and 5mm treatments (both incremental and burial) was larger than the control plants (Figure 5.7). In the 20mm treatments, trial two and three of the direct burial didn't survive and in the incremental burial trial three didn't survive. On the sand surface of these trials, remnants of dead stems were visible. After three months it was noted that in all of the treatments with healthy stems above the sand there were a number of dead stems.

Table 5.3 Linear regression analysis between the burial treatments and the number of weeks after burial.

Treatment	p-value	r²	df
5mm direct	0.00	0.64	13
5mm indirect	0.00	0.41	13
10mm direct	0.00	0.67	13
10mm indirect	0.32	0.00	13
20mm direct	0.04	0.23	13
20mm indirect	0.29	0.012	13

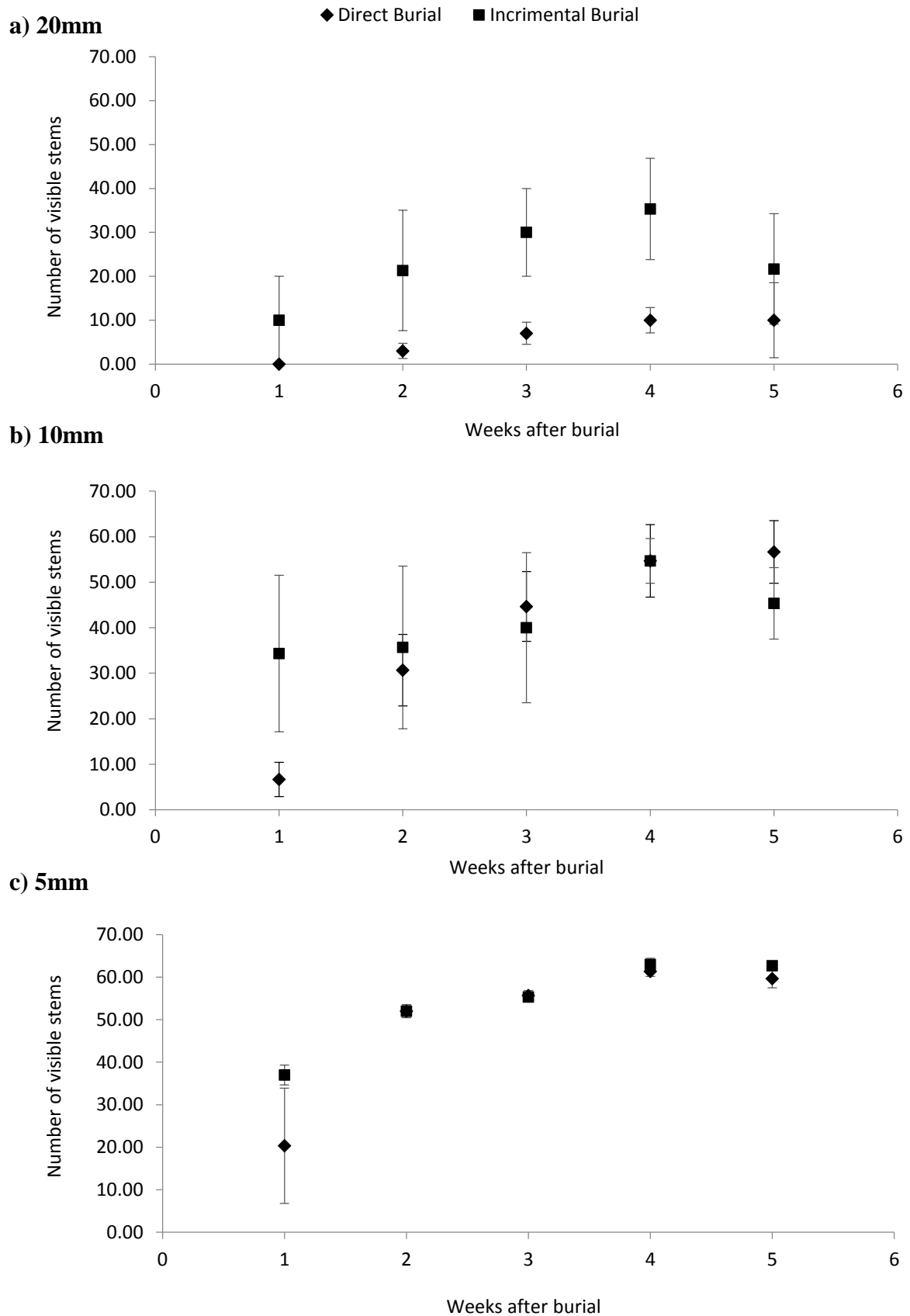


Figure 5.6: Average number of stems visible at the end of each week after burial. Direct burial is represented by a diamond, and the incremental burial is represented by a square. a) 20 mm, b) 10mm, c) 5mm. N=3 plants per burial treatment.

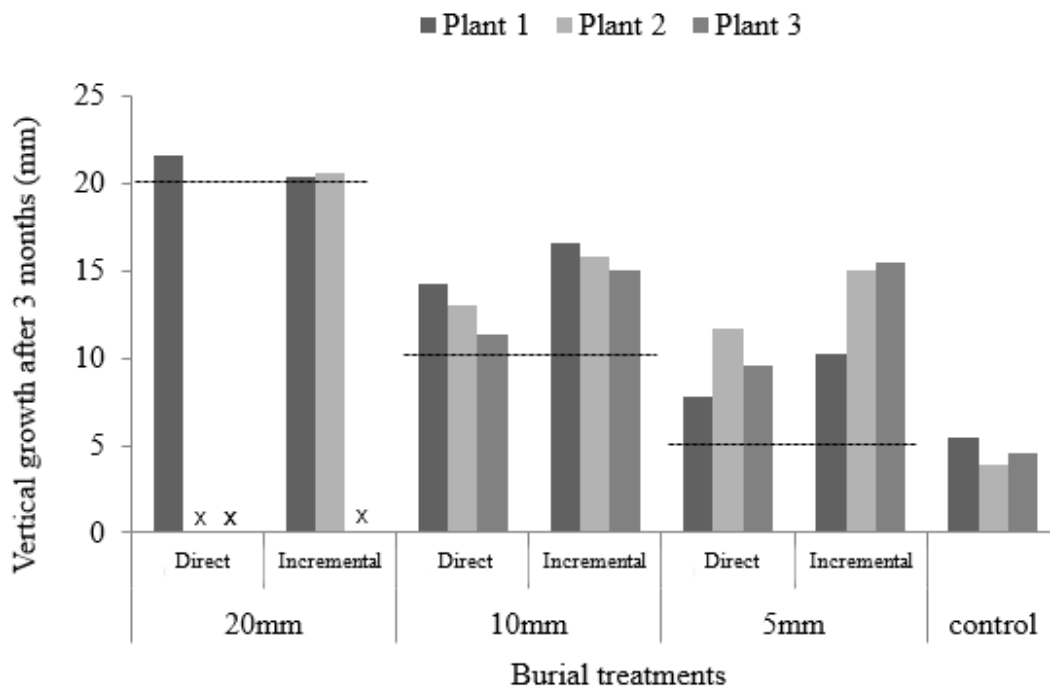


Figure 5.7: Vertical growth of individual plants in treatments three months after the start of burial treatments. The dashed lines indicate treatment burial depth, therefore growth above this line is growth above the sand surface. X indicates plants that died. The control had no sand applied, but was exposed to the same climatic conditions. N=3 plants per burial treatment. There was no statistical difference between the treatments.

5.4 Discussion

The sedimentation patterns in the stonefield over nine months were not correlated with the observed *R. hookeri* var. *hookeri* surface area patterns. The average sand accumulation observed in the stonefield over the period of a month was 1.5 mm. The lowest treatment in the burial experiment was 5mm thus representing a similar if not higher rate of sand deposition. The plants exposed to both the incremental and direct 5mm burial treatments not only survived this rate of burial, but they also grew vertically more than the control plants above the sand surface. It could be concluded that the sand accretion in the stonefield study site was not great enough to adversely affect *R. hookeri* var. *hookeri*. It should be noted that the *R. hookeri* plants used in the burial experiment were considered morphologically different so extrapolation from experimental *R. hookeri* to the Mason Bay variant *R. hookeri* var. *hookeri* should be made with caution.

Studies have shown that sand burial can stimulate growth in some dune species, for example sand binders (Zarnetske *et al.*, 2012; Sykes and Wilson, 1990). This growth has been attributed to the increased volume of sand containing small amounts of nutrients (Maun, 2004). In previous studies it was found the height of vegetation in areas of active erosion were usually lower (Levin *et al.*, 2006), however the same plants in areas of deposition were significantly taller. *R. hookeri* var. *hookeri* is not considered a sand binding species like *A. arenaria*, however the small sand accretion levels measured in the stonefield could currently be providing nutrients benefitting *R. hookeri* var. *hookeri* growth.

The observed sedimentation patterns were not an indicator of *F. spiralis* surface area. This was supported by the findings in Chapter Three where it was found that there was no growth of *F. spiralis* nabkha during the study period. Despite a positive sediment budget in the stonefield area during the study, compared to the tolerable burial rate of *F. spiralis* (two thirds of their height), this depth could be considered insignificant to elicit a growth response (Sykes and Wilson, 1990). In the Doughboy Bay, Stewart Island restoration project *F. spiralis* was planted in the foredune, and nabkha formed in association with these plantings and subsequently grew 4-5m over 10 years (Konlechner *et al.*, 2014).

The other native sand binding species growing in the stonefield study area was *P. billardierei* (present in 15.4% quadrates). Sykes and Wilson (1990) demonstrated that *F. spiralis* can tolerate greater burial than *P. billardierei*, however the presence of mature *P. billardierei* and *F. spiralis* plants within the study area does suggest that the degree of sand input occurring is enough for the germination and growth of native sand binding species plants (albeit most *F. spiralis* plants could be considered moribund, as few were seen to flower during the 2014/15 growth season).

R. hookeri var. *hookeri* was the most dominant non-sand binding species, however there was a group of other non-sand binding species present (Table 5.2). Of these species little is known of their tolerance to sand burial, but Sykes and Wilson (1990) commented that tolerance to sand deposition appeared to be as necessary for rear dune species as it is for those of the front dunes. Of the species making up the non-sand binding community, it would be of value to understand their burial tolerance enabling coastal management agencies to predict the species that will disappear first from the stonefield if sand accumulation does increase.

Species composition and distribution are strongly related to the long-term average sand deposition (Perumal and Maun, 2006). The presence of sand binders (*F. spiralis*) and non-sand binding communities (*R. hookeri* var. *hookeri*) in the study site suggests that this habitat is receiving enough sand to allow for the establishment of the sand binding community, but the sand accumulation is low enough for non-sand binding species to tolerate and possibly benefit from inputs. Based on the experimental study the sedimentation rates in the stonefield would need to at least double to begin negatively affecting *R. hookeri* var. *hookeri*. If there were a significant increase in sand accumulation in the stonefield this might cause a community shift towards a sand binder community and eventually eliminate the non-sand binding community.

Sedimentation patterns are considered one of the most important abiotic factors in coastal dunes, but this does not mean to say that other factors could not be influencing species distribution. This study was conducted in the field where multiple habitat factors are affecting plants at the same time such as climate, competition, facilitation and the magnitude of these stress factors is not controlled (Maun, 2004). The reason for focusing on the sedimentation pattern is that this abiotic factor is most likely to change in response to the destabilisation of the Mason Bay dunes system.

As dunes systems equilibrate during dynamic dune restoration projects, results suggest that there is a decline in species richness in areas directly associated with *A. arenaria* (Konlechner *et al.*, 2014 Hesp and Hilton, 2013). It is assumed that as the natural dune systems reestablish, the processes of plant dispersal and colonisation will eventually restore the mosaic of dune habitats unique to transgressive dune systems (Grootjans *et al.*, 2013). But what if there is not enough time for plant communities to respond and they are completely lost from the system? The mosaic of habitats in a natural dune system facilitates the recolonisation of recently disturbed habitats within the dune system (Grootjans *et al.*, 2002; Maun, 2009). The longevity and seed dispersal mechanisms of the non-sand binding species within the stonefield would determine their persistence in the restored dune system. The next step in understanding the implications of dune mobilisation on the stonefield communities would be to study their seed banks, longevity and dispersal mechanisms.

The surface area of the *R. hookeri* var. *hookeri* decreased moving inland through the stonefield. The surface area of the *R. hookeri* var. *hookeri* relates to the age of the plants and their recent colonisation. If the surface area is greater there are either more plants or the plants are older

both indicating a relatively earlier colonisation compared to the smaller plants (McCarthy, 1992). This relates to the evolutionary history of the stonefield, as it was determined from historic images that the landward margin of the stonefield has moved inland progressively over the last approximately 57 years (Chapter Two). This suggests that as the stonefield develops landwards *R. hookeri* var. *hookeri* is colonising, displaying a dynamic and adaptive plant species response.

The stonefield study area is in a state of limbo where both sand binding and non-sand binding communities are persisting together. The mobilisation of the parabolic dunes and foredune will inevitably increase the sand availability down wind. Once *F. spiralis* and *P. billardiarei* start to bind sand and grow, the sand accumulation may become too great for the non-sand binding communities. It is hoped that a mosaic of non-sand binding species persist to facilitate the recolonisation of deflation surfaces as the dune system equilibrates after dynamic restoration.

Chapter 6

Conclusion

6.1 Introduction

Dynamic restoration of coastal dunes aims to re-establish the natural geomorphic processes of dune systems with the goal of restoring the landform complexity and therein protecting the diversity of coastal dune ecosystems (Hesp and Hilton, 2013; Martinez *et al.*, 2013; Walker *et al.*, 2013). The deliberate removal of vegetation by either mechanical or chemical means is employed to re-establish natural geomorphic processes. In response to the growing number of dynamic restoration programmes the growth and decay of destabilised landforms such as foredunes have been investigated (Konlechner *et al.*, 2014; Arens *et al.*, 2013b; Pickart, 2013; Hilton *et al.*, 2009;). But to date few studies have examined the effect of a positive sand budget on the dune habitats and plant communities downwind of the disturbed dune landscape (Hesp and Hilton, 2013).

The dynamic restoration efforts in the Mason Bay dune complex through chemical eradication of *Ammophila arenaria*, have focused on the destabilisation of the parabolic and foredune landform elements within the wider dune system. Downwind of these landforms is a large deflation surface known locally as the ‘stonefield’. The stonefield is habitat for a distinctive assemblage of plants. Deflation surface communities play an integral role in the conservation or restoration of dune ecosystem biodiversity. The stonefield provided a unique opportunity to research the effects of *A. arenaria* invasion, then the subsequent impact of *A. arenaria* dune destabilisation (commenced in 2002) on these habitats.

The present study investigated the development of the stonefield at a range of spatial and temporal scales with the goal of predicting the future response of the stonefield to ongoing dynamic restoration. It aimed to: (i) describe the historic development of the Mason Bay stonefield in relation to *A. arenaria* invasion; (ii) assess whether sand liberated from recent and ongoing destabilisation operations is accumulating in the stonefield; and (iii) to establish the

impact of the observed sedimentation patterns on the native plant communities in the stonefield. The relevant investigations are summarised and discussed in the following section, concluding with possible future research areas.

6.2 The historic development of the Mason Bay stonefield and deflation surfaces

A. arenaria invasion has been linked to the development of large, well vegetated, foredunes and negative hinterland sand budgets (Hart *et al.*, 2012; Weidemann and Pickart, 1996; Carter *et al.*, 1990). *A. arenaria* invasion occurred relatively recently at Mason Bay, providing the opportunity to study the evolution of the stonefield in relation to *A. arenaria* invasion. It was hypothesised that due to the highly linked nature of transgressive dunes, the development of the Mason Bay foredune would have prevented sediment exchange between the beach and the backdune environment. This in turn would affect the geomorphology of the stonefield. From a series of historic photographs beginning in 1958 the stonefield was mapped in relation to the invasion of *A. arenaria*, and the start of the eradication programme in 2002.

The character of the Mason Bay study area prior to the arrival of *A. arenaria* is somewhat unclear due to the remoteness of the site and the paucity of historic information. An exhaustive search of archival material yielded photographs from the early 1900s that strongly indicate that the stonefield was a continuous feature located a lot closer to the coast than its current position. It was also smaller. As *A. arenaria* invaded the foredune and colonised the transgressing parabolic dunes (which probably formed because of *A. arenaria* invasion), the seaward margin of the stonefield moved inland approximately 280m. This inland shift was attributed to the elongation of the parabolic dunes into the stonefield recorded by Hart *et al.*, (2012). The stonefield surface area began to expand to the east in 1989 as the landward margin eroded and the seaward margin began to stabilise in response to *A. arenaria* invasion of the parabolic depositional lobes (Figure 2.6). Hesp (2013) noted that when there is a low sediment supply transgressive landforms such as parabolic dunes and deflation surfaces move away in the direction of the dominant wind direction. The dominant wind regime at Mason Bay is on shore (westerly), consistent with the long axis of the trailing arms of the parabolic dunes. Thus, the stonefield evolution demonstrates the geomorphic coupling between the foredune and hinterland environments.

The *A. arenaria* eradication programme began in the hinterland of the central dunes and here it has been rapidly effective, in part because *A. arenaria* had established many small colonies by 2002 (Jul, 1999). At this time the root and rhizome mass was probably not extensive enough to slow the erosional response, as has been documented in other studies (Hilton and Konlechner, 2010). The rapid erosion of the landward margin could may also be attributed to increased exposure of the landward portion of the stonefield (2.7m per 100m moving landwards from the seaward edge) as established in Chapter Three. The reduced vegetation cover and increased exposure could have led to the erosion of the sand sheet leaving behind a stony lag and, therefore, moving the stonefield landward margin further inland. The seaward margin remained relatively stable in the initial stages of the eradication programme allowing for the increase in stonefield area.

The parabolic dunes along the seaward margin were first sprayed in 2006 however the rhizome network of *A. arenaria* is considered to have slowed the erosion of the depositional lobes, so that erosion of these features has lagged well behind devegetation effectively slowing the geomorphic response. This is consistent with previous remobilisation efforts (through herbicide application) at Doughboy Bay, where the *A. arenaria* rhizome network inhibited an erosional response for up to five years after the initial herbicide application (Konlechner *et al.*, 2014). The destabilisation programme has not caused a loss in stonefield area, however the elongation of the parabolic depositional lobes by approximately 3m between 2011 and 2013 into the stonefield suggests that the rhizome is breaking down in the parabolic dunes generating increased rates of sand flux towards the stonefield.

6.3 Is sand liberated from recent and ongoing destabilisation accumulating in the stonefield?

As *A. arenaria* is removed and the parabolic dunes and foredune erode there is an increase in potential sand for downwind transport and deposition. Aside from encroachment of dune forms as they move downwind, the effects of increased sand mobility on downwind environments has been little studied (Hesp and Hilton, 2013; Rhind *et al.*, 2013; Walker *et al.*, 2013). Chapter Three and Four, therefore, aimed to answer the following questions across the short-term (months to years) and event-scale (hours to days) to assess (i) whether sand has accumulated over the period of this study (nine months); (ii) whether the observed patterns of sedimentation

in the plot are related to the distribution of *Ficinia spiralis* and (iii) whether sand is accumulating during discrete wind events?

Over the period of this study (nine months) there was a small positive sediment budget of 3.22mm (Chapter Three). There were, however, no changes recorded in the *F. spiralis* nabkha volume over the seven months (August 2014 and March 2015). This suggests that there had been approximately equal sand inputs and outputs from the stonefield over the study period. During one month of this study the sand accumulation recorded accounted for 66% of the (average) accumulation recorded over the total period of nine months. This suggests that the measured sedimentation patterns were a result of wind events prior to measuring the erosion pins. This highlighted the importance of measuring the event-scale sedimentation patterns.

During low wind speed events, with winds from the southwest (SW), there was no spatial gradient in wind velocity across the stonefield (Chapter Four). In periods of higher winds (5 to 6m/s), higher average wind speeds were recorded at the landward anemometer, this was attributed to a 3.5m elevation rise between the seaward and landward anemometer masts. The landward increase in elevation exposed the landward section of the stonefield reducing the potential for aeolian deposition within the stonefield. This contrasts with the study by Walker *et al.*, (2013) in which the transgressive dune downwind of the destabilised landforms acted as a sink for the eroded sand. Due to the increasing exposure inland of the stonefield any increased sand accumulations within the stonefield will probably only occur through entrainment by sand binding species like *F. spiralis*. Accumulation of sand in the absence of vegetation seems unlikely.

No pattern in the accumulation of sand across the plot was observed in the stonefield over the nine months of this study, however, the soil pits revealed that there has been (on average) a 78mm burial of the stonefield surface in the lee of the parabolic depositional lobes since 2015. Sand deposition in the lee of destabilised landforms, such as foredunes and parabolic dunes, has been noted by previous studies both through mechanical (Walker *et al.*, 2013; Arens *et al.*, 2004) and herbicide *A. arenaria* removal efforts (Konlechner *et al.*, 2014). The erosion of the parabolic depositional lobes in Mason Bay began in 2011, approximately five years after the eradication programme commenced. The use of herbicides to destabilise the landforms left the in situ *A. arenaria* rhizome and dead plant material in place, which further slowed the geomorphic response. Colonisation of *F. spiralis* on the depositional lobes suggests that some

of the sand eroding from the destabilised parabolic dunes is being trapped before reaching the stonefield (Figure 6.1). *F. spiralis* colonisation of the parabolic depositional lobes and the sand that has eroded is probably fueling the elongation of the depositional lobes into the stonefield.

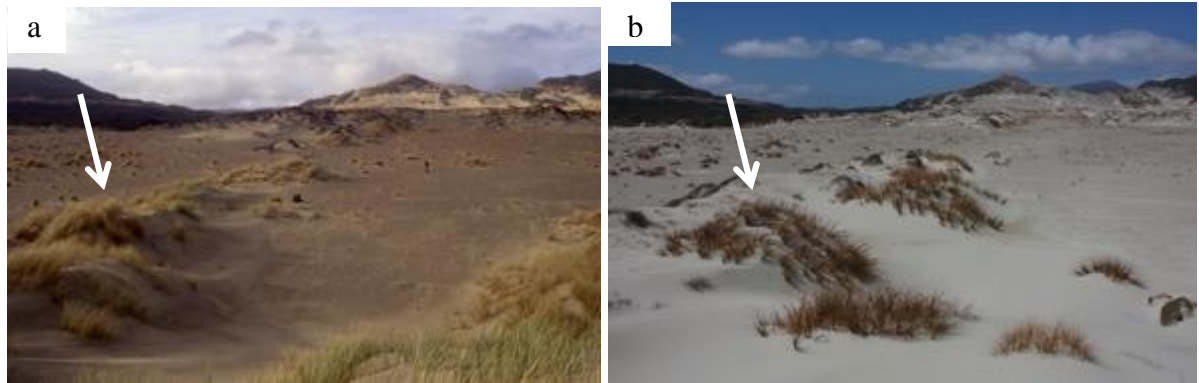


Figure 6.1: Oblique views of the parabolic depositional lobes extending into the stonefield. a) parabolic depositional lobe in 1998, white arrow indicated *A. arenaria* colonisation (source Mike Hilton). b) *F. spiralis* has since colonised the leeward side of the depositional lobes, which has slowed but not prevented this erosion parabolic, white arrow indicates *F. spiralis* colonisation.

6.4 Are the observed sedimentation patterns adversely affecting the native plant communities in the stonefield?

Two types of plant communities persist in the stonefield: the non-sand binders (*Raoulia hookeri* var. *hookeri*, *Colobanthus muelleri*, *Coprosma acerosa*, *Myosotis pygmaea*, *Luzula celata*, *Carex flagellifera*, *Gentianella saxosa* and *Isolepis nodosa*) and the sand binders (*F. spiralis* and *Poa billardiarei*). The response of these plant communities to the continued destabilisation efforts were measured by recording the distribution of *R. hookeri* var. *hookeri* and *F. spiralis* in relation to observed sedimentation patterns. This was aimed at providing an understanding into the future of the stonefield's ecological values.

The surface texture of the stonefield has not changed since the start of the destabilisation efforts. This can be seen by comparing the stonefield surface texture between 1998 and 2015 (Figure 6.2). This suggests that *R. hookeri* var. *hookeri* has not been adversely affected by sand deposition since dune destabilisation commenced. There is no relationship between the extent

of *R. hookeri* var. *hookeri* and the observed current sedimentation in the stonefield. The burial experiment suggests that *R. hookeri* is tolerant of sand burial of up to 10mm over four weeks. This is greater than the average sand accumulation of 3.22m over nine months measured in the field.

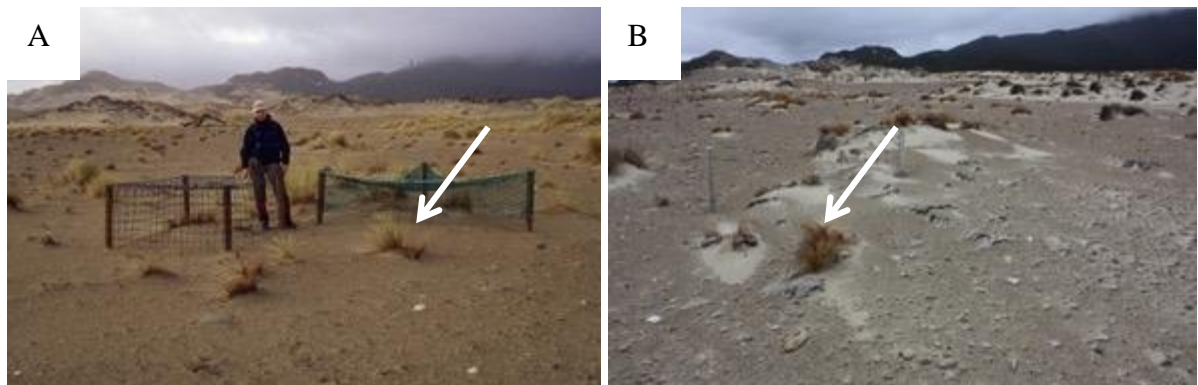


Figure 6.2: Oblique images looking landwards through the stonefield. A) Image A shows the coarse texture of the central stonefield in 1998. B) The same location in 2015. Notice the similar surface texture approximately five years after the initial destabilisation efforts began

This study suggests that there is no significant growth of *F. spiralis* plants occurring in the stonefield study area. During the nine month study there was no correlation between the recorded *F. spiralis* plants and sand accumulation. This was supported by the stable growth of the *F. spiralis* nabkha measured over seven months (Chapter Three). If sand were accumulating around *F. spiralis* plants, this would have facilitated the growth of *F. spiralis* and their related nabkha through increased sand deposition eliciting a positive growth response (Hesp 1981).

The presence of both sand binding and non-sand binding species in the stonefield suggests that enough sand is entering the system to support *F. spiralis*, however, these plants are non-thrifty. Few were seen to flower during the 2014/15 growth season. The extent and density of *R. hookeri* var. *hookeri* does not appear to have been adversely affected by significant sand deposition. It is proposed that the stonefield plant community is in a state of dynamic equilibrium, where any future increases in sand will favour the growth of *F. spiralis* and other native sand binders over non-sand binding species. Presently the advancing front of sand as the depositional lobes eroded and elongate into the stonefield, is the main threat to the stonefield plant communities.

6.4 Concluding remarks

This study has shown that the stonefield is probably a natural element in the landscape at Mason Bay but the location and extent has changed dramatically over the last 58 years. As *A. arenaria* invaded the Mason Bay dune system the seaward margin of the stonefield moved inland at an approximate average rate of 6.5m per year. The landward margin moved in land at an average rate of 2.12m per year. During this time the stonefield species were able to keep pace with the changing habitat, evidence of their ability to colonise. Since the start of the *A. arenaria* removal project and to the present day the landward margin has only increased at a maximum of 2m per year whereas the landward margin has moved inland at a considerable rate of 5.8m per year; increasing the stonefield's area. The stonefield communities are colonising the recently developed landward edge of the stonefield. Since destabilisation efforts began in the parabolic dunes in 2006 there have been no significant inputs of sand into the stonefield.

The continued break down of the *A. arenaria* rhizome in the parabolic dunes, will potentially increase the sand inputs into the stonefield. Two possible scenarios are proposed for the future of the stonefield if the sand inputs were to increase as predicted.

The first is the increased elongation of the parabolic dunes shifting the stonefield's seaward margin inland. If the elongation of the parabolic dunes exceeds the inland movement of the landward margin then the stonefield's area will eventually decrease. This occurred in 1989 as the long-walled parabolic dunes developed after the formation of the continuous foredune. However, the sand sheet began to erode at a greater rate, as the parabolic dunes were stabilised by *A. arenaria* allowing the stonefield to increase in area in 1989. If the sand sheet began to stabilise or reduce its inland movement the parabolic depositional lobes may connect with the sand sheet, breaking up the stonefield environment. This would be similar to the elongation of the southern parabolic depositional lobe that occurred between 2002 and 2011.

The second scenario is the increase in sand deposition in association with *F. spiralis* plants within the stonefield. Increased sand inputs from the destabilised landforms could elicit a positive growth response from *F. spiralis* plants forming nabkha, which could eventually join and form a dune field. This would break up the continuous stonefield and could eventually eliminate the stonefield species as the rate of deposition may become too great for the non-sand binding species to inhabit.

The stonefield species have shown that they are capable of keeping pace with the stonefield's current rate of evolution. To date the stonefield has been a continuous feature which has most likely aided in the stonefield species' ability to keep pace with the inland movement of the stonefield. However, it is unknown whether the colonisation abilities of these species will be adaptable to the possible fragmentation by sand burial from the recent destabilisation.

6.5 Future Research

Opportunities for future research areas have been presented throughout this study. The understanding of dynamic restoration in coastal dunes is limited by the lack of long term multidisciplinary monitoring (Lithgow *et al.*, 2013). Development of such monitoring, examining the relationship between geomorphic processes and coast dune plant communities, would greatly benefit the understanding of effects of destabilisation on plant communities and the ecological values of a coastal dunes system. The following areas of research aim to increase our understanding of the ecological consequences of dynamic dune restoration; (i) the importance of discrete wind events in sand transport; (ii) long term monitoring of sedimentation patterns in hinterland environments downwind of destabilisation; and, (iii) monitoring the response of dune habitats to dynamic dune restoration.

As previously outlined in Chapter Four the simultaneous analysis of sand transport and wind enables studies to identify spatial and temporal sand transports factors while including the measurement of local sand supply and transport limiting factors (Sherman and Hotta, 1990). A sediment budget analysis was unable to be conducted during this study due to lack of competent sand transporting winds during fieldwork periods. However, it was possible to examine the wind velocity across the stonefield and a slight acceleration in wind velocities was measured (Chapter Four). Wind speeds only reached 5.7m/s at the exposed landward edge of the stonefield during this study. It would be ideal to repeat this experiment during a range of wind speeds. This would help to determine whether there is a pattern of erosion or deposition in the stonefield during increased wind velocities.

The continued monitoring of sedimentation in the stonefield would greatly increase the informative power of this study. Specifically in relation to the growth of the *F. spiralis* nabkha as it was suggested that there is little potential for aeolian deposition in the stonefield (Chapter

Four). In order to completely understand where sand is coming from (in regards to the observed sedimentation patterns in the stonefield) the erosion and accretion patterns of the recently destabilised features should also be monitored. This could be carried out using a high-resolution aerial LiDAR data similar to Earmer *et al.*, (2013) or a digital terrain model derived from drone data. This would enable a detailed analysis of volumetric changes in the recently destabilised parabolic dunes and stonefield. This analysis should allow coastal managers to determine whether sand was primarily accumulating in the lee of the parabolic dunes or in the stonefield. This would be further complemented with continued surveying of *F. spiralis* nabkha across the stonefield, not just restricted to the study site.

The mosaic of habitats in the Mason Bay transgressive dune system are integral to the biodiversity and resilience of the transgressive dune ecosystem, however the relative distribution of these various habitats may change as the eradication programme progresses. Future research in the Mason Bay dune complex should focus on the response of these habitats and the ability of their associated species to facilitate the colonisation of new habitats formed through restored dynamic processes. To measure the response of the various habitats within the Mason Bay transgressive dune complex a series of large (2m²) permanent quadrats should be located in the dune complex. These quadrats should be representative of all the transgressive dune habitat types, monitoring species compositions and sedimentation patterns. This will enable the response of various coastal dune habitats to changing sedimentation patterns to be monitored and understood.

References

- Anderson, J.L. & Walker, I.J. (2006) Airflow and sand transport variations within a backshore-parabolic dune plain complex: NE Graham Island, British Columbia, Canada. *Geomorphology*, **77**, 17-34.
- Andrews, B.D., Cares, P.A. & Colby, J.D. (2002) Techniques for GIS modeling of coastal dunes. *Geomorphology*, **48**, 289-308.
- Archer, C.A. & Jacobson, M.Z. (2003) Spatial and temporal distributions of U.S. winds and wind power at 80m derived from measurements. *Journal of Geophysical Research*, **108**(9), DOI: 10.1029/2002LD002076.
- Arens, S.M. & Geelen, L.H.W.T. (2006) Dune Landscape Rejuvenation in Intended Destablisation in the Amsterdam Water Supply Dunes. *Journal of Coastal Research*, **22**(5), 1094-1107.
- Arens, S.M., Mulder, J.P.M., Slings, Q.L., Geelen, L.H.W.T. & Damsma, P. (2013a). Dynamic dune management, integrating objectives of nature development and coastal safety: Examples from the Netherlands. *Geomorphology*, **199**, 205-213
- Arens, S.M., Slings, Q.L. & Geelen, L.H.W.T. (2013b) Restoration of Dune Mobility in The Netherlands. In Martines, M.L., Gallego-Fernandez, J.B. & Hesp, P.A (eds.). *Restoration of Coastal Dunes*. Vergal, Springer, pp. 107-124
- Arens, S.M., Slings, Q. & de Varries, C.N. (2004) Mobility of a remobilized parabolic dune in Kennemerland. *Geomorphology*, **59**, 175-188.
- Arens, S., van Kaan-Peters, H. & van Boxel, J. (1995) Air flow over foredunes and implications for sand transport. *Earth Surface Processes and Landforms*, **20**, 315-332.
- Arya, S.P. (1988) *Introduction to Micrometeorology*. San Diego, CA: Academic.

- Bagnold, R.A. (1941) *The physics of blown sand and desert dunes*. London, Chapman & Hall.
- Baldwin, K.A. & Maun, M.A. (1983) Micro-environment of Lake Huron sand dunes. *Canadian Journal of Botany*, **61**, 241-255.
- Bar, P. (2013). Restoration of coastal sand dunes for conservation of biodiversity: The Israeli experience. In Martines, M.L., Gallego-Fernandez, J.B. & Hesp, P.A (eds.). *Restoration of Coastal Dunes*. Vergal, Springer, pp. 173-186.
- Bauer, B.O., Sherman, D.J., Nordstrom, K.F. & Gares, P.A. (1990) Aeolian transport measurement and prediction across a beach and dune at Castroville, California. In Nordstrom, K.F., Psuty, N.P. & Carter, B (eds.). *Coastal Dunes, Form and Process*. Chichester, Wiley, pp. 39-55.
- Bergin, D.O. & Kimberley, M.O. (1999) Rehabilitation of coastal foredunes in New Zealand using indigenous sand-binding species. *Department of Conservation Science for Conservation Series No. 122*. Wellington.
- Bullard, J.E. (1997) A note on the use of the “Fryberger Method” for evaluating potential sand transport by wind. *Journal of Sedimentary Research*, **67**(3), 499-501.
- Burkinshaw, J.R. & Rust, I.C. (1993) Aeolian dynamics on the windward slope of a reversing transverse dune, Alexandria coastal dunefield, South Africa. In K. Pye (ed.). *Aeolian Sediments Ancient and Modern*. Lancaster, Blackwell Scientific Publications, 16, 13-21.
- Carter, R.W.G., Hesp, P. A. & Nordstrom, K.F. (1990) Erosional Landforms in Coastal Dunes. In Nordstrom, K.F., Psuty, N.P. & Carter, B (eds.). *Coastal Dunes, Form and Process*. Chichester, Wiley, pp. 217-250.
- Cockayne, L. (1909a) *Report on a botanical survey of Stewart Island*. Wellington, Government Printers.

- Cockayne, L. (1909b). *Report on the sand dunes of New Zealand: The geology and Botany, with their economic bearing*. Wellington, Government Printers.
- Cockayne, L. (1982). *The vegetation of New Zealand. 2nd edition*. Leipzig, Engelmann Press.
- Cooke, R., Warren, A. & Goudie, A. (1993) *Dessert Geomorphology*. London, University College of London Press.
- Dawson, M.I., Wards, J.M., Grooves, B.E. & Hair, J.B. (1993) Contributions to a chromosome atlas of the New Zealand flora – 32 *Raoulis* (*Inuleae-Compositae* (*Asteracea*)). *New Zealand Journal of Botany*, **31**, 97-106.
- Doing, H. (1985) Coastal fore-dune zonation and succession in various parts of the world. In Beeftink, W.G., Rozema, J. & Huiskes, A.H.L (eds.). *Ecology of coastal vegetation*. Dordrecht, Dr W. Junk Publishers, pp. 65-75.
- Eamer, J.B.R., Darke, I.B. & Walker I.J. (2013) Geomorphic and sediment volume responses of a coastal dunes complex following invasive vegetation removal. *Earth Surface Processes and Landforms*, **38**, 118-1159.
- Elser, A.E. (1970) Manawatu Sand Dune Vegetation. *Proceedings of the New Zealand Ecological Society*, **17**, 41-46.
- Fryberger, S.G. (1979) Dune forms and wind regime. In McKee E.D (ed.). *A Study of Global Sand Seas, USGS Professional Paper, vol. 1052*. Washington DC, US Geological Survey and United States National Aeronautics and Space Administration, pp137-169.
- Fryberger, S.G. (1978) Techniques for the evaluation of surface wind data in terms of eolian sand drift. U.S. Geological Survey, Open-File 78-405.
- Garcia-Mora, M.R., Gallego-Fernandez, J.B. & Francisco, G. (1999) Plant function types in coastal foredunes in relation to environmental stress and disturbance. *Journal of Vegetation Science*, **10**, 27-34.

- Grootjans, A.P., Dullo, B.S., Kooijman, A.M., Bekker, R.M. & Aggenbach, C. (2013) In Restoration of Dune Vegetation in the Netherlands. In Martines, M.L., Gallego-Fernandez, J.B. & Hesp, P.A (eds.). *Restoration of Coastal Dunes*. Vergal, Springer, pp. 235-254.
- Grootjans, A.P., Geelen, H.W.T., Jansen, A.J.M. & Lammerts, E.J. (2002) Restoration of coastal dune slacks in the Netherlands. *Hydrobiologia*, **478**, 181-203.
- Hart, A.T., Hilton, M.J., Wakes, S.J. & Dickinson, K.J. (2012) The impact of *Ammophila arenaria* foredune development on downwind aerodynamics and parabolic dune development. *Journal of Coastal Research*, **28**(1), 112-122.
- Hayes, M. & Kirkpatrick, J.B. (2012) Influence of *Ammophila arenaria* on half a century of vegetation change in eastern Tasmanian sand dune systems. *Australian Journal of Botany*, **60**, 450-460.
- Havholm. K.G., Ames, D.V., Whittecar, G.R., Wenell, B.A., Riggs, S.R., Jol, H.M., Berger, G.W. & Holmes, M.A. (2004) Stratigraphy of Back-Barrier Coastal Dunes, Northern North Carolina and Southern Virginia. *Journal of Coastal Research*, **20**(4), 980-999.
- Hernandez-Calvento, L., Jackson, D.W.T., Medina, R., Hernandez-Cordero, A.L., Cruz, N. & Requejo, S. (2014) Downwind effects on an arid dunefield from an evolving urbanized area. *Aeolian research*, **15**, 301-309.
- Hesp, P.A. (2013) Conceptual models of the evolution of transgressive dune field systems. *Geomorphology*, **199**, 138-149.
- Hesp, P.A. & Hilton, M.J. (2013) Restoration of Foredune and Transgressive Dunefields: Case Studies from New Zealand. In Restoration of Dune Vegetation in the Netherlands. In Martines, M.L., Gallego-Fernandez, J.B. & Hesp, P.A (eds.). *Restoration of Coastal Dunes*. Vergal, Springer, pp. 253-288.

- Hesp, P.A. & Martinez, M. L. (2007). Disturbance Processes and Dynamics in Coastal Dunes. In Johnson, E.A. & Miyanishi, K (eds.). *Plant Disturbance Ecology: The Process and The Response*. Burlington, Academic Press, pp. 215-247.
- Hesp, P.A., Davidson-Arnott, R., Walker, I.J. & Ollerhead, J. (2005) Flow dynamics over a foredune at Prince Edward Island Canada. *Geomorphology*, **65**(1-2), 71-84.
- Hesp, P.A. (2002) Foredunes and blowouts: initiation, geomorphology and dynamics. *Geomorphology*, **48**, 245-268.
- Hesp, P.A. & Thom, B.G. (1990) Geomorphology and Evolution of Active Transgressive dunefields. In Nordstrom, K. F., Psuty, N. P. & B, Carter (eds.). *Coastal Dunes, Form and Process*. Chichester, Wiley, pp. 253-288.
- Hesp, P. A. (1981) The Formation of Shadow Dunes. *Journal of Sedimentary Petrology*, **51**(1), 101-112.
- Hilton, M.J. (2006) The loss of New Zealand's active dunes and the spread of marram grass (*Ammophila arenaria*). *New Zealand Geographer*, **62**, 105-121.
- Hilton, M., Duncan, M. & Jul, A. (2005) Processes of *Ammophila arenaria* (Marram Grass) Invasion and Indigenous Species Displacement, Stewart Island, New Zealand. *Journal of Coastal Research*, **21**(1), 175-185.
- Hilton, M.J. & Konlechner, T.M. (2010) A review of the marram grass eradication programme (1999-2009), Stewart Island, New Zealand. *Proceeding of the 17th Australasian Weeds Conference, Christchurch, New Zealand, 26-30 September 2010*. pp. 386-389.
- Hilton, M., Woodley, D., Sweeney, C. & Konlechner, T. (2009) The Development of a Prograded Foredune Barrier Following *Ammophila arenaria* Eradication, Dough Boy, Stewart Island. *Journal of Coastal Research*, **56**(1), 317-321.
- Holdaway, R.J., Wiser, S.K. & Williams, P.A. (2012) A threat status assessment of New Zealand's naturally uncommon ecosystems. *Conservation Biology*, **4**, 619-629.

- Hugenholtz, C.H., Levin, N., Barchyn, T.E. & Baddock, M.C. (2012). Remote sensing and spatial analysis of aeolian sand dunes: A review and outlook. *Earth Science Review*, **111**, 319-334.
- Jackson, N.L., Nordstrom, K.F., Feagin, R.A. & Smith, W.K. (2013) Coastal geomorphology and restoration. *Geomorphology*, **199**, 1-7.
- Jewell, P.W. & Nicoll, K. (2011) Wind regimes and aeolian transport in the Great Basin, U.S.A. *Geomorphology*, **129**, 1-13.
- Johnson, P.N. (1992) *The sand dune and beach vegetation inventory of New Zealand: II South Island and Stewart Island*. Christchurch: Land Resources Scientific Report No.16, Department of Scientific and Industrial research, 278p.
- Jul, A., Hilton, M.J. & Handerson, R. (1999) *Patterns and process of marram grass invasion, Mason Bay, Stewart Island and recommendations for management*. Unpublished report. Department of Conservation and Department of Geography, University of Otago.
- Kim, D. & Yu, K.B. (2012) A Conceptual Model of Coastal Dune Ecology Synthesizing Spatial Gradients of Vegetation, Soil and Geomorphology. *Plant Ecology*, **202**, 135-148.
- Klijn, J.A. (1990) The younger dunes in the Netherlands; chronology and causation. geomorphology-hydrology-soils. *Catena Supplement*, **18**, 89-100.
- Konlechner, T.M., Hilton, M.J. & Arens, S.M. (2014) Transgressive dune development following deliberate de-vegetation for dune restoration in the Netherlands and New Zealand. *Dynamic environments*, **33**, 141-154.
- Korner, C. (2003) *Alpine plant life*. 2nd ed. pp. 45-47. Berlin, Springer.
- Lang, L., Wang, X., Hasi, E. & Hua, T. (2013) Nebkha (coppice dune) formation and significance to environmental change reconstructions in arid and semiarid areas. *Journal of Geographical Sciences*, **23**(2), 344-358.

- Ledendre, P., and Legendre, L. (2012) *Numerical Ecology 3rd edition*. Elsevier, Amsterdam, Netherlands.
- Levin, N., Kidron, G.J., and Ben-Dor, E. (2006) The spatial and temporal variability of sand erosion across a stabilizing coastal dune field. *Sedimentology*, **53**, 697-715.
- Litcher, J. (2000) Colonisation constraints during primary succession on coastal Lake Michigan sand dunes. *Journal of Ecology*, **88**, 825-839.
- Lithgow, D., Martinez, M.I., Gallego-Fernandez, J.B., Hesp, P.A., Flores, P., Guchuz, S., Rodriguez-Revelo, N., Jimenez-Orocio, O., Mendoza-Gonzalez, G. & Alvarez-Molina, L.I. (2013). Linking restoration ecology with coastal dune restoration. *Geomorphology*, **199**, 214-224.
- Luna, M.C.M.de M., Parteli, E.J.R., Duran, O. & Herrmann, H.J. (2011) Model for the genesis of coastal dune fields with vegetation. *Geomorphology*, **129**, 215-224.
- Martines, M.L., Hesp, P.A. & Gallego-Fernandez, J.B. (2013) Coastal dunes: Human Impact and Need for Restoration. In Restoration of Dune Vegetation in the Netherlands. In Martines, M.L., Gallego-Fernandez, J.B. & Hesp, P.A (eds.). *Restoration of Coastal Dunes*. Vergal, Springer, pp 1-142.
- Maun, M.A. (2009) *The biology of coastal sand dunes*. Oxford University Press, Oxford.
- Maun, M.A. (1994) Adaptations enhancing survival and establishment of seedlings on coastal dune systems. *Vegetation*, **111**, 59-70.
- Maun, M.A. (1998) Adaptations of plants to burial in coastal sand dunes. *Canadian Journal of Botany*, **76**, 713-738.
- McCarthy, D.P. (1992) Dating with Cushion Plant: Establishment of a *Silene acaulis* Growth Curve in the Canadian Rockies. *Arctic and Alpine Research*, **24**(1): 50-55.

- Mori, A.S. (2011) Ecosystem management based on natural disturbances: hierarchical context and non-equilibrium paradigm. *Journal of Applied Ecology*, **48**, 280-292.
- Mounteny, N.P. & Russell, A.J. (2006) Coastal aeolian dune development, Sólheimasandur, southern Iceland. *Sedimentary Geology*, **192**, 167-181.
- Musaya, A.M. & de Lange, P.J. (2010) *Ficinia spiralis* (Cypetaceae) a new genus and combination for *Desmoschoenus spiralis*. *New Zealand Journal of Botany*, **48**(1), 31-39.
- Nordstrom, K.F. (2008) *Beach and dune restoration*. Cambridge, Cambridge University Press.
- Nordstrom, K.F., Lampe, R. & Vandemark, L.M. (2000) Reestablishing Naturally Functioning Dunes on Developed Coasts. *Environmental Management*, **25**, 37-51.
- Olson, J. (1958) Lake Michigan dune development; Wind velocity profiles. *Journal of Geology*, **66**, 254-327.
- Park, J.S., Ahn, I. & Lee, E.J. (2012) Influence of soil properties on the distribution of *Deschampsia antarctica* on King George Island. *Maritime Antarctica, Polar Biology*, **35**, 1703-1711.
- Parttridge, T.R. (1992) Vegetation recovery following sand mining on coastal dunes at Kaitorete Spit, Canterbury, New Zealand. *Biological Conservation*, **61**, 59-71.
- Pearce, K.I. & Walker, I.J. (2002) Frequency and magnitude biases in the 'Fryberger' model, with implications for characterizing geomorphically effective winds. *Geomorphology*, **68**, 39-55.
- Perumal, V.J. & Maun, M.A. (2006) Ecophysiological response of dune species to experimental burial under field and controlled conditions. *Plant Ecology*, **13**, 560-566.
- Peterson, P.S., Hilton, M.J. & Wakes, S. J. (2011) Evidence of aeolian sediment transport across an *Ammophila arenaria*-dominated foredune, Mason Bay, Stewart Island. *New Zealand Geographer*, **67**, 174-189.

- Pickart, A.J. (2013) Dune Restoration Over Two Decades at Lanphere and Ma-le'l Dunes in Northern California. In Restoration of Dune Vegetation in the Netherlands. In Martines, M.L., Gallego-Fernandez, J.B. & Hesp, P.A (eds.). *Restoration of Coastal Dunes*. Vergal, Springer, pp 159-171.
- Provoost, S., Jones, M.L.M. & Edmondson, S.E. (2011) Changes in Landscape and Vegetation of Coastal Dunes in Northwest Europe: a Review. *Journal of Coastal Conservation*, **15**, 207-226.
- Rhind, P., Jones, R., & Jones, L. (2013) The Impact of Dune Stabilisation on the Conservation Status of Sand Dune Systems in Wales. In Restoration of Dune Vegetation in the Netherlands. In Martines, M.L., Gallego-Fernandez, J.B. & Hesp, P.A (eds.). *Restoration of Coastal Dunes*. Vergal, Springer, pp 125-143.
- Robertson-Rintoul, M. J. (1990) A quantitative analysis of the near surface wind flow pattern over coastal parabolic dunes. In Nordstrom, K.F., Psuty, N.P. & Carter, B (eds.). *Coastal Dunes, Form and Process*. Chichester, Wiley, pp. 57-78.
- Roman, C.T. & Nordstrom, K.F. (1988) The effect of erosion rate on vegetation patterns of a east coast barrier island. *Estuarine, Coastal and Shelf Science*, **26**(3), 233-242.
- Sherman, D.J. (1995) Problems of scale in the modeling and interpretation of coastal dunes. *Marine Geology*, **124**, 339-349.
- Sherman, D.J. & Hotta, S. (1990) Aeolian Sediment Transport: Theory and Measurement. In Nordstrom, K. F., Psuty, N. P. & Carter, B (eds.). *Coastal Dunes, Form and Process*. Chichester, Wiley, pp. 17-37.
- Smissen, R.D., Brietwiser, I., Ward, J.M., McLenachan, P.A. & Lockhart, P.J. (2003) Use of ISSR profiles and ITS-sequences to study the biogeography of alpine cushion plants in the genus *Raoulia* (Asteraceae). *Plant Systems Evolution*, **230**, 79-94.

- Sommerville, P., Mark, A.F. & Wilson, J.B. (1982) Plant succession on moraines of the upper Dart Valley, southern South Island, New Zealand. *New Zealand Journal of Botany*, **20**(3), 227-244.
- Spence, J.R. (1990) Seed rain in grassland, herbfield, snowbank, and fellfield in the alpine zone, Craigieburn Range, South Island, New Zealand. *New Zealand Journal of Botany*, **28**, 439-450.
- Sturgess, P. & Atkinson, D. 1993. The clear-felling of sand-dune plantations: soil vegetational processes in habitat restoration. *Biological Conservation*, **66**, 171-183.
- Swetnam, T.W., Allen, C.D. & Betancourt, J.L. (1999) Applied Historical Ecology: Using the past to manage for the future. *Ecological Applications*, **9**(4), 1189-1206.
- Sykes, M.T. & Wilson, J.B. (1990) An experimental investigation into the response of New Zealand sand dune species to different depths of burial by sand. *Acta Botanica Neerlandica*, **39**, 171-181.
- Tsoar, H. & Blumberg, D.G. (2002) Formation of parabolic dunes from brachan and transverse dunes along Israel's Mediterranean coast. *Earth Surfaces Processes and Landforms*, **27**, 1147-1161.
- Tsoar, H. (2000) Geomorphology and paleogeography of sand dunes that have formed the kurkar ridges in the coastal plain of Israel. *Israel Journal of Earth Sciences*, **49**, 189-196.
- Ullmann, I., Banister, J.M. & Bannister, P. (2007) The *placopis trachyderma*-*Raoulia*-community, a special type of biological soil crusts in the braided rivers of southern New Zealand. *Flora*, **202**, 687-694.
- Van der Meulen, F., Jungerius, P.D. & Visser, J.H. (1989) *Perspectives in coastal dune management*. The Hague, SPB Academic Publishing.

- Visser, S.M., Sterk, G. & Ribolzi, O. (2004) Techniques for simultaneous quantification of wind and water erosion and semi-arid regions. *Journal of Arid Environments*, **59**, 699-717.
- Wakes, S.J., Maegli, T., Dickinson, K.J. & Hilton, M.J. (2010) Numerical modelling of wind flow over a complex topography. *Environmental Modelling & Software*, **25**(2), 237-247.
- Walker, I.J., Earmer, J.B.R. & Darke, I.B. (2013) Assessing significant geomorphic changes and effectiveness of dynamic restoration in a coastal dune ecosystem. *Geomorphology*, **199**, 192-204.
- Wiedemann, A.M. & Pickart, A. (2004) Temperate Zone Coastal Dunes. In Martinez, M.L. & Psuty, N.P. (eds.). *Coastal Dunes Ecology and Conservation*. Verlag, Springer, pp. 53-65.
- Wiedemann, A.M. & Pickart, A. (1996) The *Ammophila* problem on the North West Coast of North America. *Landscape and Urban Planning*, **34**, 287-299.
- Zarnetske, P.L., Hacker, S.D., Seabloom, E.W., Ruggiero, P., Killian, J.R., Maddax, T.B. & Cox, D. (2012) Biophysical feedback mediates effects of invasive grasses on coastal dune shape. *Ecology*, **93**(6), 1439-1450.

Appendix I

Average sedimentation (mm), *Raoulia hookeri* var. *hookeri* and *Ficinia spiralis* surface area (cm³) per 10m² quadrant in the 200mx50m ground survey.

Co-ordinates (meters) of the centre of each 10m ² quadrant					Average erosion pin height change per 10m ²		Species surface area per 10m ²	
E	N	X	Distance from the start of the survey area (m)	Distance from the parabolic depositional lobe (m)	6/14-3/15 (mm)	2/15-3/15 (mm)	Average <i>Raoulia hookeri</i> var. <i>hookeri</i> (cm ³)	Average <i>Ficinia spiralis</i> (cm ³)
1202058.95	4789593.60	12.89	5	719.5	1.00	7.80	489.80	NA
1202058.62	4789568.91	12.59	15	729.5	-1.00	4.67	258.70	163.57
1202059.07	4789543.21	11.91	25	739.5	7.00	3.00	962.28	NA
1202058.96	4789518.42	11.31	35	749.5	2.67	3.00	327.08	NA
1202059.31	4789493.57	10.88	45	759.5	5.20	3.20	455.01	55.76
1202059.13	4789468.52	10.27	55	769.5	-2.33	1.75	424.70	NA
1202059.34	4789443.42	9.88	65	779.5	-7.00	3.67	628.01	NA
1202059.85	4789418.83	9.40	75	789.5	-3.00	3.75	539.49	24.80
1202061.12	4789581.62	12.81	85	799.5	4.50	5.75	306.39	NA
1202061.86	4789531.11	11.66	95	809.5	1.67	1.67	556.19	3.69
1202062.20	4789481.10	10.53	105	819.5	6.00	0.25	399.13	47.06
1202062.18	4789430.88	9.67	115	829.5	16.00	4.00	568.09	199.27
1202064.42	4789418.55	9.44	125	839.5	8.00	0.75	726.49	NA
1202064.45	4789443.45	9.97	135	849.5	5.00	-0.50	542.32	NA
1202064.76	4789468.68	10.30	145	859.5	2.50	NA	691.71	99.17
1202064.64	4789493.48	10.77	155	869.5	2.40	2.20	533.55	NA
1202064.30	4789518.32	11.44	165	879.5	11.50	-2.00	572.52	NA
1202064.31	4789543.30	12.02	175	889.5	-2.50	3.00	268.25	85.00
1202063.83	4789569.42	12.52	185	899.5	3.00	-3.00	469.67	52.03
1202063.88	4789594.39	13.12	195	909.5	1.33	2.33	309.08	107.80
1202068.79	4789594.56	13.06	5	719.5	3.33	4.50	638.17	80.19
1202068.81	4789569.78	12.52	15	729.5	1.25	5.50	1003.83	NA
1202069.26	4789543.22	12.03	25	739.5	2.00	0.50	666.10	NA
1202069.33	4789518.36	11.57	35	749.5	4.67	3.80	1216.10	10.99
1202069.62	4789493.40	10.86	45	759.5	3.00	2.00	838.31	45.70
1202069.76	4789468.55	10.44	55	769.5	9.00	5.50	1418.60	34.06

E	N	X	Distance from the start of the survey area (m)	Distance from the parabolic depositional lobe (m)			Average <i>Raoulia</i> <i>hookeri</i> var. <i>hookeri</i> (cm ³)	Average <i>Ficinia</i> <i>spiralis</i> (cm ³)
					6/14- 3/15 (mm)	2/15- 3/15 (mm)		
1202069.47	4789443.44	10.04	65	779.5	9.00	1.67	818.70	184.14
1202069.75	4789418.66	9.46	75	789.5	7.00	1.50	667.53	NA
1202072.55	4789431.53	9.68	85	799.5	-4.33	2.00	619.71	70.18
1202072.39	4789481.18	10.70	95	809.5	3.33	-1.00	671.60	NA
1202072.09	4789531.30	11.73	105	819.5	0.00	1.33	435.99	204.33
1202071.45	4789582.26	12.78	115	829.5	10.00	3.50	591.96	687.52
1202074.36	4789595.22	13.12	125	839.5	3.33	-0.50	543.40	47.68
1202073.86	4789570.28	12.53	135	849.5	6.00	3.00	479.01	271.64
1202074.57	4789543.35	11.91	145	859.5	-2.00	1.67	509.05	80.74
1202074.72	4789518.38	11.37	155	869.5	3.75	0.50	481.39	NA
1202074.93	4789493.50	10.97	165	879.5	-2.50	1.00	907.40	32.81
1202074.91	4789468.65	10.40	175	889.5	2.00	8.00	296.08	620.79
1202074.78	4789443.53	9.91	185	899.5	-2.00	3.00	345.28	72.76
1202074.82	4789418.73	9.55	195	909.5	-2.00	4.00	564.00	20.88
1202079.79	4789418.60	9.46	5	719.5	10.50	10.33	340.74	53.60
1202079.70	4789443.63	10.01	15	729.5	7.00	1.00	1453.27	34.74
1202079.77	4789468.58	10.40	25	739.5	NA	4.00	1265.23	NA
1202079.86	4789493.62	10.93	35	749.5	5.00	6.67	625.14	68.85
1202079.66	4789518.52	11.41	45	759.5	5.00	1.00	664.63	NA
1202079.54	4789543.41	11.94	55	769.5	8.25	1.75	1763.74	NA
1202078.77	4789570.23	12.50	65	779.5	2.67	2.00	872.12	98.40
1202078.87	4789595.35	13.03	75	789.5	13.00	3.50	394.15	NA
1202080.24	4789583.04	12.78	85	799.5	7.67	3.00	785.46	40.64
1202082.04	4789531.13	11.64	95	809.5	2.50	9.50	763.21	58.27
1202082.47	4789481.10	10.61	105	819.5	4.75	0.50	671.05	40.09
1202082.81	4789431.02	9.64	115	829.5	0.00	-4.33	914.09	NA
1202084.80	4789418.68	9.58	125	839.5	2.67	1.67	649.27	NA
1202084.76	4789443.63	9.91	135	849.5	4.33	1.50	1079.60	NA
1202084.81	4789468.59	10.42	145	859.5	7.50	-2.75	560.87	NA
1202084.74	4789493.58	10.87	155	869.5	-0.25	9.50	479.93	93.83
1202084.62	4789518.52	11.35	165	879.5	-2.75	3.40	574.32	54.09
1202084.46	4789543.43	11.91	175	889.5	-4.00	-0.33	373.61	101.58
1202083.64	4789570.70	12.45	185	899.5	0.33	3.25	309.58	33.44
1202083.75	4789596.07	12.98	195	909.5	7.00	5.33	809.53	NA
1202088.71	4789595.83	12.94	5	719.5	6.50	5.00	559.96	NA
1202088.67	4789571.19	12.44	15	729.5	5.00	2.50	748.64	40.41

E	N	X	Distance from the start of the survey area (m)	Distance from the parabolic depositional lobe (m)			Average <i>Raoulia</i> <i>hookeri</i> var. <i>hookeri</i> (cm ³)	Average <i>Ficinia</i> <i>spiralis</i> (cm ³)
					6/14- 3/15 (mm)	2/15- 3/15 (mm)		
1202089.39	4789543.57	11.82	25	739.5	6.50	0.50	680.52	151.90
1202089.70	4789518.47	11.33	35	749.5	8.33	1.33	975.41	118.08
1202089.87	4789493.56	10.91	45	759.5	9.00	2.50	750.74	NA
1202089.75	4789468.54	10.46	55	769.5	7.50	1.50	303.88	NA
1202089.94	4789443.60	9.99	65	779.5	10.00	0.67	777.41	46.94
1202089.90	4789418.74	9.53	75	789.5	5.33	2.40	640.23	NA
1202092.36	4789431.16	9.83	85	799.5	0.00	-1.00	651.29	884.00
1202092.41	4789481.06	10.79	95	809.5	-1.00	-0.50	816.71	NA
1202092.15	4789520.91	11.45	105	819.5	-0.50	2.00	354.15	15.28
1202091.11	4789573.89	12.60	115	829.5	1.25	1.00	629.06	153.64
1202093.90	4789601.75	13.20	125	839.5	9.50	0.33	742.52	43.29
1202094.06	4789576.82	12.70	135	849.5	5.00	1.67	213.16	22.28
1202094.47	4789548.60	11.94	145	859.5	12.00	2.20	428.72	38.12
1202094.64	4789523.49	11.51	155	869.5	-1.25	1.00	359.81	NA
1202094.84	4789498.57	11.05	165	879.5	1.33	-2.00	340.15	39.92
1202095.02	4789473.50	10.59	175	889.5	-3.50	-1.67	405.60	87.73
1202094.92	4789448.78	10.11	185	899.5	-1.00	4.50	649.51	51.78
1202094.83	4789423.49	9.64	195	909.5	0.00	-12.00	490.69	NA
1202099.76	4789413.64	9.47	5	719.5	0.33	0.60	802.68	27.77
1202100.07	4789438.29	9.90	15	729.5	0.00	1.00	672.85	NA
1202099.95	4789463.65	10.40	25	739.5	-1.50	1.40	377.15	604.66
1202099.82	4789488.45	10.80	35	749.5	2.50	1.00	562.03	NA
1202099.66	4789513.38	11.35	45	759.5	0.50	3.00	630.71	NA
1202099.61	4789538.38	11.78	55	769.5	-1.50	1.25	455.61	NA
1202099.11	4789563.31	12.28	65	779.5	0.33	0.75	436.42	NA
1202098.64	4789592.13	13.04	75	789.5	2.00	2.00	378.06	349.00
1202101.26	4789594.82	13.18	85	799.5	3.80	5.40	735.41	23.45
1202102.22	4789541.04	11.97	95	809.5	12.50	4.50	195.79	30.74
1202102.46	4789490.98	10.98	105	819.5	3.50	0.00	332.55	10.57
1202102.62	4789441.11	9.93	115	829.5	4.67	3.33	715.89	NA
1202104.63	4789413.73	9.43	125	839.5	9.25	7.25	285.50	169.63
1202105.05	4789438.50	9.87	135	849.5	3.60	4.80	542.42	77.84
1202104.91	4789463.68	10.35	145	859.5	3.00	3.00	253.79	41.43
1202104.95	4789488.42	10.86	155	869.5	-1.50	-2.00	282.10	16.94

			Distance from the start of the survey area (m)	Distance from the parabolic deposition nal lobe (m)	6/14- 3/15 (mm)	2/15- 3/15 (mm)	Average <i>Raoulia</i> <i>hookeri</i> var. <i>hookeri</i> (cm ³)	Average <i>Ficinia</i> <i>spiralis</i> (cm ³)
E	N	X						
1202104.89	4789513.15	11.38	165	879.5	-10.50	3.00	105.89	96.43
1202104.48	4789538.35	12.03	175	889.5	0.00	4.75	2.36	244.53
1202104.95	4789563.39	12.42	185	899.5	-3.25	-3.00	NA	NA
1202103.44	4789592.64	13.13	195	909.5	13.50	0.75	NA	NA

Appendix II

The results of the morphological changes in the *Ficinia spiralis* nabkha surveyed in the stonefield between August 2014 and March 2015.

<i>F. spiralis</i> nabkha number	Distance from start of survey (m)	Distance from parabolics (m)	Net volume (3/15)	Net volume change (m ³) 8/14-3/15	Max height change (mm) 8/14 -3/15
1	11.72	16.22	-0.35	0.01	-0.81
2	16.75	21.25	-1.46	0.083	-1.31
3	30.08	34.58	-0.29	0.025	-0.61
4	41.12	45.62	0.68	0.115	-1.21
5	47.66	52.16	0.44	0.046	-0.78
6	58.31	62.81	0.74	0.054	-1.49
7	65.89	70.39	0.84	0.022	-0.34
8	78.21	82.71	0.85	0.022	-0.81
9	88.89	93.39	0.35	0.004	-0.38
10	99.67	104.17	2.36	0.047	-0.65
11	110.74	115.24	4.47	0.101	-0.7
12	120.48	124.98	0.83	0.022	-0.84
13	132.26	136.76	1.79	0.024	-0.65
14	142.01	146.51	5.09	0.056	-0.51
15	154.09	158.59	1.06	0.002	-0.63
16	164.14	168.64	4.18	-0.021	-0.42
17	175.51	180.01	4.26	-0.019	0.06
18	185.36	189.86	5.29	-0.029	-0.08